Annual Report of Research Performed on the LIBRA Project Between 1 January and 31 December 1982 by Fusion Power Associates for the Kernforschungszentrum Karlsruhe GmbH, Karlsruhe, FRG

B. Badger, J. Billen, D. Bruggink, R. Engelstad, G.L. Kulcinski, E.G. Lovell, G.A. Moses, K. O'Brien, R.R. Peterson, L. Pong, I.N. Sviatoslavsky, D.K. Sze, W.F. Vogelsang, J. Watrous

December 31,

FPA-82-7

FUSION POWER ASSOCIATES

2 Professional Drive, Suite 248
Gaithersburg, Maryland 20879
(301) 258-0545

1500 Engineering Drive
Madison, Wisconsin 53706
(608) 263-2308

ANNUAL REPORT

of

RESEARCH PERFORMED ON THE LIBRA PROJECT

between

JANUARY 1 and DECEMBER 31, 1982

by

FUSION POWER ASSOCIATES

for the

KERNFORSCHUNGSZENTRUM KARLSRUHE GmbH

Karlsruhe, Federal Republic of Germany

B. Badger
J. Billen
D. Bruggink
R. Engelstad
G. Kulcinski
E. Lovell
G. Moses
K. O'Brien
R. Peterson
L. Pong
I. Sviatoslavsky
D. Sze
W. Vogelsang
J. Watrous

FPA-82-7

December 31, 1982

TABLE OF CONTENTS

INTRODUCTION

This is a progress report of work performed between January 1, 1982 and December 31, 1982 by Fusion Power Associates under contract to Kernforschungszentrum Karlsruhe. The purpose of the work was to make a preliminary assessment of the suitability of light ion beam driven fusion for reactor applications, in order to set the stage for a full scale conceptual reactor design in calendar year 1983. This preliminary assessment includes:

(1) Review of past work in light ion beam fusion (LIBF);

(2) Definition of a reactor to be designed in 1983;

(3) Investigations of critical elements of LIBF reactors, drivers, targets, beam propagation, fireball generation, cavity gas pumping and cavity design; and

(4) Preparation of a bibliography of LIBF related papers.

These topics as well as others are reported in the remainder of this report.

1. Review of Other Light Ion Beam Fusion Reactor Designs

1.1 Light Ion Beam Fusion Target Development Facility

For the last four years the University of Wisconsin Fusion Engineering Program has been working in collaboration with Sandia National Laboratory on the design of a Light Ion Fusion Target Development Facility. Some of the general features of this facility are given in Table 1.1. Its purpose is to test high gain target concepts using a pulsed power multimodule light ion driver capable of delivering 4 MJ of energy onto a target. Target yields in the range of 50-200 MJ are expected and the target shot rate is 10/day. Hence this facility will experience many of the same phenomena within one shot as one would expect to find in a reactor. However, low shot frequency removes problems such as heat transfer and radiation damage. There is also no blanket or tritium breeding in this design. A list of specific parameters is given in Table 1.2 and a review of the TDF design is shown in Fig. 1.1. A cut-view is shown in Fig. 1.2. The reaction vessel itself is made of Al 6061 and consists of curved panels or plates supported from behind by a structure of ribs and stringers. These are shown in more detail in Fig. 1.3. All of these components have been conservatively designed to a fatigue lifetime of 10^4 shots -- the expected life of the facility. The flexure stress in a plate and rib are plotted as a function of time in Figs. 1.4 and 1.5 respectively. Hence there is no anticipated replacement of the reaction vessel.

Because this is an experimental facility there is a great emphasis on accessibility. The radiation shield is a water filled annulus between the reaction chamber and the water-vacuum interface of the pulsed power machine as shown in Fig. 1.2. This region contains the magnetically insulated transmission lines. The water can be quickly drained to gain access to the re-

TABLE 1.1

General Features of the Light Ion Beam Target Development Facility

General Characteristics

- Test Bed for 50-200 MJ Targets
- Operational Life - 5 y
- Target Rate - 10/day; 3000/y
- Facility Rate = 3 Times Target Rate
- Initial Construction - Est. 1988
- Initial Operation - Est. 1992-93

TABLE 1.2

Specific Parameters for the Light Ion Beam

Target Development Facility Parameters

Pellet	
Nature	Cryogenic
Energy requirement	< 4 MJ
Gain	50
Yield	< 200 MJ
Mass	0.5 gm
Radius	0.5 cm
Driver	
Energy in store	15 MJ
Energy at diodes	8 MJ
Diode voltage	4 MV
Ion specie	He^{++}
Ion energy	8 MeV
Power at diodes	200 TW
Pulse width at diodes	40 ns
Response time	1.5 μs
Jitter time	10 ns
Channel	
Length	4.0 m
Current	85 kA
Current rise time	1 μs
Radius at firing time	0.5 cm
Density rarefaction factor	4
Number	60
Channel Laser System	
Laser pulse width	1 μs
Distance from last mirror to pellet	10 m
Beam-aiming mirror radius	5 cm
Beam-aiming mirror mass	0.2 kg
Pellet tracking distance	10 cm

TABLE 1.2. (continued)

Hydromotion at firing time	Negligible
Aperture vane port radius	2 cm
Aperture open time	200 μs
Blanket port radius	10 cm
Pellet Injection and Tracking	
Pellet acceleration	500 m/s^2 (500 g's)
Accelerator tube length	9 m
Pellet injection velocity	300 m/s
Allowable beam incidence error	1 mm
Beam-aiming mirror actuator energy	1 J
Cavity Gas	
Type	99.8% Ar, 0.2% Na or N_2
Density	$7 \times 10^{23}/m^3$
Temperature	300°K
Cavity	
Shape	Cylinder
Height	6.0 m
Radius	3.0 m
Overpressure incident on wall	1.7 MPa
Shot repetition rate	10/day
First Wall	
Thickness	3 cm
Material	Aluminum
Design	Solid plate panels
Number of panels	60
Panel width	0.47 m
Panel height	2 m
Cycles to failure	1.5×10^4

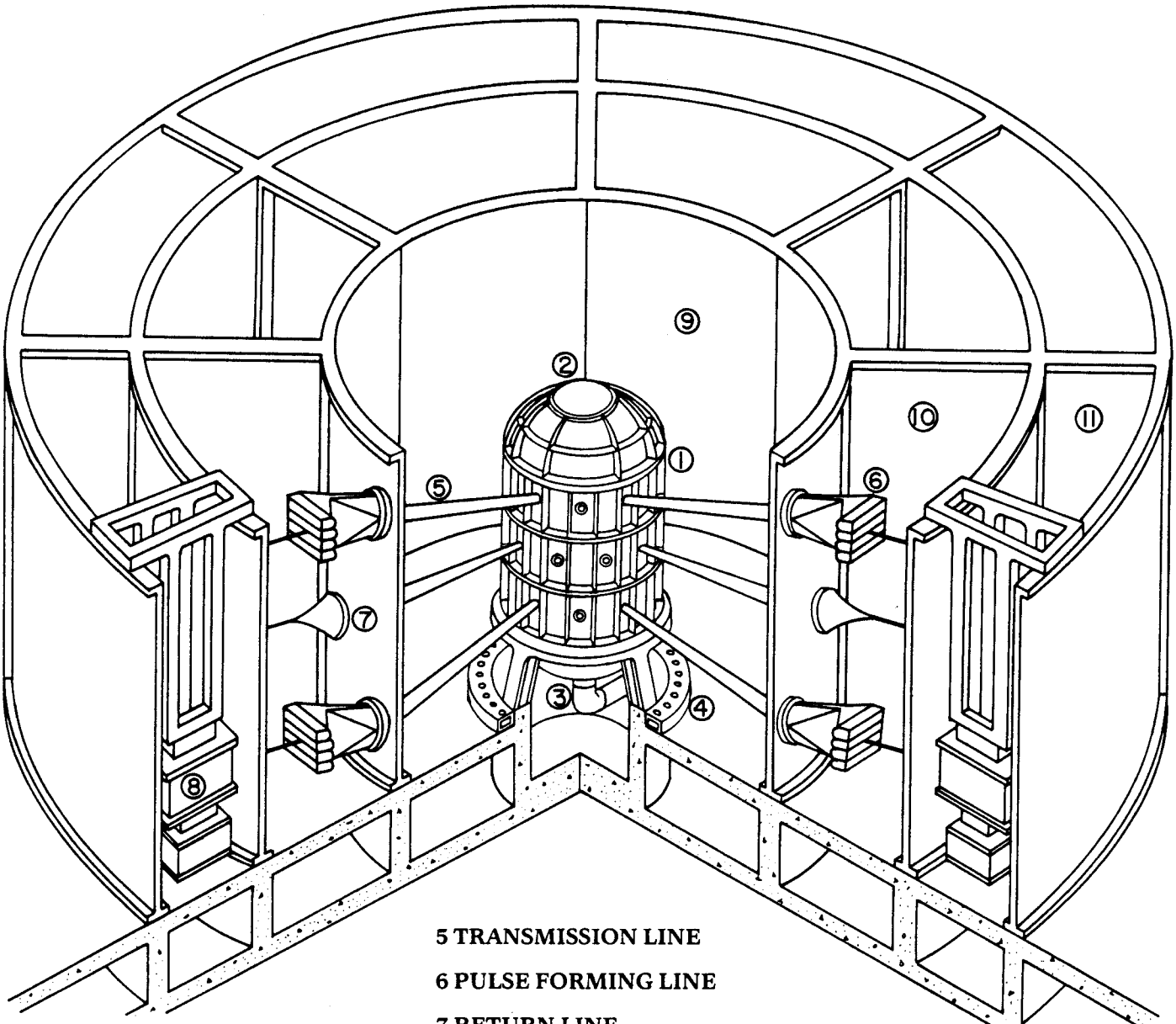

Fig. 1.1 Light Ion Beam Target Development Facility.

Fig. 1.2 Cross-sectional view of the LIB-TDF.

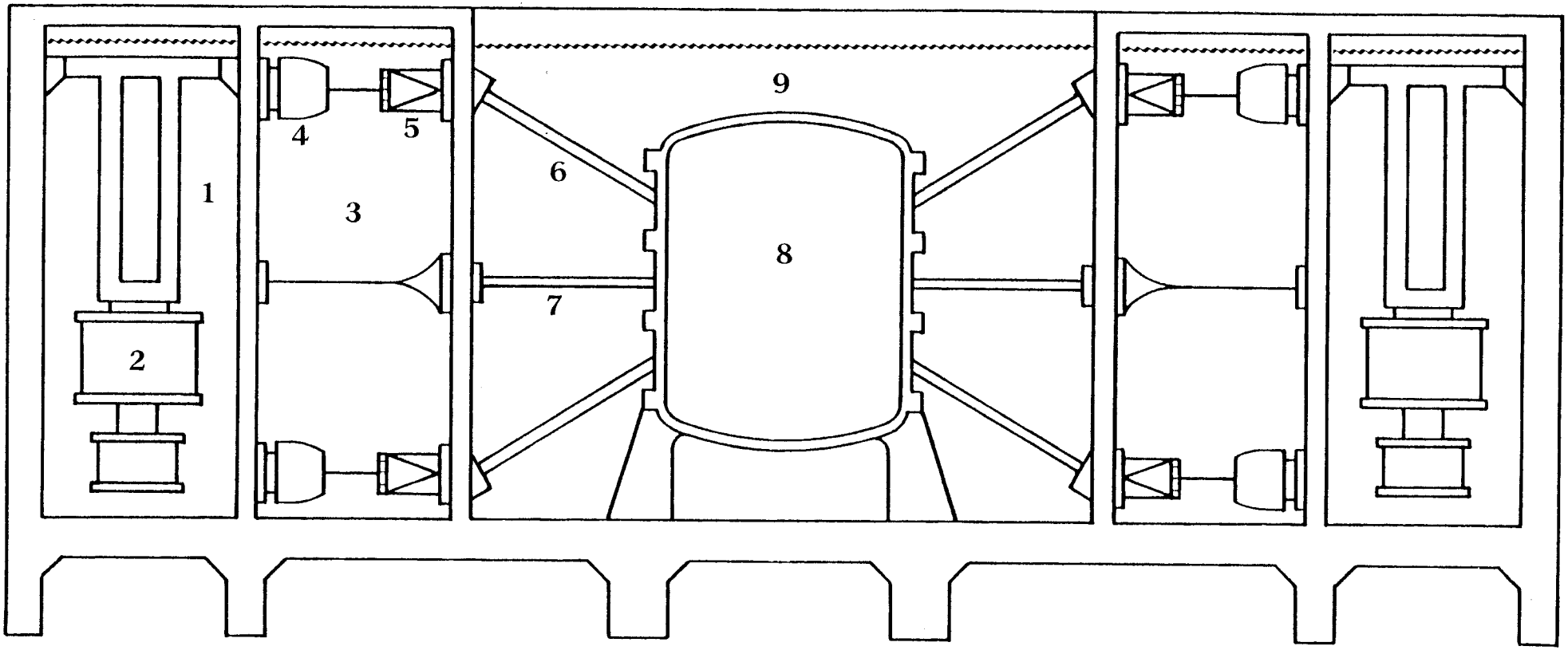

1 ENERGY STORAGE SECTION – OIL

2 BEAM MARX GENERATOR

3 PULSE FORMING SECTION – WATER

4 INTERMEDIATE STORAGE CAPACITOR

5 PULSE FORMING LINE

6 TRANSMISSION LINE

7 RETURN LINE

8 REACTION CHAMBER

9 SHIELDING POOL – WATER

CONCEPTUAL FIRST WALL
STRUCTURAL SYSTEM

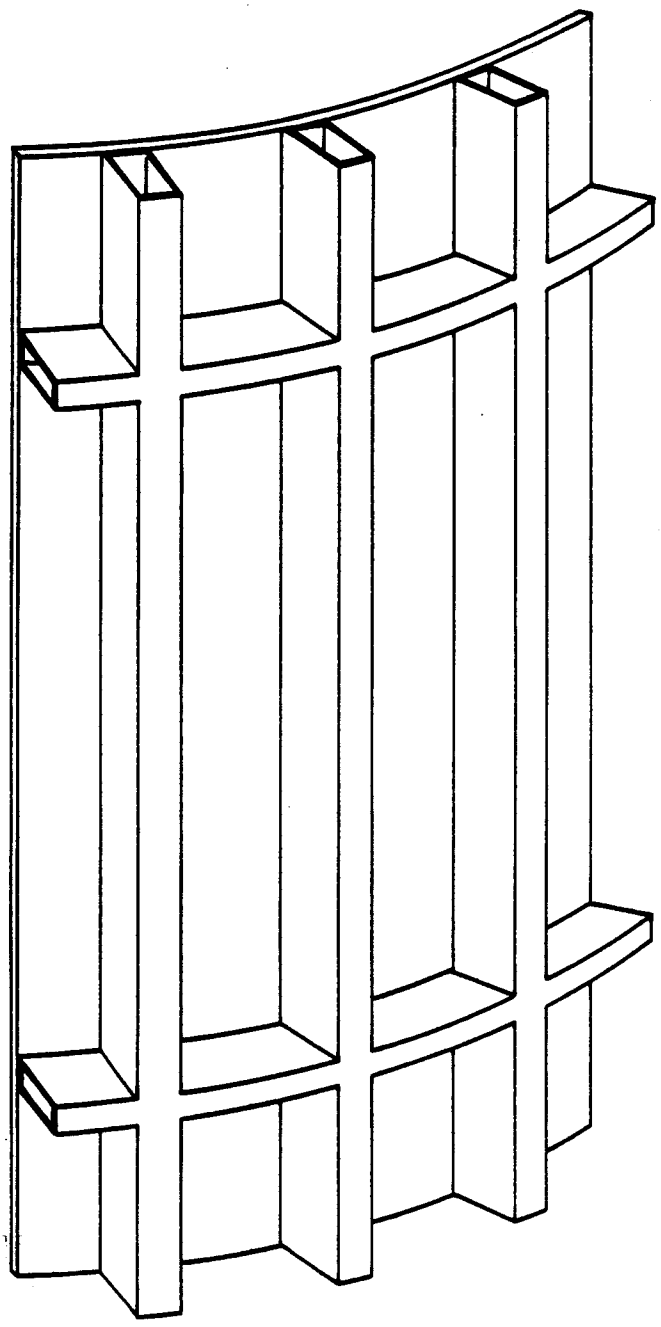

Fig. 1.3 First wall and structural frame for the LIB-TDF.

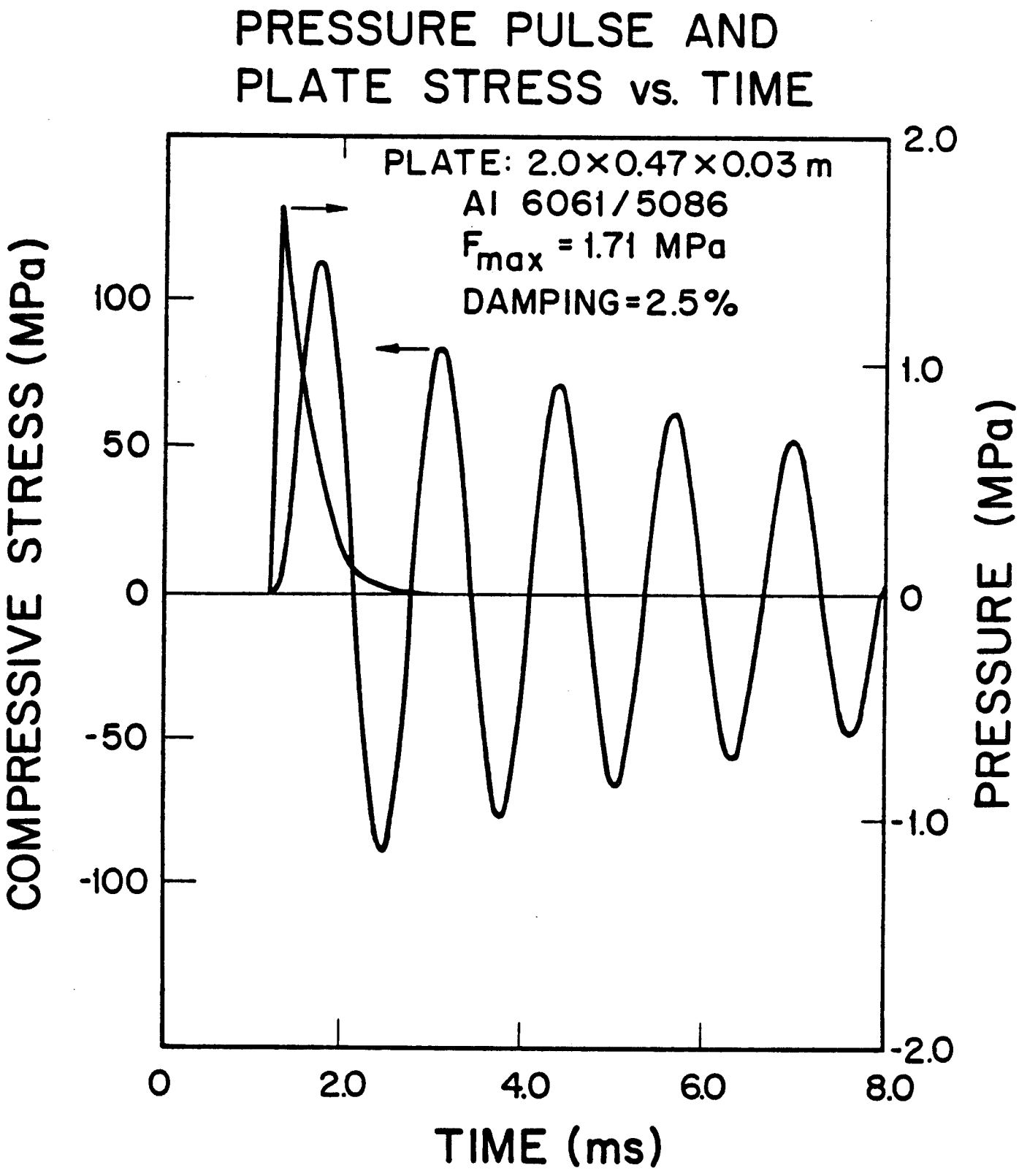

Fig. 1.4 Flexural stress vs. time for a supported first wall plate in the LIB-TDF.

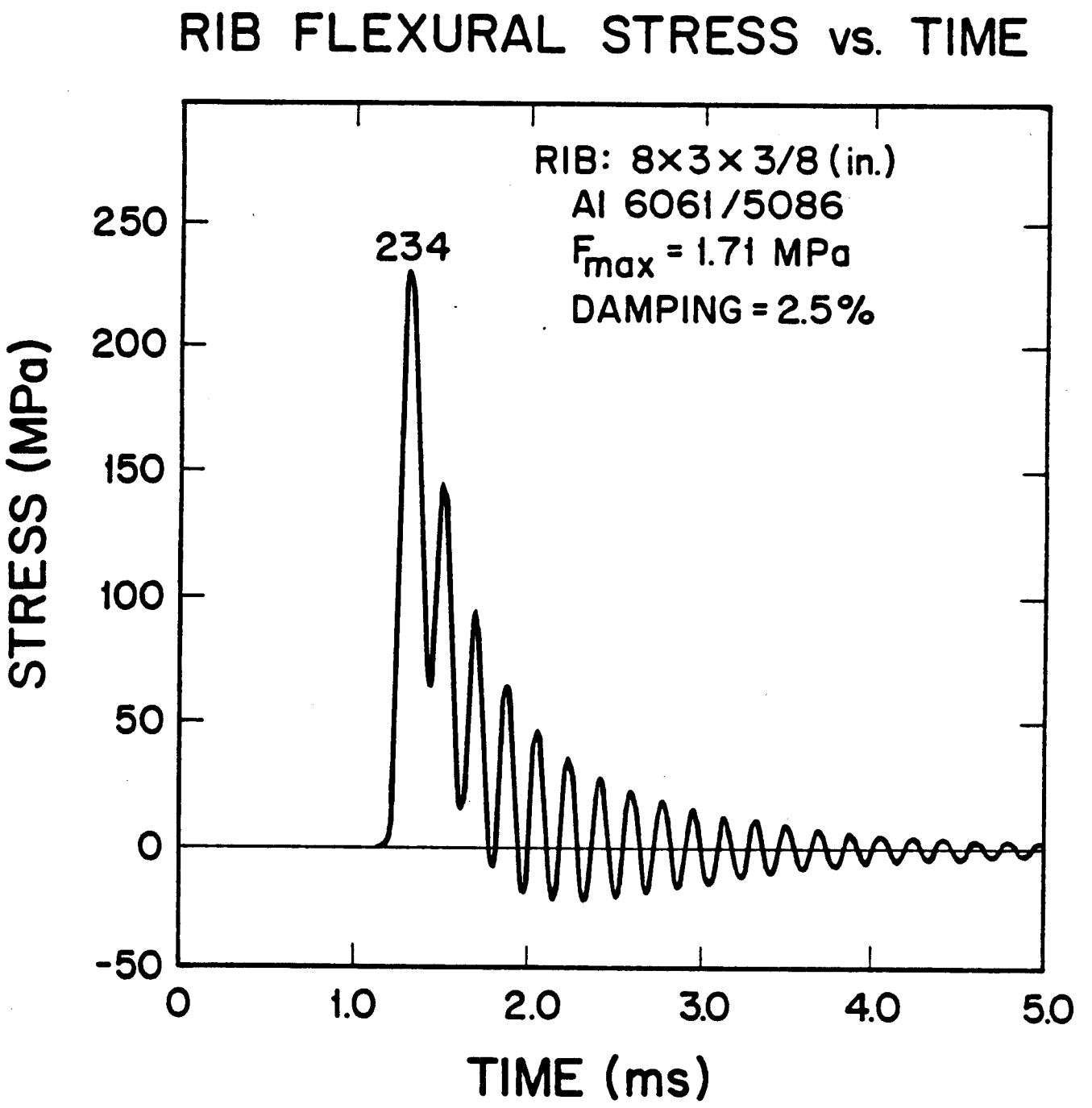

Fig. 1.5 Flexural stress vs. time for a supporting rib member in the LIB-TDF.

action chamber by removal of the top end-cap as shown in Fig. 1.6. The use of aluminum as the structural material allows hands-on maintenance with the reaction chamber at one week after shutdown. Many different metal alloys were investigated as candidates for the structure and aluminum had the clearest advantage due to its low radioactivity as shown in Table 1.3.

The vibrating reaction vessel will induce pressure waves in the water shield following a target explosion. These waves are suppressed by introducing bubbles in the shield to reflect and attenuate the pressure waves. The plenum for introducing the screen of bubbles is shown in Fig. 1.1. Attenuation calculations have been done and show that properly designed bubble screens will effectively attenuate the pressure waves.

A report summarizing the work to date on TDF will be issued in early 1983. However, work continues on this design to further investigate the optimum chamber size and design. Work is also underway to improve the stress analysis models used for the design of the target chamber.

1.2 Comparison of EAGLE, UTLIF, ADLIB, and LIBRA

We have reviewed the most recent work in the area of light ion fusion conceptual reactor design and compared these designs with the proposed LIBRA design. Three other designs were identified and these are listed in Table 1.4 along with their sponsor and the organization responsible for the work. We see that two of these designs were done by the Japanese and one was sponsored by EPRI. The major parameters for each of these reactor designs are given in Table 1.5. The two Japanese designs, UTLIF and ADLIB, are characterized by optimistic target gain (135 and 170), moderately high repetition rate (6 and 3 Hz) and consequently high fusion power (2844 and 2562 MW_t). Both use high energy protons (8 and 10 MeV) as the driver ion. The EAGLE design, conceived

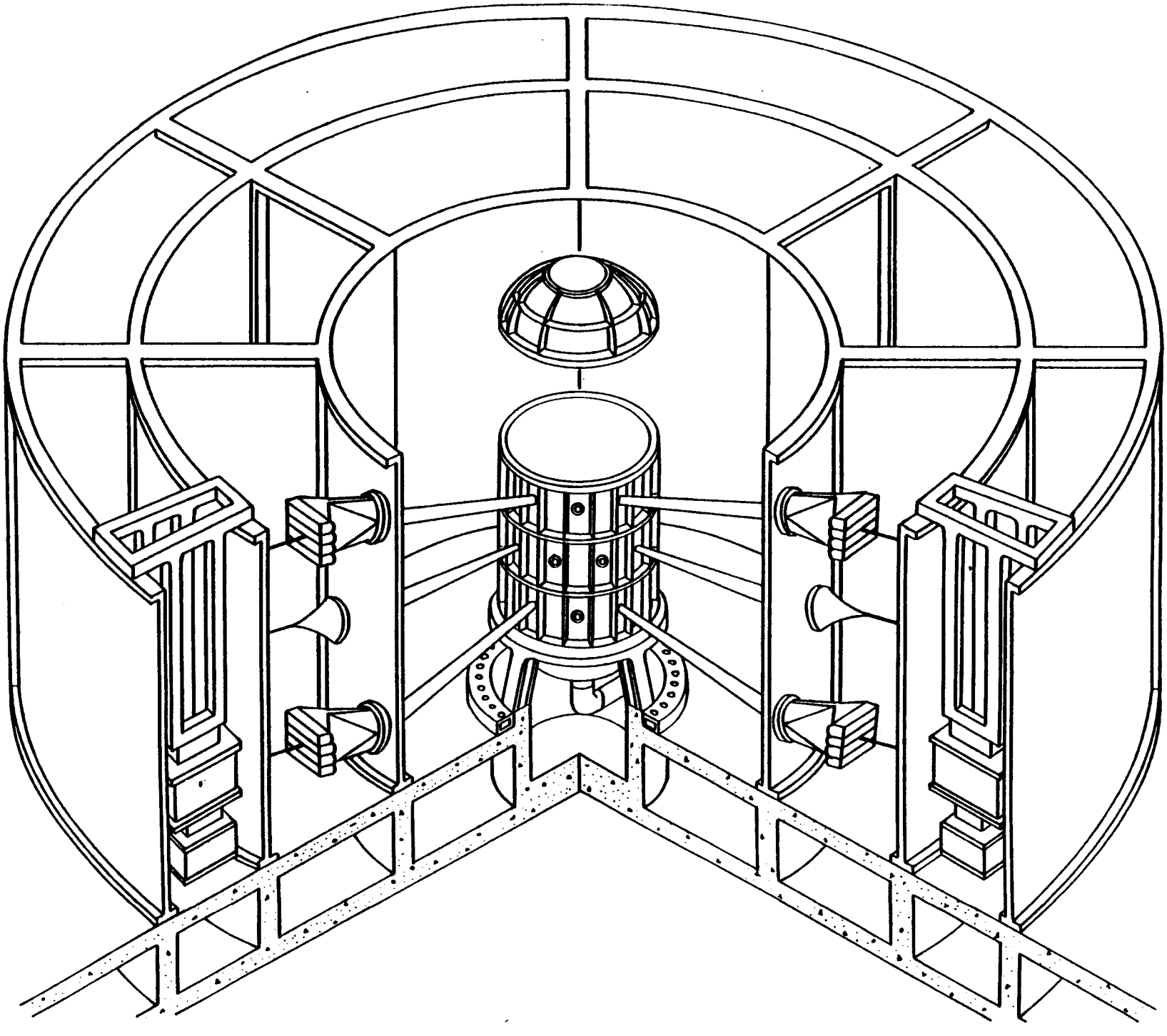

Fig. 1.6 Access to the LIB-TDF is achieved by removing the top end-cap.

TABLE 1.3

Radioactive Dose After Shutdown for the LIB-TDF

Dose at First Wall (mr/hr)

Material	Time After Shutdown 0	1 day	1 week
Al 6061	2,100	260	1.65
HT-9	489	114	101
304 SS	481	109	105
Ti-6Al-4V	515	177	66
Cu-Be	1,060	204	7

Dose At Operating Floor (mr/hr)

Material	Time After Shutdown 0	1 day	1 week
Al 6061	230	28	0.18
HT-9	55	13	11
304 SS	54	12	12
Ti-6Al-4V	59	20	7.5
Cu-Be	118	22	0.82

TABLE 1.4

Current Status of Light Ion Beam Power Reactor Studies

Name	Sponsor	Start	Lead Organizations
Eagle	EPRI-U.S.	1981	Bechtel Physics International Sandia (Fall 1982)
UTLIF	Minis. of Ed., Japan	Fall 1981	Univ. of Tokyo
ADLIB	Minis. of Ed., Japan	Fall 1981	Univ. of Tokyo
LIBRA	KfK, FRG	1982	Univ. of Wisconsin Kernforschungszentrum Karlsruhe

TABLE 1.5

Major Parameters of Current LIB Reactors

	LIBRA	EAGLE	UTLIF(1)	ADLIB-1
Cavity shape	cyl.	cyl.	cyl.	cyl.
Cavity radius, m	5	4	5	4
Total driver energy, MJ/shot	4	5	3.5	5
Pellet Gain	80	60	135.4	170.8
$n_D G$	16	12	13.5	17
Repetition rate, Hz	1.5	3	6	3
Fusion yield, MJ/shot	320	300	474	854
Fusion power, MW_t	480	900	2844	2562
Driver eff., %	20	20	10	10
Ion type (MeV)	Li(21)	D(6.3)	p(8)	p(10.2)
Number drivers	40	24	36	36
Cavity gas, torr	Ar(10) + Li(0.002)	undecided	Ne(10) + Na(0.1)	Ne(10) + Li(0.3)
Max. neutron wall loading, MW/m^2	1.09	3.1	7.24	10.2
Tritium breeding ratio	?	1.05-1.2	1.38	1.70
First wall and blanket structure	PbLi INPORT units	Li spray + HT-9 tubes	V-20Ti tube bundles	Liq. Li in rotating V-20Ti vessel
Blanket breeding and heat transp. medium	$Li_{17}Pb_{83}$	Li	Li	Li
Li inlet temp., °C	?	500	350	350
Li outlet temp., °C	?	610	550	550
Total thermal power, MW_t	514	1040	3014	2772
Gross elec. output, MW_e	206	380	1410	1300
Net elect. output, MW_e	144	290	1140	1100
Net plant eff., %	30	27.9	38	40

by Bechtel and Physics International, has a fusion power of 900 MW_f and uses the heavier deuterium isotope of hydrogen at 6 MeV. In this case the target gain is a very conservative 60. This compares to a proposed target gain of 80 with 4-8 MJ of 21 MeV Li for LIBRA.

These parameters are plotted in Fig. 1.7 and compared to the gain curves of Bangerter for short wavelength lasers and heavy ion beams. (We must emphasize that the parametric curves on this graph for heavy ion ranges and spot size do not directly carry over to light ions.) Light ion gain curves for similar targets are likely to be more pessimistic than the heavy ion curves and under no circumstances will they exceed the short wavelength laser band. This comparison leads us to the conclusion that the ADLIB and UTLIF designs assume quite optimistic fusion performance while the EAGLE design assumes the most conservative fusion performance. This is likely to result from the varied sources of target physics information used by each of these design studies. As more is learned about target implosions and the real-world effects that tend to ruin their spherical symmetry, the more conservative the gain predictions become. The EAGLE design uses information from Sandia National Laboratory and Sandia target designers have historically been very conservative.

The LIBRA design falls into the middle of these two extremes. Gain of 80 at 4 MJ of input energy is quite optimistic, gain of 80 at 6 MJ of input energy is nominal, and gain of 80 at 8 MJ of input energy could be considered "conservative." The exact value of input energy awaits further target scaling investigations.

It is interesting to note that the driver efficiency in the ADLIB and UTLIF studies is much more conservative than the LIBRA or EAGLE designs, 10%

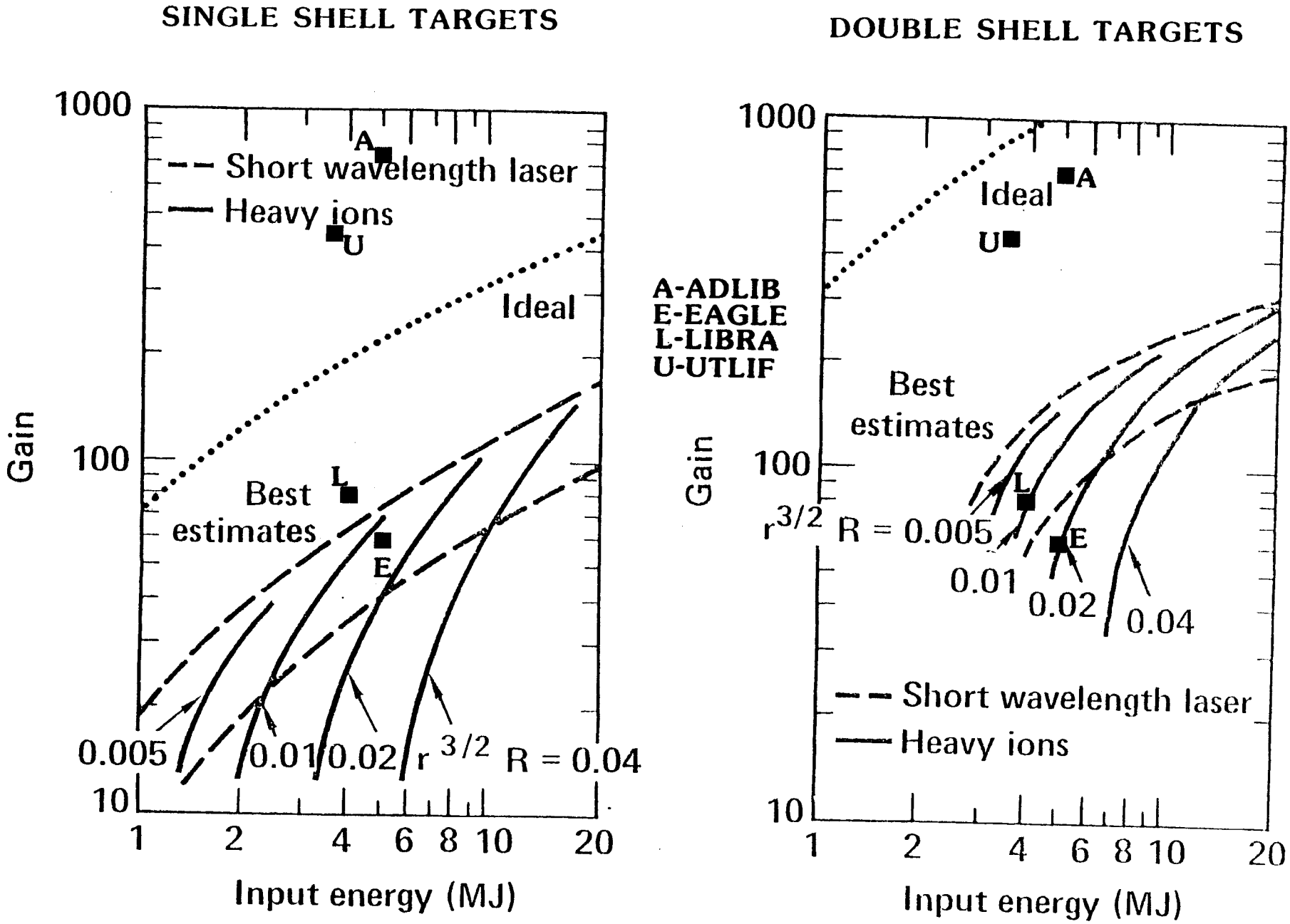

Fig. 1.7 Gain and driver energy proposed for current LIB reactor studies.

as compared to 20%. It is difficult to determine the reason for this difference. The LIBRA design uses 20% only as a goal and is not supported by any detailed calculations at this time.

The repetition rate in the four designs varies by a factor of 4, from a low of 1.5 Hz for LIBRA to a high of 6 Hz for UTLIF. The other two designs use 3 Hz. The repetition rate in light ion systems is limited by the time required to reestablish the cavity environment. Hence the LIBRA design represents the most conservative estimate of cavity reestablishment time. This is the result of our past experience in cavity gas radiation hydrodynamics and heat transfer. This appears to be one of the most difficult problems in LIB reactor design because of the presence of a background gas at 1-20 torr to support ion beam propagation in plasma channels. This is the reason for our conservative choice. As a result our power level is much lower than the other designs and the LIBRA neutron wall loading is much lower. This lower neutron wall loading is a signal that our design is not optimum and work will continue on reducing the size of the cavity.

The cavity and blanket designs for EAGLE, UTLIF, and ADLIB are shown in Figs. 1.8, 1.9, and 1.10, respectively. The EAGLE reactor uses some background gas to support channel formation and a Li spray or mist near the wall to absorb the fireball energy through latent heat of vaporization and ionization. This is meant to decrease the cavity reestablishment time. The coolant and breeding materal in EAGLE is lithium. A sequence of schematics showing the cavity phenomenology in EAGLE is shown in Fig. 1.11.

The UTLIF design uses banks of tubes as the blanket and first wall as shown in Fig. 1.9. As the fireball expands out through these tubes they act in the same manner as a cross-flow heat exchanger. The cavity is pumped from

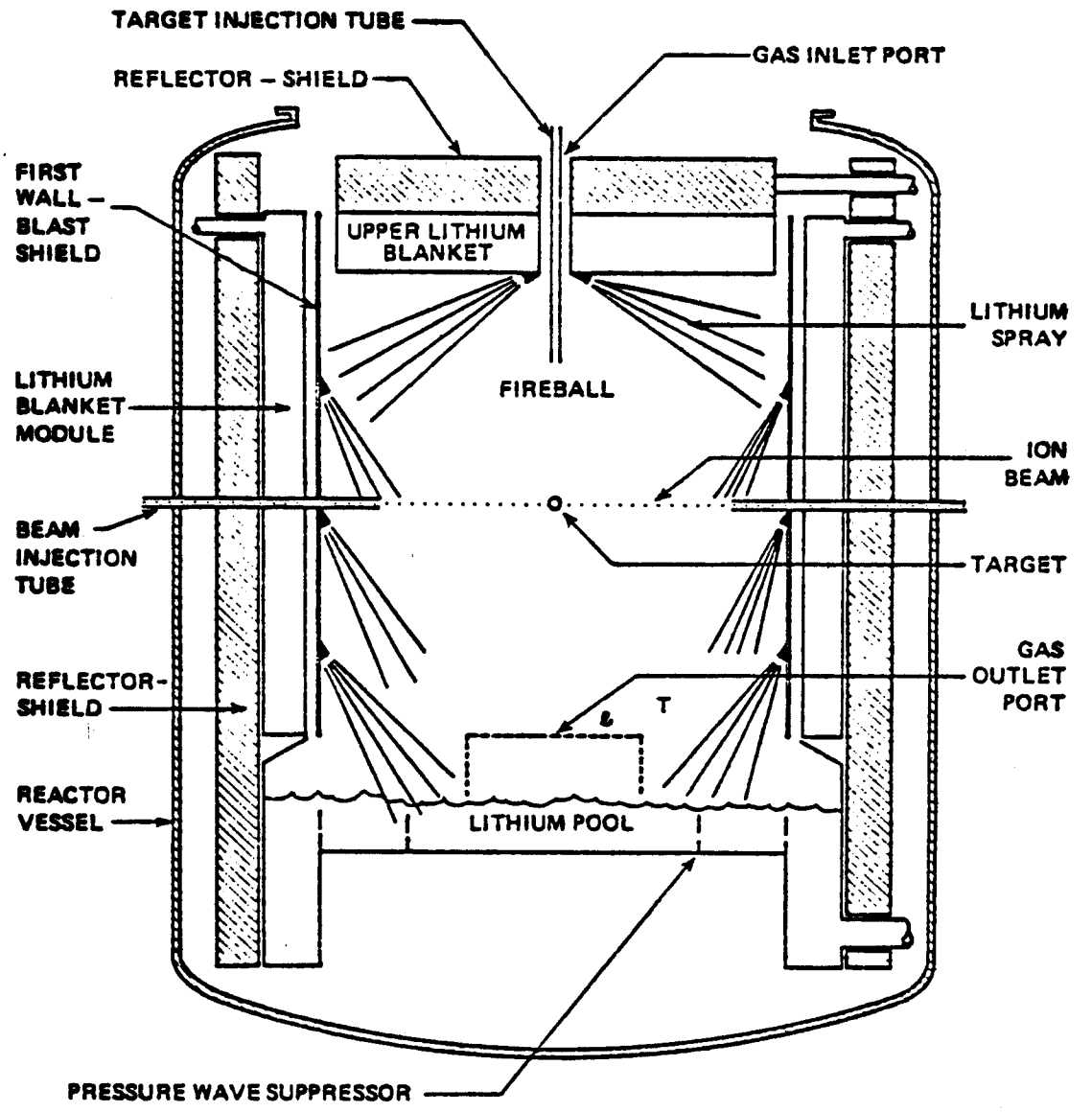

Fig. 1.8 · Schematic of EAGLE reactor cavity and blanket.

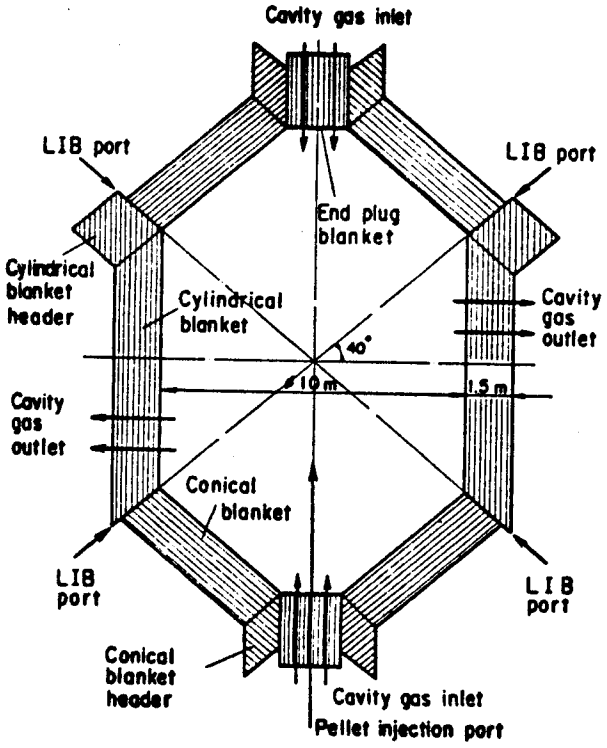

Configuration of cavity and blanket

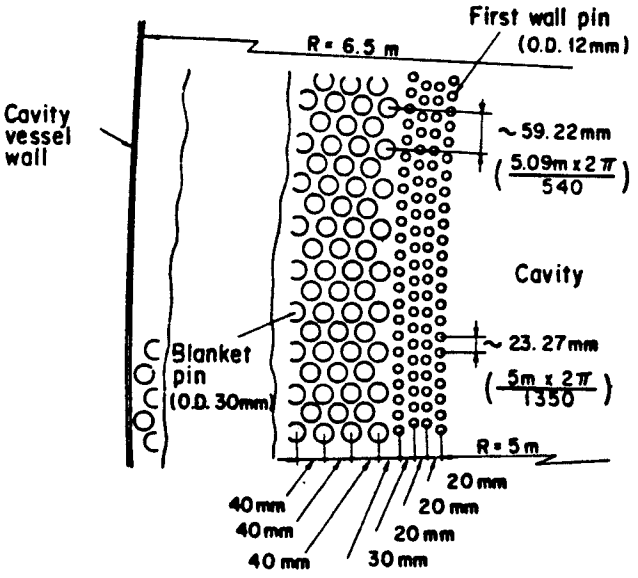

Arrangement of pins in cylindrical blanket

Fig. 1.9 Schematic of UTLIF reactor cavity and blanket.

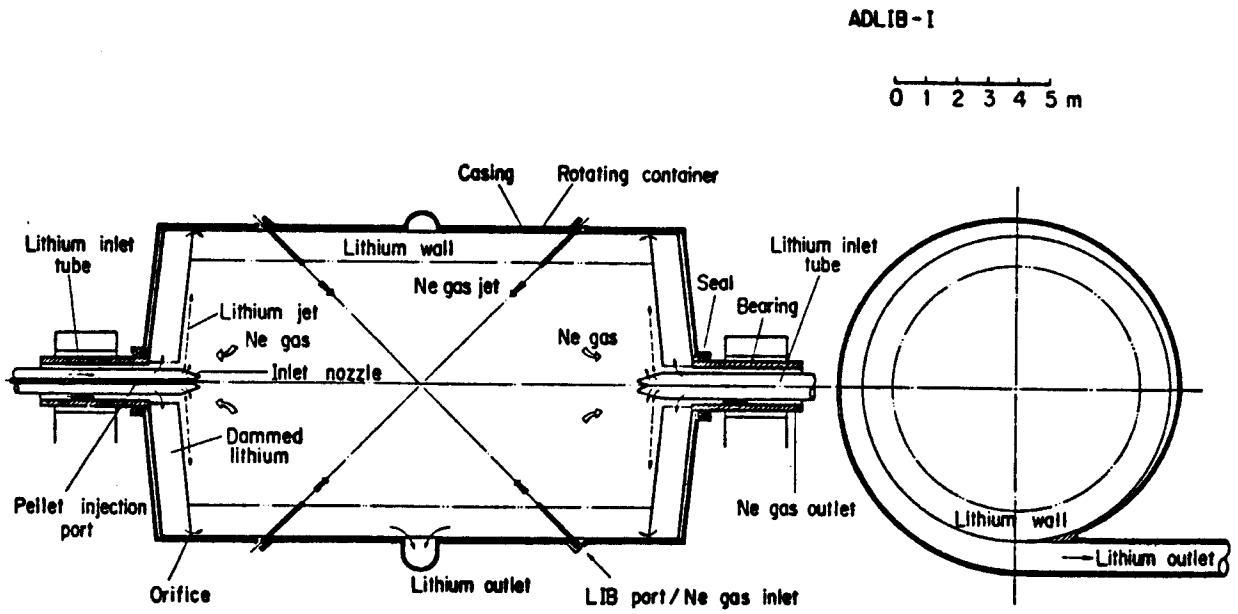

Fig. 1.10 Schematic of ADLIB reactor cavity and blanket.

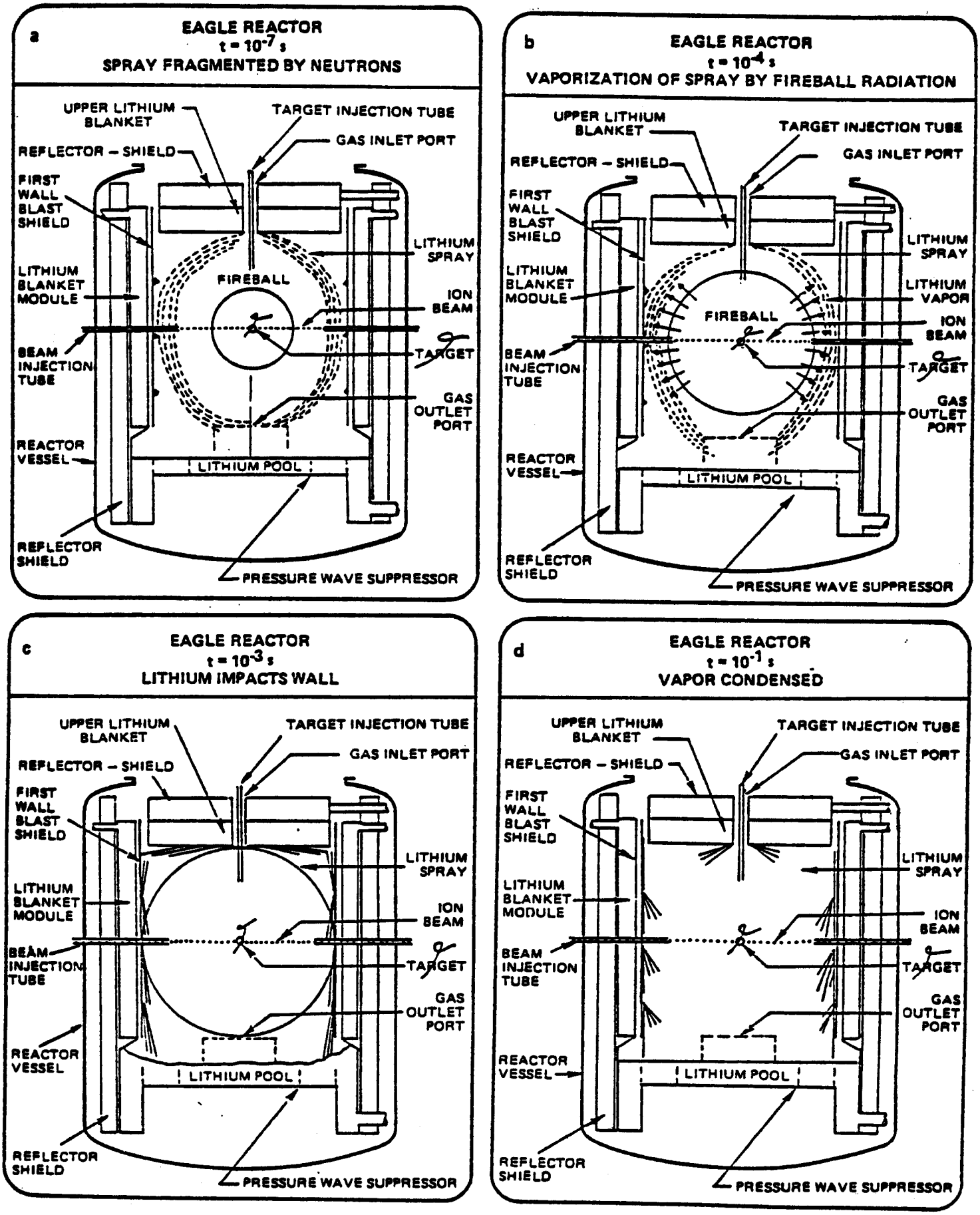

Fig. 1.11 Phenomenology of EAGLE reactor cavity following a target explosion.

behind these tubes so that the nominal flow is along a path that comes in the top and bottom of the cavity and out the sides. Neutron energy deposition is in the lithium coolant flowing within the tubes. This is very much along the lines of the HIBALL INPORT units only the tubes are metallic, V-20Ti, and are not porous.

The UTLIF design in Fig. 1.10 uses a horizontal rotating drum to hold liquid lithium against its inner wall by centrifugal force. The cavity itself is filled with Ne gas seeded with lithium.

These four studies represent the state-of-the-art in light ion fusion reactor design. They show a wide range of possible cavity configurations. Some of the designs use specific parameters that we feel are inconsistent with the current understanding of target performance and cavity gas dynamics and we believe that the LIBRA design is more in line with the state-of-the-art in these areas. None of the designs represent a level of effort that is comparable to the HIBALL design. In fact, all of these designs are less than one-half of the HIBALL effort. This gives us great motivation to perform the LIBRA design for we feel that it will still represent the best design to date when it is completed.

2. Light Ion Beam Fusion Reactor (LIBRA) Definition

A bilateral decision was made in June 1982 at a joint UW-KfK meeting in Karlsruhe that the LIBRA reactor would be a demonstration reactor. In the path to commercialization a demonstration reactor serves the role of proving all required technology but not necessarily in an economic fashion. This is shown in Table 2.1. With this decision as guidance, the basic features shown in Table 2.2 were chosen for the LIBRA reactor. We will assume technology levels extrapolated to the 2010 time frame for the demonstration reactor. Under current ICF funding in the U.S., and certainly for FRG, this implies an accelerated program over the current funding levels. The power level will be approximately 500 MW_{th} which should provide ~ 150 MW_e if the driver system is 20% efficient. At this level, full scale power handling equipment will be used in the reactor. Furthermore, this will allow us to investigate the potential attractiveness of LIBF as a basis for "small reactors" in the hundreds of megawatt range. We will look at only electricity production and will leave hybrid and synthetic fuel production studies for future analysis. This of course places a greater pressure on the economic performance of the reactor. The conventional multimodule pulsed-power/diode driver system has been tentatively chosen for LIBRA. Because in the current situation there is no provision for the detailed design of this driver, the cavity design will be performed in a way that is hopefully generic to the specific form that the driver eventually takes. The ion type is Li^{+1} at an energy of greater than 20 MeV. Diode scaling indicates that heavier ions accelerated to higher voltage have better focusing or brightness than protons. Lithium diodes are under active investigation today although the results of these studies are very prelimi-

TABLE 2.1

Path to Commercialization

Reactor Type	Description
10th of a kind commercial reactor	Fully commercial, economy of scale, proven technology, mature industry.
1st of a kind commercial reactor	Fully commercial, not yet an economy of scale, proven technology, immature industry.
Demonstration reactor	Not necessarily commercial, designed to prove technology needed for commercialization.
Prototype reactor	Basic features are same as for commercial applications but some non-commercializable technology may be included.
Experimental reactor	Testing of basic engineering concepts. The first real non-physics experiment.
Physics experiments	

TABLE 2.2

Basic Features of the LIBRA Demonstration Reactor

Feature	Description
Reactor type	Demonstration reactor
Technology time frame	2010
Power level	~ 500 MW_{th} (150 MW_e)
Fusion product	Electricity (rather than fissile fuel, synthetic fuel, etc.)
Driver approach	Look first at conventional pulsed-power diode
Type of ion	~ 20 MeV Li^{+1}
Target type	Single shell cryogenic
Illumination uniformity	Axisymmetric or clustered
Target gain	60-80
Energy on target	4-8 MJ
Repetition rate	1-2 Hz
Number of cavities	1
Beam transmission mode	Preformed plasma channels
Cavity gas	Argon or neon with lithium doping
Cavity gas pressure	~ 1-20 torr
First wall	INPORT units, possibly modified
Blanket breeding/cooling material	$Pb_{83}Li_{17}$
Shield	Water swimming pool
Power cycle	Double wall heat exchanger, no intermediate loop
Cost goal	< $1,000,000,000

nary. The target type is a single shell with a cryogenic layer of DT. Recently, there has been serious doubt raised that high performance double shell targets with a central ignitor will perform as previously calculated. Such targets have been abandoned by target designers at LLNL and we have chosen to take this direction in the definition of the LIBRA target. Single shell targets have the added complication of requiring driver power pulse shaping. The illumination arrangement will be axisymmetric as in the HIBALL design or clustered as in HYLIFE, depending on the type of channel and target that is used. The energy on target and target gain are "conservatively" in the ranges of 4-8 MJ and 60-80 respectively. This is far less than the maximum theoretical gain but best represents today's understanding of target performance. The considerations leading to this reduction in gain from the maximum possible are not particularly sensitive to the passage of time and the resultant greater understanding of target dynamics. These so-called conservative figures are likely to be the best that can be expected. With 250-500 MJ per shot, the shot repetition rate need only be 1-2 Hz in one cavity to produce the specified 500 MW_{th}. Beam propagation will be from multi-diodes into plasma channels to the target. Two types of plasma channels will be investigated; (1) many small diameter channels, one per diode, and (2) few large diameter channels, possibly one for several diodes. In the first case the diodes will be arranged axisymmetrically. In the second case the diodes will be clustered and a sophisticated focusing structure must surround the target. Preformed channels require a background gas in the cavity and this will be argon or neon doped with trace amounts of lithium at a pressure of 1-20 torr depending on the detailed dynamics of the plasma channel formation. The first wall will be protected from neutron damage by INPORT-like structures. The

exact design of these structures is yet to be determined. The breeder/coolant will be liquid $Pb_{83}Li_{17}$ and the power cycle will include double wall heat exchangers with no intermediate loop. A novel swimming pool-type water shield will be investigated for LIBRA. Finally, the cost goal is not driven by commercial considerations since this is a demonstration reactor. However, it is driven by the practical consideration of the maximum amount of money that is likely to be spent on a high risk system such as this. We place a goal of $1,000,000,000 as the maximum cost of LIBRA.

3. Parameter List for LIBRA

Just as in the HIBALL study we have started LIBRA by assembling a parameter list that includes as many important parameters about the system as we can identify. This list is given in Table 3.1. At this time the list is very sparcely filled. Many of these parameters are best guesses and will be firmed up as the full scale design proceeds.

TABLE 3.1

LIBRA PARAMETER LISTING #1

I. GENERAL PARAMETERS

	10/13/82	DATE	DATE	DATE
Average DT power - 17.6 MeV/fusion (MW)	480			
Target power (MW)	475.2			
Target multiplication	0.99			
Target yield (MJ)	320			
Ion type	Li^+			
Ion energy (MeV)	21			
Ion beam pulse energy (MJ)	4			
Target gain	80			
Overall accelerator efficiency (%)	20			
Fusion gain nG	16			
Blanket multiplication	1.4			
Total nuclear thermal power (MW)	612			
Gross power	612			
Net thermal efficiency (%)	40			
Gross electrical output (MW)	245			
Recirculating power fraction	0.12			
Net electrical output (MW)	215			
Chamber repetition rate (Hz)	1.5			
Chamber geometry	cylindrical			
Chamber diameter (m)	10			
Chamber height (m) (at vacuum wall)	10			
Chamber material	HT-9/SiC			
# of beam ports	60			
ion diodes	40			
return paths	20			
Breeding material	$Pb_{83}Li_{17}$			
Tritium breeding ratio	1.1			
Chamber gas	Ar+0.002 Li			
Chamber gas pressure (torr)	10			
Neutron wall loading (MW/m^2)	1.09			

II. TARGET PARAMETERS

	10/13/82	DATE	DATE	DATE
Composition				
D (mg)	1.28			
T (mg)	1.92			
DT load (mg)	3.2			
Material #1 (mg) - PbLi	53.68			
Material #2 (mg) - Pb	230.4			
Burnup (%)	30			
Total mass (mg)	287.28			
Configuration (# of shells)	1			
Target diameter (cm)	0.6			
Absorbed ion energy (MJ)	4			
DT yield (MJ)	320			
Target yield (MJ)	316.8			
Target energy multiplication	0.99			
Target gain	80			
Average DT power (MW)	480			
Target power (MW)	475.2			
Neutron yield (MJ)	227.84			
Ave. neutron energy (MeV)	11.98			
Neutron multiplication	1.046			
Fraction of yield in neutrons	0.72			
Gamma yield (MJ)	0.48			
Ave. gamma energy (MeV)	1.53			
Fraction of yield in gammas	0.0015			
X-ray yield (MJ)	71.6			
X-ray spectrum - blackbody (keV)	1			
Fraction of yield in X-rays	0.23			
Debris yield (MJ)	16.8			

	10/13/82	DATE	DATE	DATE
Debris spectrum (keV/amu)	0.6			
Fraction of yield in debris	0.05			
Radioactivity production (Ci/target @ t = 0)				
Target injection velocity (m/s)				
Max. DT temperature (K)	12			
Target injector type	gas gun			
Target tracking				
Target cost				

III. TARGET MANUFACTURE AND DELIVERY PARAMETERS

	DATE	DATE	DATE	DATE
Target manufacture				
Production rate (#/s)				
Material stored within target factory (kg)				
Deuterium				
Tritium				
Material #1				
Material #2				
Cost/target (cents)				
Target storage				
# of targets in storage				
Average target storage time (hr)				
Target delivery				
Longitudinal positioning tolerance (mm)				
Lateral positioning tolerance (mm)				
Target velocity (m/s)				
Repetition frequency (Hz)				
Injection:				
Type				
Projectile (sabot+target) mass (g)				
Propellant gas amount (torr liters/shot)				
Propellant gas				
Total prop. gas handled (mg/shot)				
Buffer cavity pressure, min. (Torr)				
max. (Torr)				
Buffer cavity volume (m^3)				

	DATE	DATE	DATE	DATE
Injection channel diameter (mm)				
Prop. gas entering reactor cavity (mg/shot)				
Gas gun total efficiency				
Gun barrel diameter (mm)				
Pressure of prop. gas reservior (bar)				
Acceleration distance (m)				
Acceleration (m/s^2)				
Acceleration time (ms)				
Total target travel time (ms)				
Tolerance on total travel time (ms)				
Distance muzzle to focus (m)				
Tracking:				
Lateral tracking				
Longitudinal tracking, type				
Tracking position 1, distance from focus (m)				
Tracking position 2, distance from focus (m)				
Light beam diameter (mm)				
Precision of arrival time prediction (μs)				
Duration of processing tracking results (ms)				

IV. DRIVER PARAMETERS

	DATE	DATE	DATE	DATE
Ion				
Type				
Charge state				
Energy (MeV)				
Velocity (m/s)				
Beta, $\beta = v/c$				
Gamma, $\gamma = (1 - \beta^2)^{-1/2}$				
Mass number (amu)				
Accelerator - general				
Type				
Efficiency				
Number of modules				
Number of stores/module				
Number of return current paths				
Outer radius of oil section (m)				
Inner radius of oil section (m)				
Outer radius of water section (m)				
Inner radius of water section (m)				
Radius of water-vacuum interface (m)				
Radius of diodes (m)				
Energy in primary store (MJ)				
Energy at diodes (EM) (MJ)				
Power at diodes (EM) (TW)				
Voltage across diodes (MV)				
Impedance (ohms)				
Marx Banks				
Number				
Volume (m^3)				

	DATE	DATE	DATE	DATE
Energy density (MJ/m^3)				
Charge time (s)				
Discharge time (s)				
Charging voltage (MV)				
Discharging voltage (MV)				
Dielectric				
Intermediate Storage Capacitors				
Number				
Length (m)				
Diameter (m)				
Gap (m)				
Material				
Charging time (μs)				
Discharging time (μs)				
Switch type				
Dielectric				
Voltage (MV)				
Pulse Forming Lines				
Number				
Length (m)				
Height (m)				
Width (m)				
Gap width (m)				
Geometry				
Material				
Switch type				
Dielectric				
Charging time (ns)				
Discharging time (ns)				
Voltage (MV)				
Water-vacuum interface				
Insulating material				

	DATE	DATE	DATE	DATE
Area (m^2)				
Distance to target (m)				
Radiation dose - peak (rad)				
average (rad)				
Voltage (MV)				
Magnetic insulated transmission lines				
Number				
Length (m)				
Vacuum gap (cm)				
Height (cm)				
Width (cm)				
Material				
Voltage (MV)				
Diodes				
Type				
Gap width (cm)				
Radius (cm)				
Source				
Source area (cm^2)				
Voltage drop (MV)				
Voltage ramp				
Total current (MA)				
Ion current (MA)				
Impedance (ohms)				
Material				
Brightness ($TW/cm^2/ster$)				
Focal spot size (cm^2)				
Divergence half-angle (degrees)				
Pressure pump down time (ms)				
Laser triggered switches				
Number				
Gas type				

	DATE	DATE	DATE	DATE
Gas pressure (torr)				
Gas flow rate (torr-ℓ/s)				
Jitter (ns)				
Pulse rise time (ns)				
Laser power (W)				
Laser type				
Diode Protection				
Shutter speed (rev/s)				
Aperture diameter (cm)				
Pump down time (ms)				
ΔP (MPa)				

V. CHANNEL LASER SYSTEM PARAMETERS

	DATE	DATE	DATE	DATE
Laser type				
Wavelength (μm)				
Laser beam diameter (cm)				
Intensity (W/cm^2)				
Pulse energy/channel (J)				
Total energy in laser beams (J)				
Laser efficiency				
Energy to drive lasers (J)				
Ionization/excitation mechanism				
Energy hitting target (J)				

VI. PREFORMED PLASMA CHANNEL PARAMETERS

	DATE	DATE	DATE	DATE
Number of ion channels				
Number of return current channels				
Channel length (m)				
Channel diameter (cm)				
Cavity gas density before discharge (cm^{-3})				
Cavity gas temperature before discharge (eV)				
Channel density				
g/cm^3				
$\#/cm^3$				
Channel temperature (eV)				
Before ion beam				
After ion beam				
Discharge current (kA)				
Discharge current density (kA/cm^2)				
Discharge rise time (μs)				
Energy in capicitor banks (MJ)				
Circuit inductance (μH)				
Magnetic field strength (T)				
Ion cyclotron freq. (s^{-1})				

VII. ION BEAM PARAMETERS

	DATE	DATE	DATE	DATE
Ion type				
Ion charge state				
Ion energy (MeV)				
At channel entrance				
At channel exit				
Energy/Channel (MJ)				
At channel entrance				
At channel exit				
Average power/channel (TW)				
At channel entrance				
At channel exit				
Peak power/channel (TW)				
At channel entrance				
At channel exit				
Beam current/channel (MA)				
At channel entrance				
At channel exit				
Pulse bunching factor				
Energy loss in channel (MJ)				
Total beam energy (MJ)				
At channel entrance				
At channel exit				
Total average beam power (TW)				
At channel entrance				
At channel exit				
Total average beam power (TW)				
At channel entrance				
At channel exit				

	DATE	DATE	DATE	DATE
Beam overlap radius (cm)				
Overlap efficiency				
Energy on target (MJ)				
Average power on target (TW)				
Peak power on target (TW)				
Beam divergence half-angle (degrees)				
At channel entrance				
At channel exit				
Beam brightness ($TW/cm^2/ster$)				
At channel entrance				
At channel exit				
Focal spot size (cm)				
At channel entrance				
At channel exit				

VIII. "CAVITY" REGION PARAMETERS

	10/13/82	DATE	DATE	DATE
Coolant and breeding material				
Li-6 enrichment, %				
Tube Region				
Inport tube structural material and v/o				
Inport tube coolant v/o				
Tube region support structure v/o				
First surface radius (m)				
Region thickness (m)				
Region density factor				
Effective coolant thickness (m)				
Mass of coolant in tubes (tonnes)				
Tubes				
Length (m)				
Diameter (cm)				
First two rows				
Wall thickness (mm)				
Remainder				
Wall thickness (mm)				
Number				
First two rows				
Remainder				
Number of penetrations in region				
Total area of beam penetrations at first surface (m^2)				
Cavity gas				
Type	Ar+0.2% Li			
Pressure @ 0°C (torr)	10			

	10/13/82 DATE	DATE	DATE
Density (g/cm^3)	2.36×10^{-5}		
($\#/cm^3$)	3.55×10^{17}		
Temperature (eV)	0.07		
(K)	800		
Pressure at op. temp. (torr)	30		
Flow rate (kg/s)			
(torr-ℓ/s)			
Speed (m/s)			
Outlet			
At channel			
Eqm. radioactivity (Ci)			
Cavity Gas			
Target			
Fireball			
Initial size (cm)	50		
Initial temperature (eV)	100		
Initial energy (MJ)	89		
Max. heat flux on first surface (kW/cm^2)	680		
Total energy flux on first surface (J/cm^2)	18.6		
Arrival time of max. heat flux (ms)	7.3×10^{-5}		
Max. overpressure on first surface (MPa)	0.2		
Arrival time of max. overpressure (ms)	1.1		
Duration of pressure pulse (ms)	0.5		
Cool down time of cavity gas (s)			
Time between shots (s)	0.67		
Chamber top			
Structural material and v/o			
Coolant v/o			
Height at chamber centerline (m)			

	DATE	DATE	DATE	DATE
Region thickness (m)				
Mass of coolant in cavity top (tonnes)				
Number of penetrations in top region				
Total area of penetrations at chamber inner surface (m^2)				
Chamber bottom pool				
Structural material and v/o				
Coolant v/o				
Height at chamber centerline (m)				
Region thickness (m)				
Mass of coolant in bottom pool (tonnes)				
Maximum 1st surface neutron energy current - at chamber midplane (MW/m^2)				
Neutrons passing through each beam line penetration per shot				
DT power (MW)				
Total n & γ power in cavity (MW)				
Tube region				
Cavity top				
Cavity bottom				
Total power in cavity, including X-rays and debris (MW)				
Energy multiplication[1]				
n & γ energy multiplication[2]				
Average power density (W/cm^3)				
Tube region				
neutron				

[1]Total energy deposited in region/DT yield

[2]Total n & γ energy deposited in region/n & γ energy incident on 1st surface.

	DATE	DATE	DATE	DATE
gamma				
Top region				
neutron				
gamma				
Bottom region				
neutron				
gamma				
Peak/average spatial power density in tube region				
Impulse on first row of tubes (dyne-s/cm^2)				
Amount of coolant blown off per shot (kg)				
Maximum dpa/FPY				
Tube region				
Top region				
Bottom region				
Maximum H production (appm/FPY)				
Tube region				
Top region				
Bottom region				
Maximum He production (appm/FPY)				
Tube region				
Top region				
Bottom region				
Maximum SiC burnup (appm/FPY)				
Tube region				
Top region				
Bottom region				
Tritium breeding ratio				
^6Li				
Tube region				

	DATE	DATE	DATE	DATE
Top region				
Bottom region				
^{7}Li				
Tube region				
Top region				
Bottom region				
Coolant				
Inlet temperature (°C)				
Outlet temperature (°C)				
Flow rate (kg/hr)				
Maximum velocity within tubes in first two rows (m/s)				
Maximum velocity within tubes not in the first two rows (m/s)				
Pressure (MPa)				
ΔP for entire loop (MPa)				
Pumping power delivered to coolant (MW)				

IX. "NON-CAVITY" REGION PARAMETERS

	DATE	DATE	DATE	DATE
A. Vacuum Boundary Wall				
Structural material				
Side wall				
Inside diameter (m)				
Thickness (m)				
Height (m)				
Top liner				
Height above midplane (m)				
at centerline				
at side wall				
Thickness				
Maximum neutron wall loading (MW/m^2)				
- side wall at midplane				
Average power density (W/cm^3)				
Side wall				
neutron				
gamma				
Top liner				
neutron				
gamma				
n & γ energy multiplication				
Power deposited in vacuum wall (MW)				
Side wall				
Top liner				
Maximum dpa/FPY				
Side wall				
Top liner				

	DATE	DATE	DATE	DATE
Peak instantaneous dpa rate (dpa/s)				
- side wall at midplane				
Maximum H production (appm/FPY)				
Side wall				
Top liner				
Maximum He production (appm/FPY)				
Side wall				
Top liner				
Peak instantaneous He production rate				
(appm/s) - side wall at midplane				
Maximum temperature (°C)				
Expected lifetime (FPY)				
Radioactivity at shutdown (Ci)				
B. Reflector				
Structural material				
Coolant				
Side reflector				
Inside diameter (m)				
Thickness (m)				
Mass of structure (tonnes)				
Mass of coolant (tonnes)				
v/o of structure				
v/o of coolant				
Top reflector				
Thickness (m)				
Mass of structure (tonnes)				
Mass of coolant (tonnes)				
v/o of structure				
v/o of coolant				
Bottom of reflector (splash plate)				
Thickness (m)				
Mass of structure (tonnes)				

	DATE	DATE	DATE	DATE
Mass of coolant (tonnes)				
v/o of structure				
v/o of coolant				
Total mass of structural material in reflector (tonnes)				
Total mass of coolant in reflector (tonnes)				
n & γ energy multiplication				
Average power density (W/cm^3)				
Side reflector				
neutron				
gamma				
Top reflector				
neutron				
gamma				
Bottom reflector (splash plate)				
neutron				
gamma				
Peak/average spatial power density - in side reflector				
Power deposited in reflector (MW)				
Side				
Top				
Bottom				
Maximum DPA/FPY				
Side reflector				
Top reflector				
Bottom reflector				
Maximum H production in structural material (appm/FPY)				
Side reflector				
Top reflector				

	DATE	DATE	DATE	DATE
Bottom reflector				
Maximum He production in structural material (appm/FPY)				
Side reflector				
Top reflector				
Bottom reflector				
Tritium breeding ratio				
^{6}Li				
Side				
Top				
Bottom				
^{7}Li				
Side				
Top				
Bottom				
Coolant				
Mass of coolant within reflector (tonnes)				
Flow rate (kg/hr)				
Inlet temperature (°C)				
Outlet temperature (°C)				
Maximum coolant velocity (m/s)				
Pressure (MPa)				
ΔP for entire loop (MPa)				
Pumping power delivered to coolant (MW)				
Maximum structure temperature (°C)				
C. Shield				
Structural material and v/o				
Coolant and v/o				
Side shield				
Inside diameter (m)				
Thickness (m)				

	DATE	DATE	DATE	DATE
Top shield				
Height above midplane at centerline (m)				
Thickness (m)				
Bottom shield				
Height below midplane (m)				
Thickness (m)				
Maximum power density at midplane (W/cm^3)				
Average power density (W/cm^3)				
Power deposited in shield (MW)				
Power deposited in neutron & debris dump per beam line (MW)				
Energy flux at outer surface of shield at midplane (W/cm^2)				
neutron				
gamma				
Dose rate at outer surface of shield at midplane (mrem/hr)				
neutron				
gamma				
Coolant				
Inlet temperature (°C)				
Outlet temperature (°C)				
Flow rate (kg/hr)				
Maximum velocity (m/s)				
Pressure (MPa)				
ΔP in entire loop (MPa)				
Pumping power delivered to coolant (MW)				
Peak structure temperature (°C)				

X. BALANCE OF PLANT

	DATE	DATE	DATE	DATE
Steam temperature (°C)				
Steam pressure (MPa)				
Steam flow rate (kg/hr)				
Feedwater temperature (°C)				
Reheat temperature (°C)				
Steam generator surface area (m^2)				

XI. SYSTEM PARAMETERS

	DATE	DATE	DATE	DATE
Average DT power (MW)				
Total power recoverable (MW)				
System energy multiplication				
Total pumping power delivered to coolant (MW)				
Gross power (MW)				
Gross power (MW)				
Gross thermal efficiency (%)				
Gross plant output (MWe)				
Recirculating power (MWe)				
Driver system				
Pulsed power machine				
Channel capacitor banks				
Channel lasers				
Target manufacture and delivery (MW)				
Coolant pumps				
Vacuum pumps				
Plant auxiliaries				
Net plant output (MWe)				
Net plant efficiency (%)				

XII. TRITIUM PARAMETERS (FOR 29% BURNUP)

	DATE	DATE	DATE	DATE
Material inserted per shot				
D - target (mg)				
(# of atoms)				
T - target (mg)				
(# of atoms)				
Li - target (mg)				
(# of atoms)				
Pb - target (mg)				
(# of atoms)				
Li - ion beam (mg)				
(# of atoms)				
Li - INPORT (g)				
(# of atoms)				
Pb - INPORT (g)				
(# of atoms)				
Nonvolatiles (mg)				
(# of atoms)				
Total (mg)				
Total # of atoms				
D_2 (target injector) mg/shot				
# of atoms				
Total D, T, D_2 (mg)				
(# of atoms)				
Fractional burnup, $f_b = T_b/(T_b + T_p)$				
Material pumped per shot				
D - target, unburned (mg)				
(# of atoms)				
T - target, unburned (mg)				

	DATE	DATE	DATE	DATE
(# of atoms)				
D_2 (target injector) - mg/shot				
- # atoms				
T - lost from coolant (mg)				
(# of atoms)				
He-DT fusion reaction (mg)				
(# of atoms)				
He-T decay (mg)				
(# of atoms)				
He-T production (mg)				
(# of atoms)				
He - total (mg)				
(# of atoms)				
Li - ion beam (mg)				
(# of atoms)				
Li - not condensed (mg)				
(# of atoms)				
Pb - not condensed (mg)				
(# of atoms)				
Nonvolatiles (mg)				
(# of atoms)				
Total (D, T, He, D_2 Target inj.)				
Total # of atoms				
# of shots per second				
Total condensibles pump rate (g/s)				
Total noncondensibles pump rate (g/s)				
Cavity pressure (torr @ 0°C)				
Coolant breeding region				
Breeding material				
Flow rate (kg/hr)				
Breeder mass (kg)				
Inlet temperature (°C)				

	DATE	DATE	DATE	DATE
Outlet temperature (°C)				
Breeding ratio				
Steady state tritium concentration (wppm)				
Tritium pressure (torr @ 0°C)				
Extractor				
Inlet temperature (°C)				
Outlet temperature (°C)				
Inlet concentration (wppm)				
Outlet concentration (wppm)				
Extraction method				
Size of extractor				
Mass of breeding material within extractor (kg)				
% of total breeding material within extractor				
Steam generator				
Material composition				
Wall thickness (mm)				
Primary inlet temperature (°C)				
Primary outlet temperature (°C)				
Secondary inlet temperature (°C)				
Secondary outlet temperature (°C)				
Secondary pressure (MPa)				
Surface area (m^2)				
Tritium permeation rate to H_2O (Ci/s)				
Tritum inventory - steady state				
Breeding material				
Reactor chamber - kg				
Reflector - kg				
Cryopumps (2 hr on-line) - kg				
Cryogenic distillation columns (kg)				

	DATE	DATE	DATE	DATE
Fuel cleanup (kg)				
Structural material and piping (kg)				
Steam generator piping (kg)				
Storage - 3 days fuel supply (kg)				
Total (kg)				
Total (Ci)				
Containment				
Total building volume (m^3)				
Volume of reactor & auxiliaries (m^3)				
Cleanup volume (m^3)				
Containment pressure (torr @ 0°C)				
Time for tritium cleanup (hr)				

4. Target Considerations

4.1 Single vs. Double Shell Targets

Two basic target designs have received a great deal of attention during the past few years, particularly in Lawrence Livermore National Laboratory publications. These are the so-called single and double shell targets depicted schematically in Fig. 4.1. (Here we have chosen to display the light ion beam rather than the laser driven variety of these targets.) The single shell target consists of contiguous layers of Pb tamper, PbLi ablator/pusher and DT fuel with an interior void. For high gain this target uses hot spot ignition. In this ignition configuration, only the inner 1% of the fuel mass is raised to ignition temperatures of 4 keV while the surrounding DT fuel is kept cold on a low isentrope. The achievement of this highly nonequilibrium situation requires very careful pulse shaping of the driver power as shown in Fig. 4.1. Shock waves must converge at the center of the DT fuel just as the fuel reaches its highest density. Furthermore, ρR requirements in the bulk DT fuel and the hot spot must correspond to approximately 3 g/cm^2 and 0.5 g/cm^2 respectively for there to be high gain.

In the case of double shell targets this situation is quite different. Here the ignition or "spark plug" fuel is encapsulated in a gold shell in the center of the interior void. Now the pulse need only isentropically compress the bulk fuel, hence the pulse shape is not as critical. The collision of the bulk fuel with the spark plug capsule shock heats and compresses the spark plug fuel along a high isentrope until it burns. The burn wave and resultant shock wave from this spark plug is expected to ignite the surrounding bulk fuel.

Fig. 4.1 Single and double shell target designs.

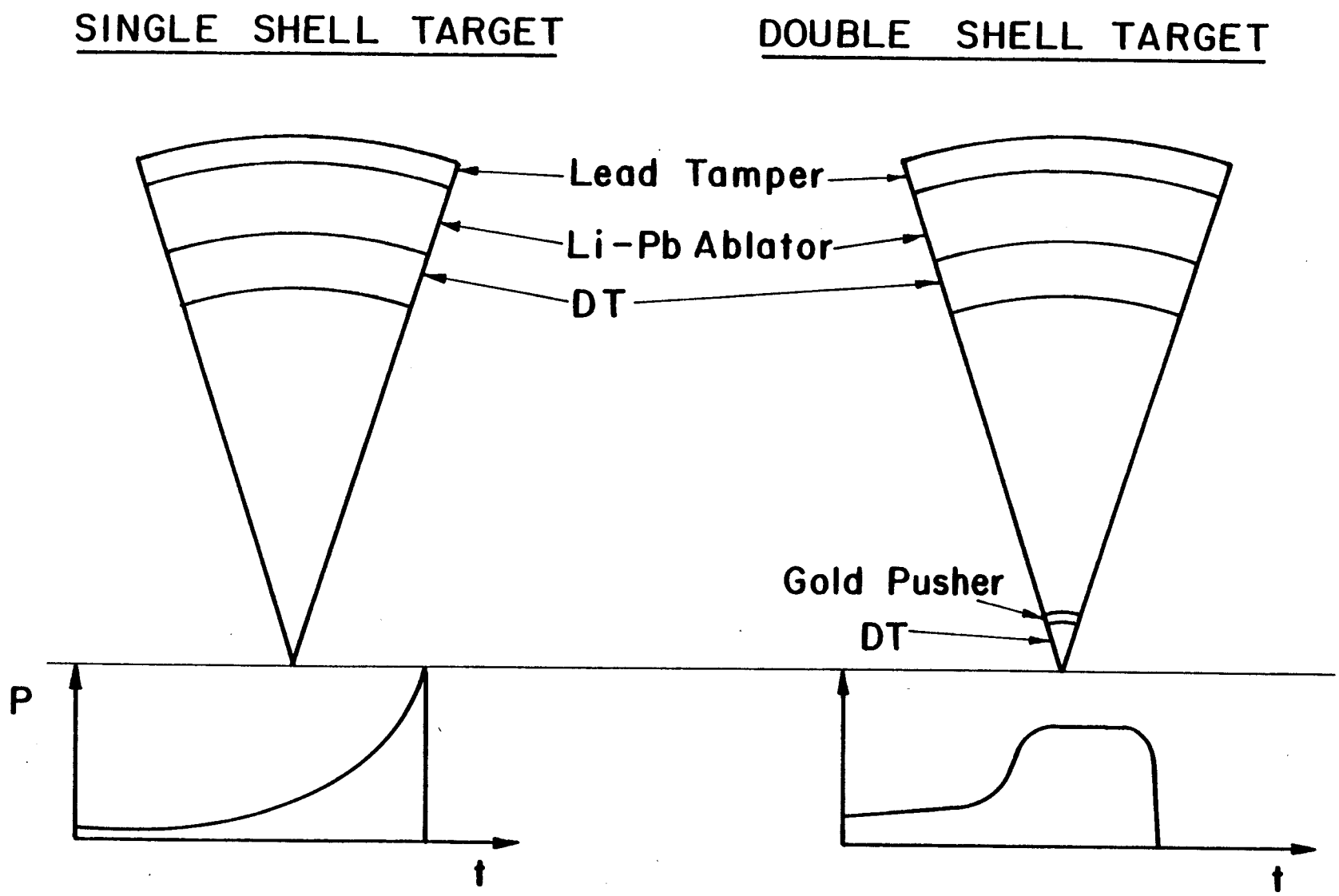

If this target were to work as predicted by optimized one-dimensional hydrodynamics simulations then it would have a considerably higher gain than an equivalent single shell target as shown by the "Ideal" curves in Fig. 4.2. (Note: These gain curves were computed for short wavelength lasers and heavy ions. They do not correspond to scaling for light ions because the short wavelength laser and heavy ion targets used for these scaling studies are not the same as the light ion targets considered in this report. However, the basic features and the differences between single and double shells should carry over to the light ion case.) When the standard factors for non-ideal implosion and burn inefficiencies are applied to each of these gain curves, the double shell target again looks better. This case is made even stronger when one looks at the power requirements predicted for single and double shell targets as shown in Fig. 4.3.

These potential advantages of the double shell target may unfortunately be outweighed by its disadvantages. First of all, it is difficult to fabricate shells that meet the concentricity requirements of the target designers. Also, the support structure for the inner Au shell must be nearly massless to avoid perturbing the implosion symmetry. These are very important practical problems. However, the most serious problem is the question of fluid instabilities when the shells collide. More careful, detailed investigations show that instabilities may lead to contamination of the DT bulk fuel with gold from the inner shell and this will quench the burn of the bulk DT before it can ignite. This is a catastrophic situation since iginition of the bulk fuel is the crux of this design. For these reasons the double shell target has lost much of the promise that it has held during the past few years and target designers are turning back to the single shell target. We have therefore

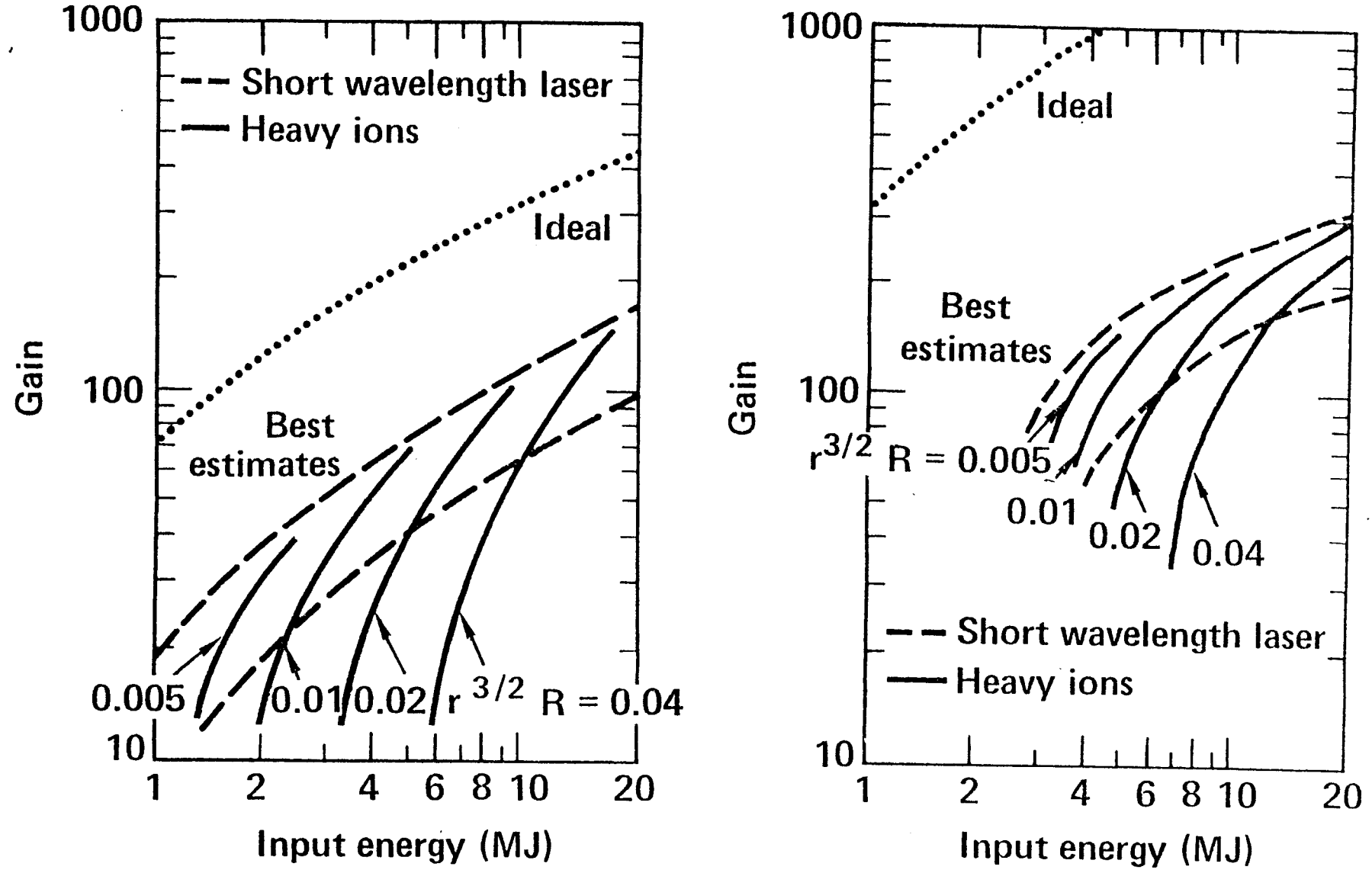

Fig. 4.2 Gain curves for heavy ion beam and short wavelength laser driven double and single shell targets.

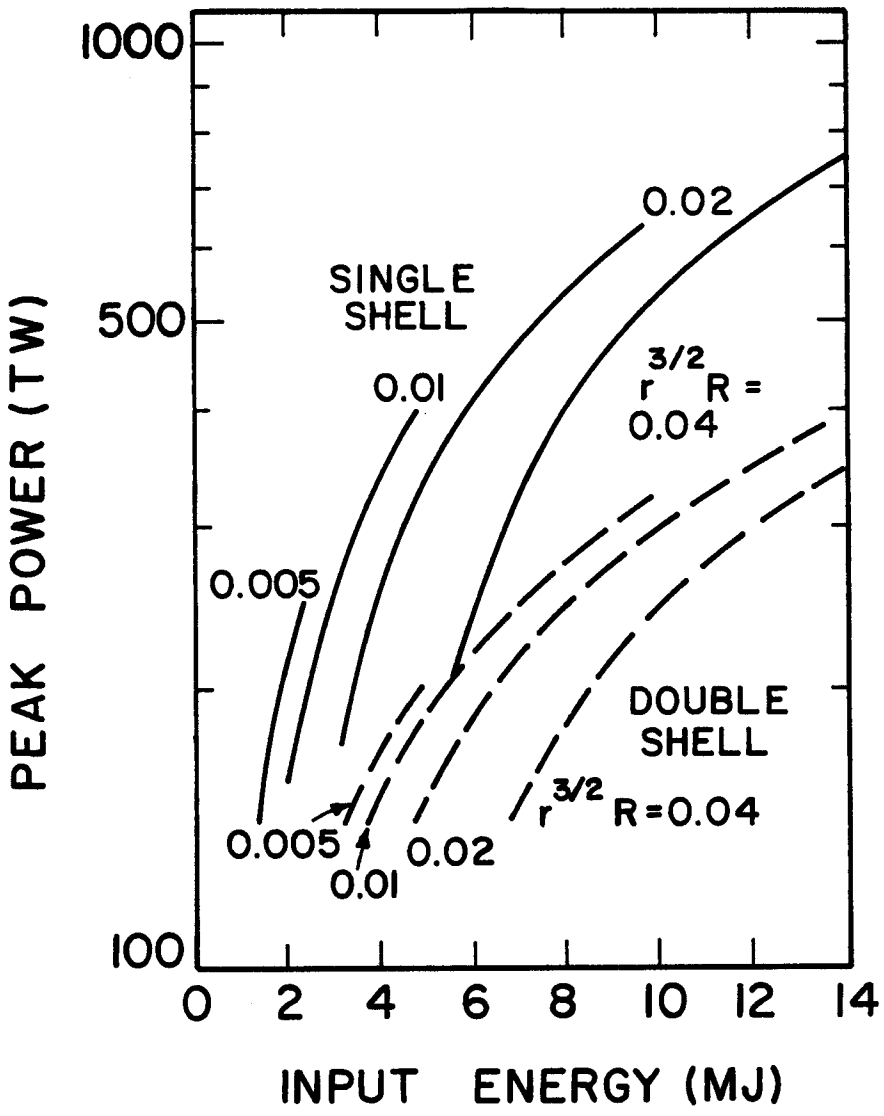

Fig. 4.3 Power requirements for heavy ion beam and short wavelength laser driven double and single shell targets.

chosen the single shell target as the basis for this preliminary LIBRA assessment.

4.2 Preliminary Target Characteristics for LIBRA

Initial proposals for the choice of input energy and target gain presented at KfK in June 1982 by FPA were E_D = 8-12 MJ, G = 60-80. This initial proposal was rejected on the basis that ever-escalating input energy would eventually ruin any prospect for attractive ICF reactors. It was then agreed upon that the LIBRA design should investigate the implication of a more optimistic set of parameters (E_D = 4 MJ, G = 80). Using these more optimistic assumptions we obtain the parameters shown in Table 4.1. The partitioning of the yield into neutrons, x-rays, and debris was derived by scaling the "100 MJ" target design from HIBALL up to 320 MJ by multiplying all masses by 3.2 and assuming the spectra would not change. The neutron, gamma, and x-ray spectra are given in Figs. 4.4, 4.5, and 4.6 respectively. This is not a good assumption in this case and more care must be taken before a final target design is established.

The most serious problem with this target design is the high ion intensity of 280 TW/cm^2 that is required to drive this single shell target. Focusing of ions to this intensity will be a significant challenge.

TABLE 4.1

Preliminary Target Parameters for LIBRA

Parameter	Value
Input energy	4 MJ
Target gain	80
Yield	320 MJ
neutrons	228 MJ
gamma rays	0.48 MJ
x-rays	72. MJ
debris	17 MJ
endothermic	2.52 MJ
DT mass	3.2 mg
Fractional burnup	30%
Power on target	317 TW
Target diameter	0.6 cm
Intensity on target	280 TW/cm^2
Ion type	Li^{+1}
Ion energy	21 MeV
Ion range	50-100 mg/cm^2

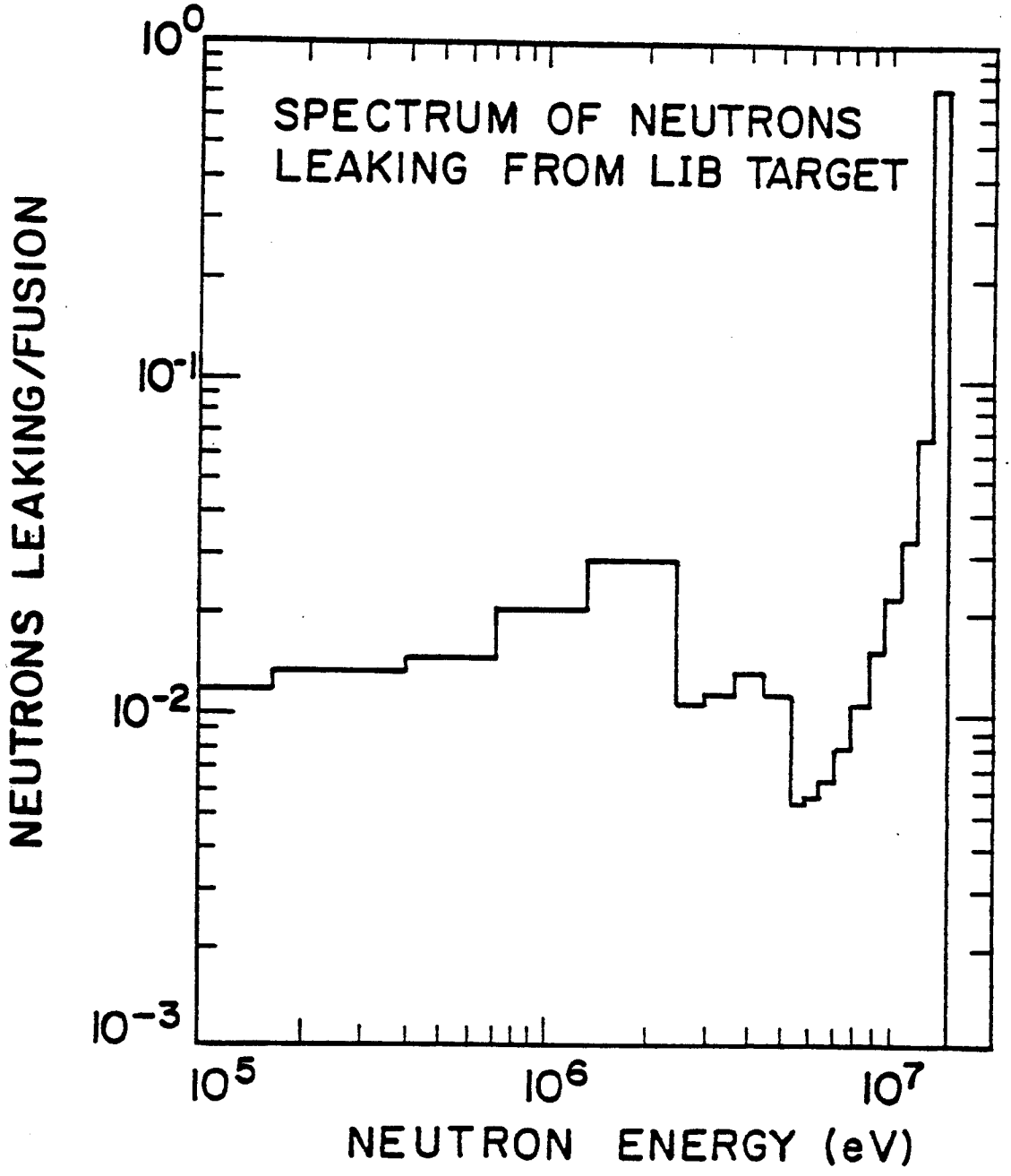

Fig. 4.4 Neutron spectrum for canonical 100 MJ ion beam target.

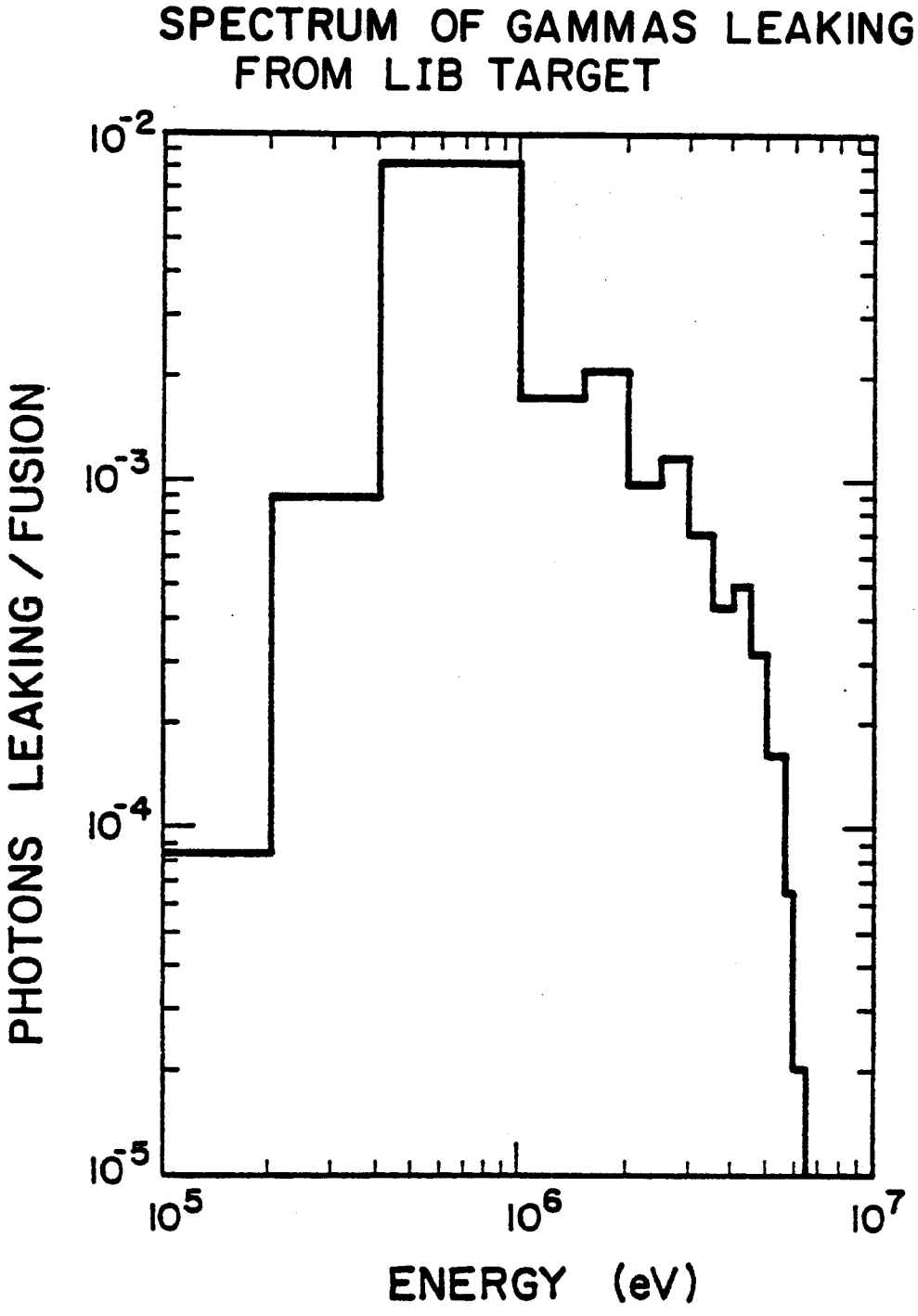

Fig. 4.5 Gamma ray spectrum for canonical 100 MJ ion beam target.

5. Ion Trajectories in Channels

The problems of ion generation, focusing, propagation, and target interaction are critical to the success of light ion beam driven fusion. We have therefore begun the analysis of these systems. The reactor designer's problem is shown schematically in Fig. 5.1. A pulsed power machine delivers an electromagnetic pulse to the diode and this is converted to ion energy with an ion generation efficiency η_{IG}. These ions are then focused through a drift region into the throat of a channel with an efficiency η_{CF}. They propagate through the channel and emerge at the other end with an efficiency η_p. Finally, they are focused onto the target, either passively or actively with an efficiency η_{TF}. The energy on target is therefore given as

$$E_{Target} = E_{EM}\eta_{IG}\eta_{CF}\eta_p\eta_{TF}$$

or more importantly, the required machine energy for a specified energy on target is

$$E_{EM} = E_{Target}(\eta_{IG}\eta_{CF}\eta_p\eta_{T_F})^{-1} .$$

Each of these efficiency factors must be nearly 1 to have a high net efficiency driver. We are hoping for a net driver efficiency of 20%.

We have undertaken the task of calculating each of these efficiency factors. We have reviewed the literature to understand the problems of ion generation in various types of diodes -- although it is unclear at this time whether any of these diodes is suitable for repetitive operation. We have also reviewed and rederived the current and space charge limitations on the

ION GENERATION AND PROPAGATION

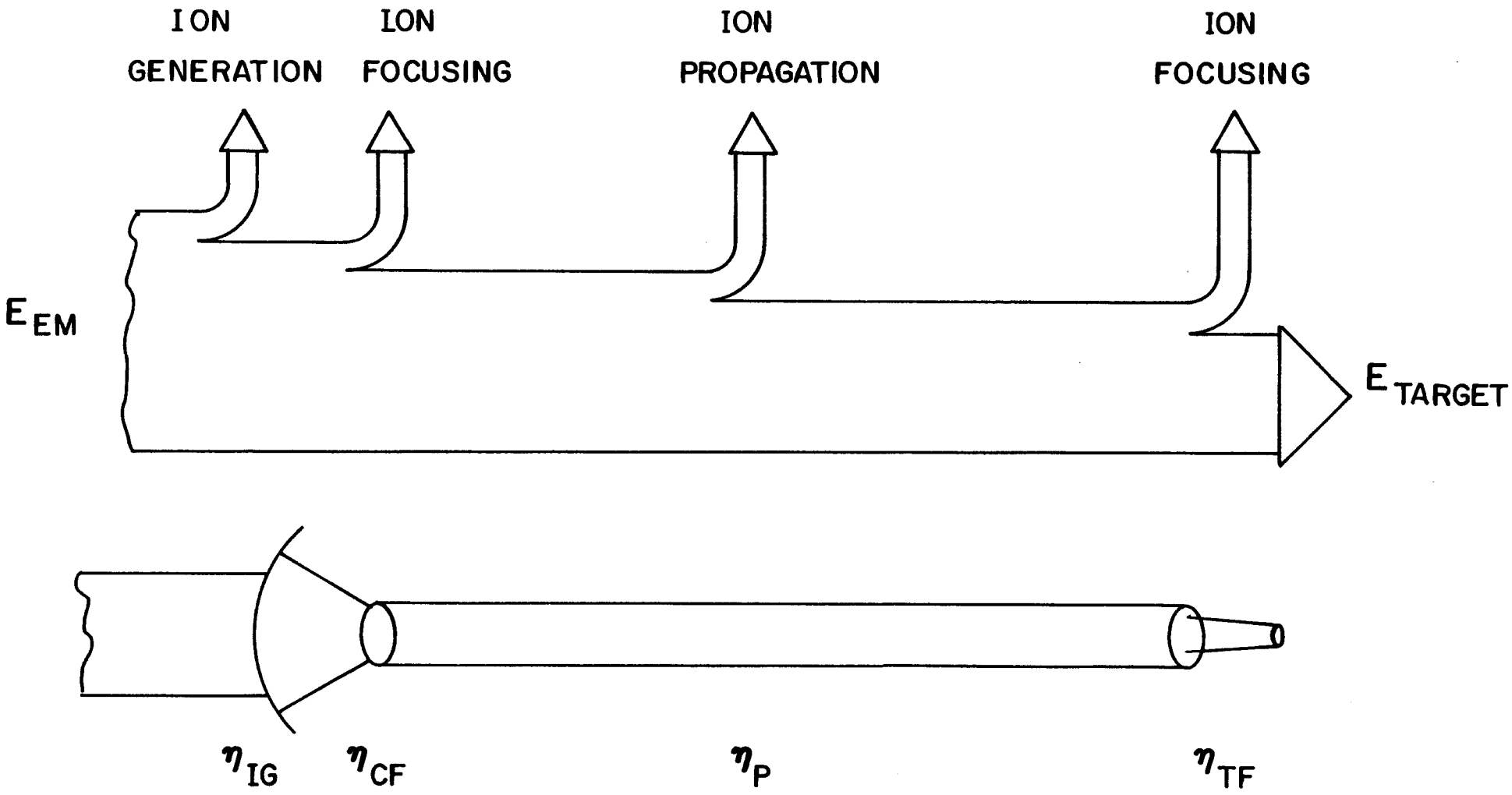

$$E_{TARGET} = E_{EM}\eta_{IG}\ \eta_{CF}\ \eta_{P}\ \eta_{TF}$$

Fig. 5.1 Ion generation, propagation, and focusing efficiencies.

beam in the focusing and drift region of the diode. Space charge neutralization in this focusing region is very important to the propagation of high current beams.

Another important problem associated with ion propagation in plasma channels is the initial creation of the z-pinch channel. Here we intend to modify the MF-FIRE hydrodynamics code by including a one-dimensional magnetic field diffusion equation and external circuit equations to the cylindrical option in the hydro code. This is outlined in Table 5.1. The MF-FIRE code is a one-dimensional lagrangian hydrodynamics code with a multifrequency group radiative transfer option. It uses the flux limited diffusion theory model of energy transfer. To this we will add a magnetic field equation of the form:

$$-\frac{1}{C}\frac{\partial \underline{H}}{\partial t} + \frac{1}{C}\nabla \times \underline{u} \times \underline{H} = \nabla \times \lambda \nabla \times \underline{H}$$

The magnetic field boundary conditions are obtained from the total current flowing in the channel which can be computed from the circuit shown in Fig. 5.2. The magnetic field couples to the equation of motion through a force term and the plasma energy equation is augmented with a resistive heating term. When this code is completed it will allow us to compute the cavity gas characteristics that are necessary for high quality channel formation. We are now just beginning to modify the MF-FIRE code.

We have currently done a significant amount of work in studying ion propagation in plasma channels. A code has been written to follow the trajectories of ions in idealized plasma channels with uniform current and no beam energy loss due to collisions. This code gives us the capability of studying the effects of focusing into the channel on the focusing at the

TABLE 5.1

Changes to MF-FIRE Required to Create a Channel MHD Code

- One-dimensional radiation-magneto-hydrodynamics model of channel
  - One-dimensional lagrangian hydrodynamics
  - One fluid plasma model - artificial viscosity
  - One temperature plasma
  - Multigroup treatment of radiation
  - Tabulated equations of state and multigroup opacities (MIXERG)

  + Magnetic field diffusion equation
  + External circuit equations
  + Magnetic field forces
  + Resistive energy losses in plasma

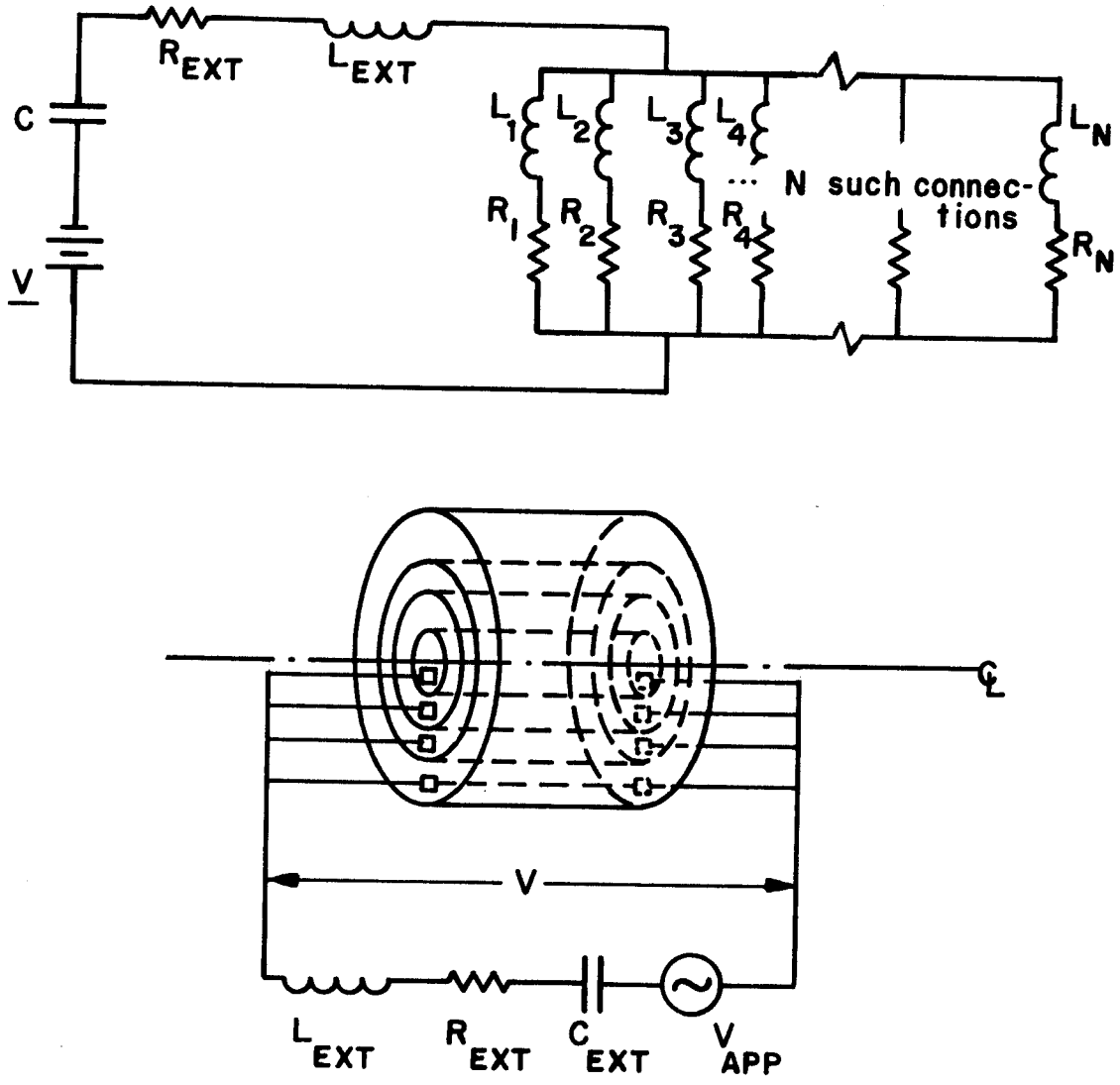

Fig. 5.2 Electrical circuit for channel MHD code.

target. We can also study beam time-of-flight bunching and rippling of the beam due to coherence effects in the ion trajectories. The parameters for a typical calculation are given in Table 5.2. This is what we will call a "small channel" case. Figure 5.3 shows the trajectories of the leading edge of the ion pulse as they leave the entrance to the channel. The ions are distributed in a Gaussian distribution in space over a diameter of 0.5 cm and in a Gaussian distribution in angle with a FWHM of 0.4 radians. The figure clearly shows how some of the ions are immediately lost from the channel due to initial trajectories that could not be turned around by the channel's magnetic field. Figure 5.4 shows this leading edge as it is focused onto the target. Again, there are focusing losses evident from this figure. These calculations can therefore provide us with estimates of η_p and η_{TF} for our net efficiency determination. Figures 5.5 and 5.6 show the spread in the leading edge of the pulse at 40 ns and 250 ns after the ions enter the channel. These are configuration space plots that show the position of each ion at an instant in time. We see that as the leading edge of the pulse reaches the target, there is a significant spread in the arrival time of the ions. The combination of this information and the trajectory information on Fig. 5.4 gives the detailed time-angle-ion energy pulse shape that the target will experience. Such detailed information will eventually be important to the target design exercise.

To compress the ion pulse in time from about 40 ns in length to 13 ns we can use time of flight compression in the channel. This is shown in Fig. 5.7 and 5.8 where the pulse envelope is shown just as the tail leaves the channel entrance and at the target. The factor of 3 pulse compression is obvious. This was achieved by ramping the voltage from 21 MeV at the head of the pulse

TABLE 5.2

Parameters for Preliminary Ion Beam Trajectory Calculations

Focus angular dispersion (HWHM)	0.2 rad
Focus diameter (spot size)	0.5 cm
Channel diameter	1.0 cm
Channel length	600 cm
Target diameter	0.6 cm
Total energy on target	4 MJ
Number of beam channels	50
Return current channels	25
Channel plasma density	$3.55 \times 10^{16}/cm^3$
Initial pulse density	$2.8 \times 10^{14}/cm^3$
Initial pulse length	40 ns
Final pulse length	13 ns
Leading edge ion energy	21 MeV
Trailing edge ion energy	26.6 MeV
Beam temperature	0.2 MeV
Ions	$(Li\text{-}7)^{+3}$
Peak azimuthal magnetic field	40 kG
Beam current/channel	350 kA
Magnetic field current/channel	100 kA

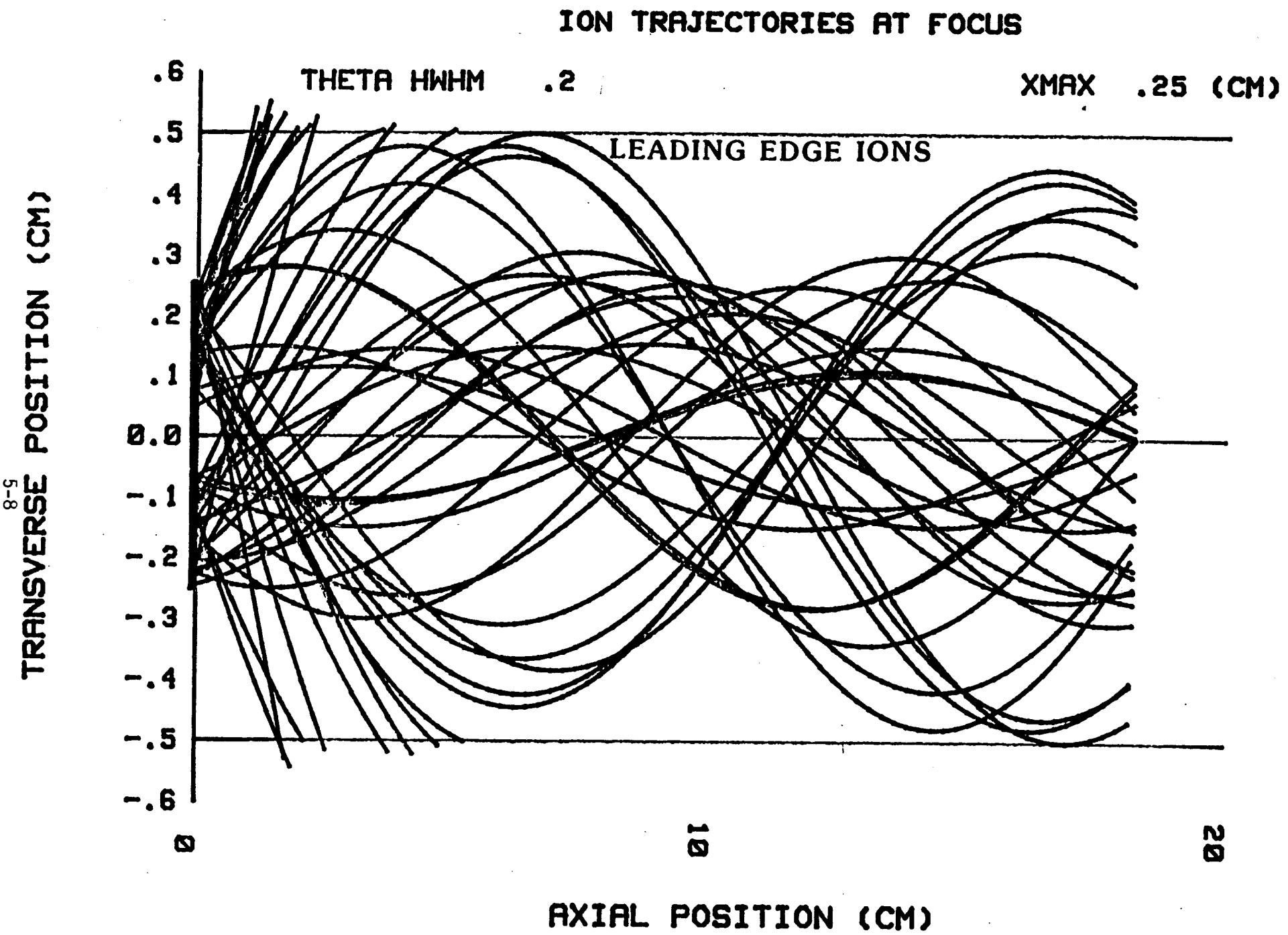

Fig. 5.3 Trajectories of the leading edge of the ion pulse entering the channel.

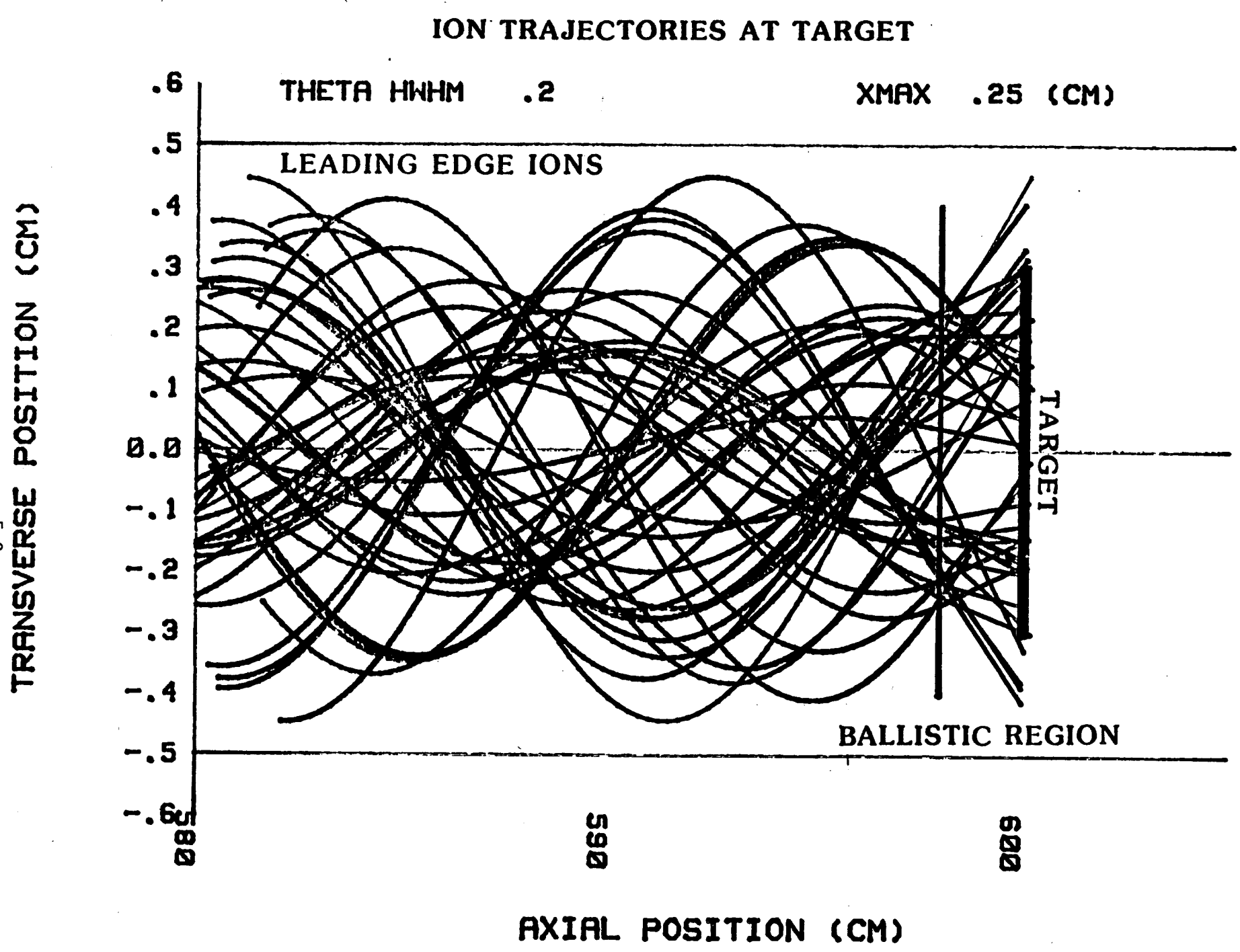

Fig. 5.4 Leading edge of the ion pulse as it is focused onto the target.

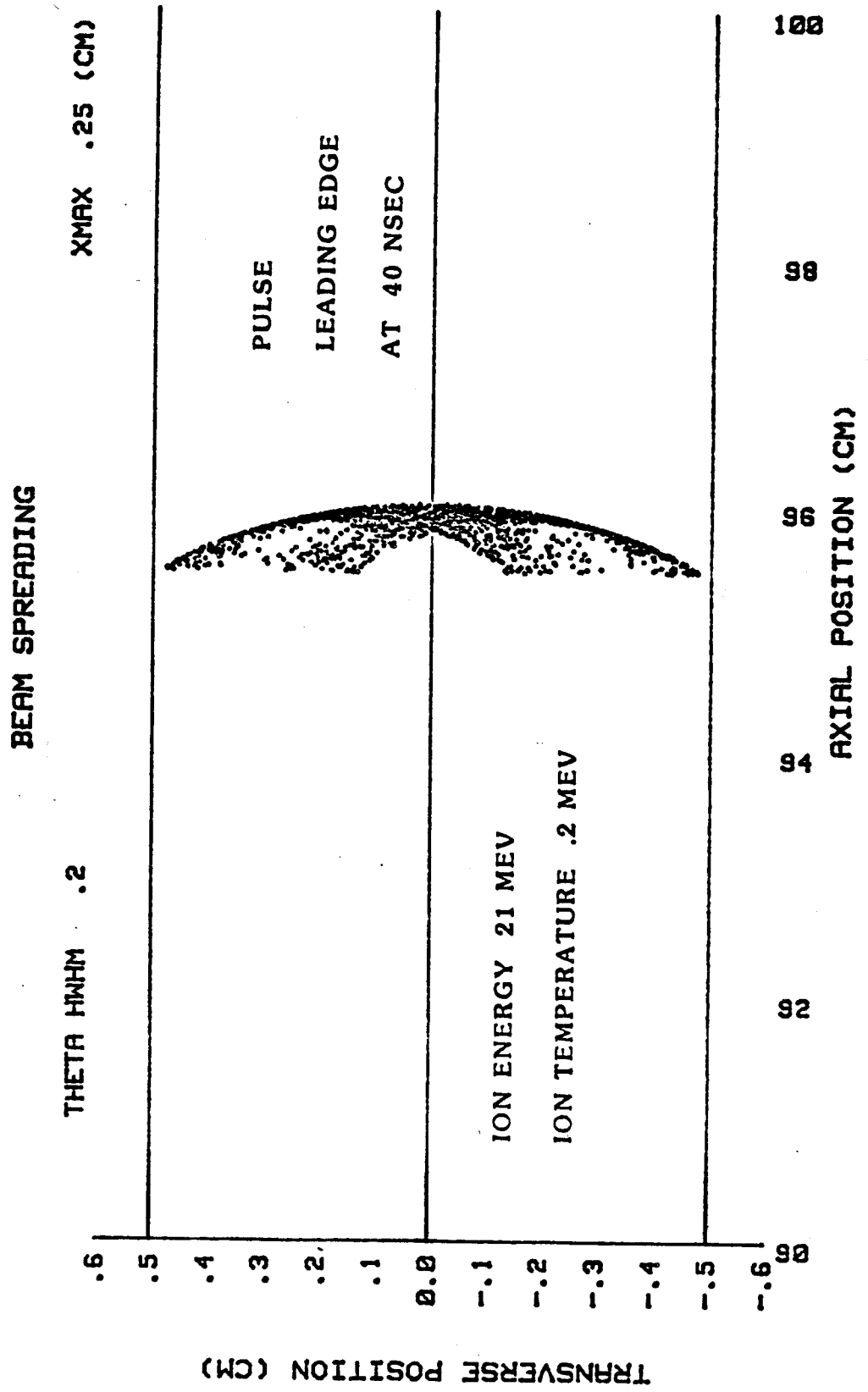

Fig. 5.5 Configuration space plot of leading edge of ions at 40 nsec after injection.

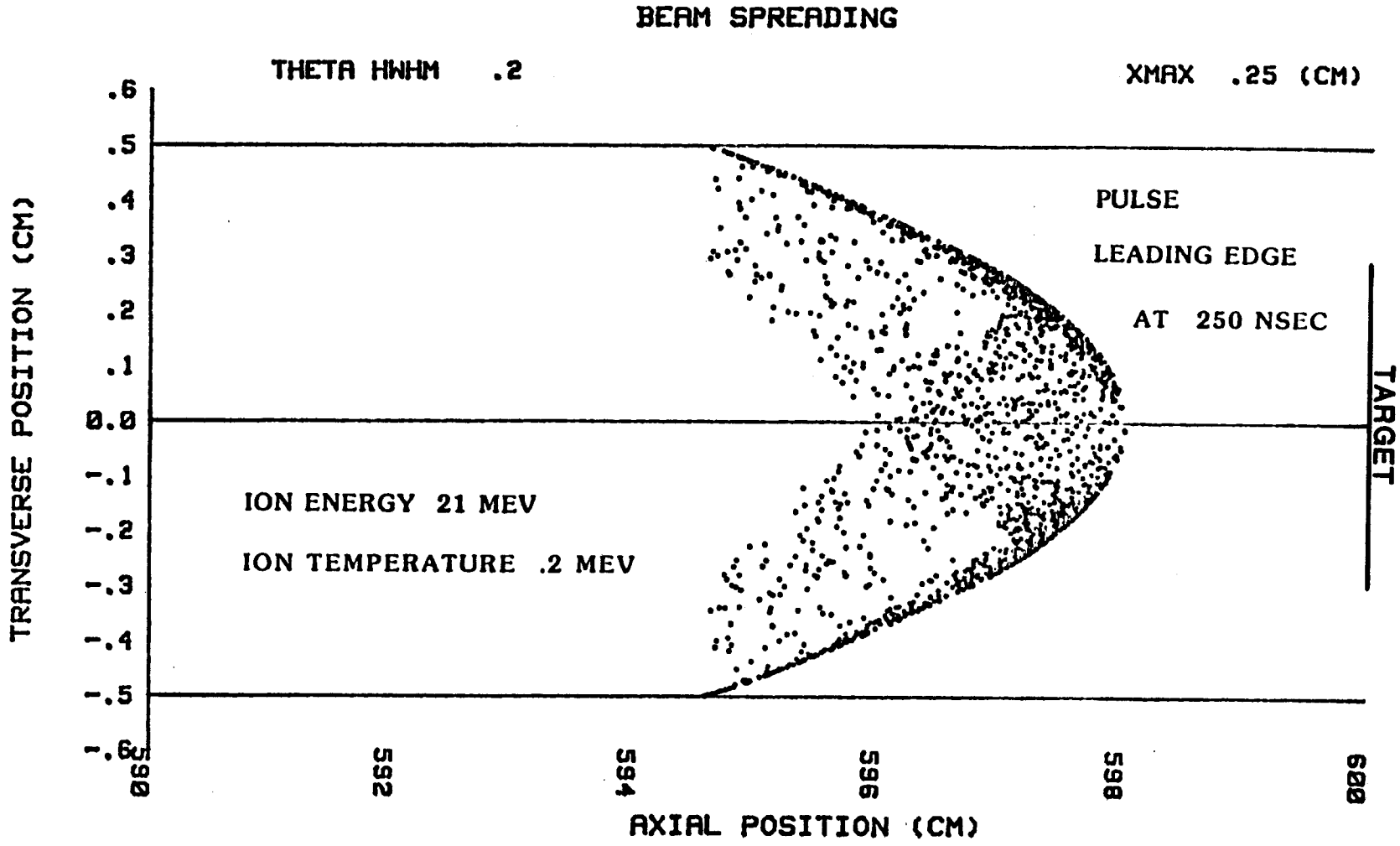

Fig. 5.6 Configuration space plot of leading edge ions at 250 nsec after injection.

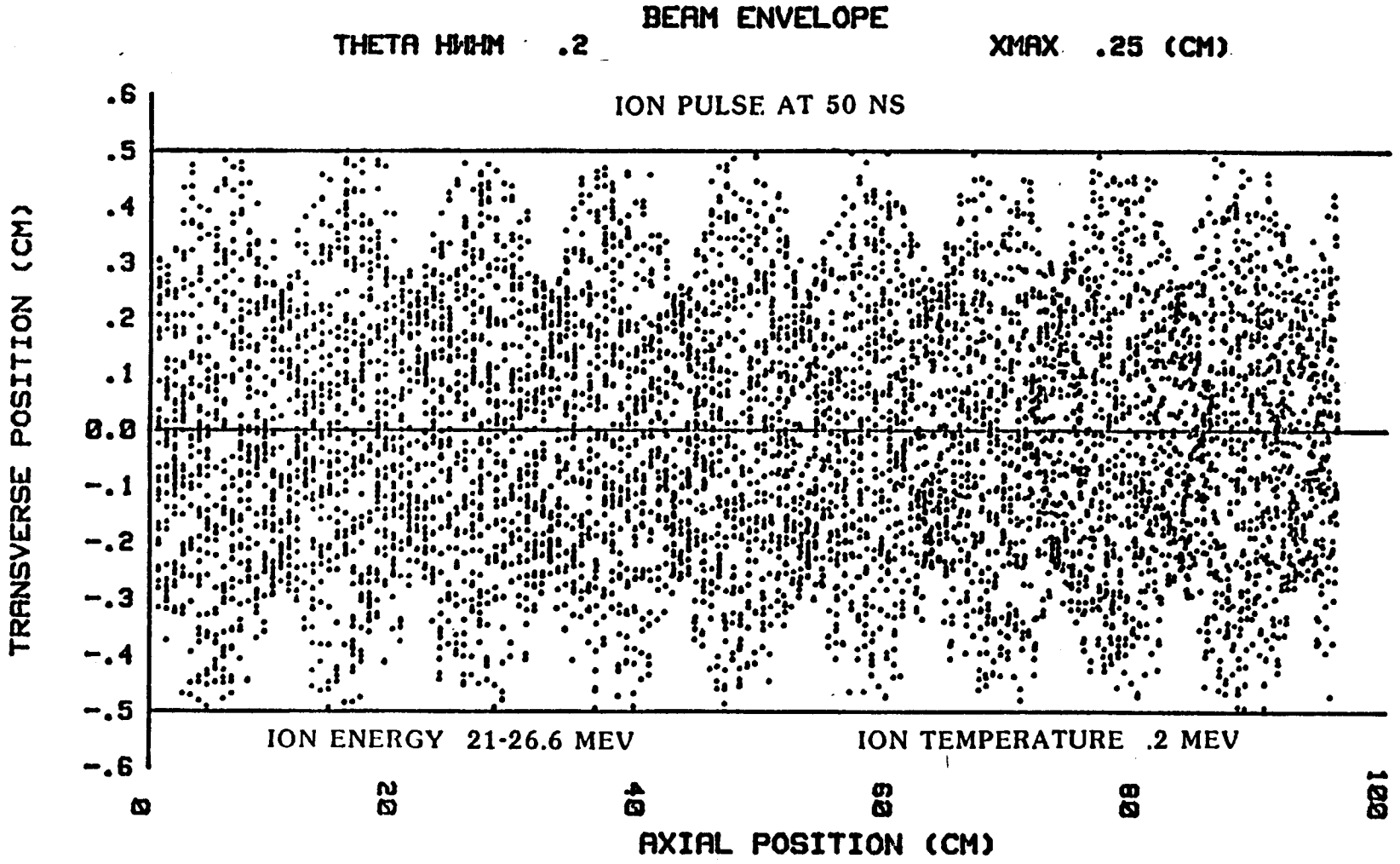

Fig. 5.7 Configuration space plot of entire ion pulse as it starts propagation.

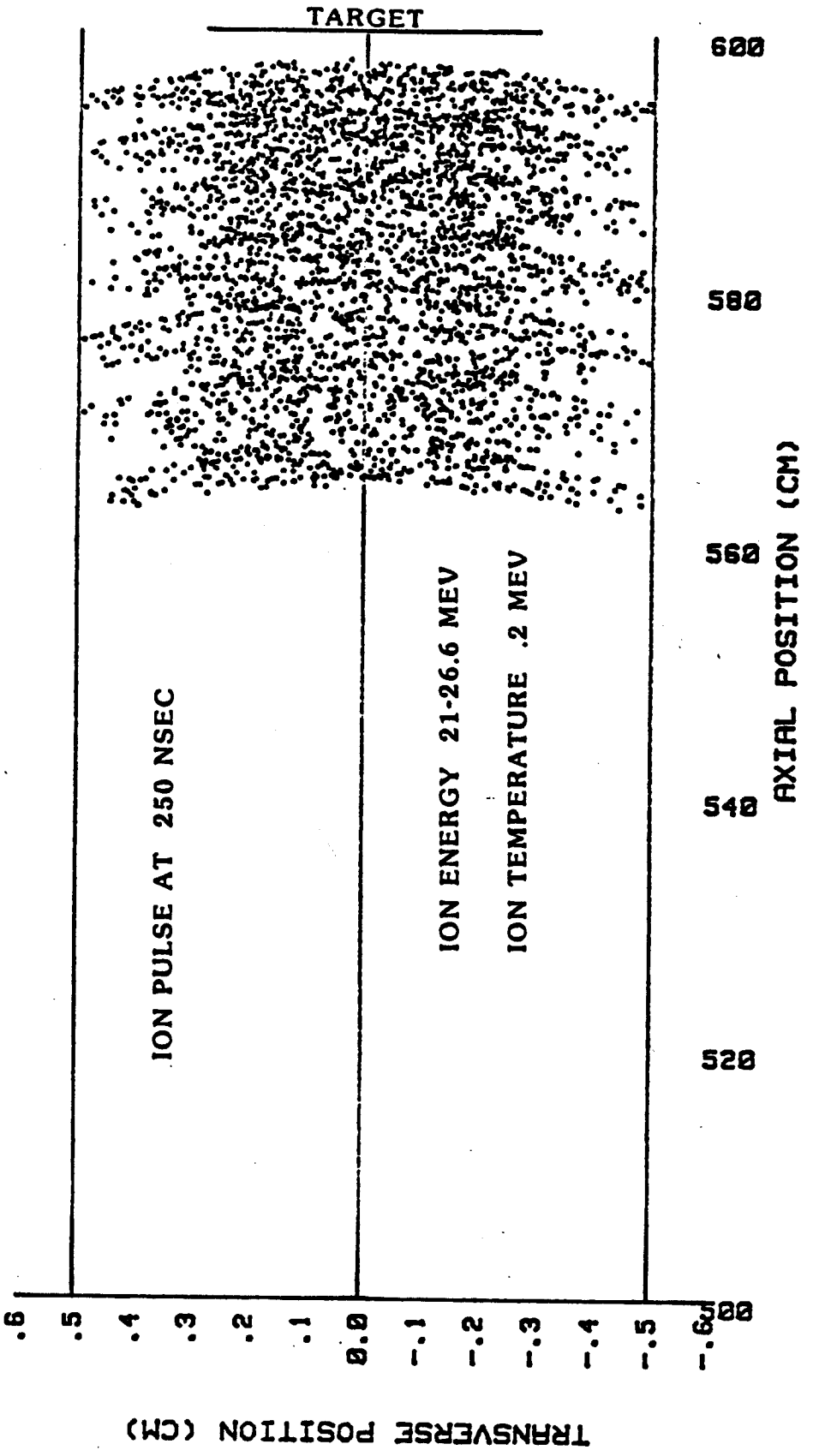

Fig. 5.8 Configuration space plot of entire ion pulse as it ends propagation and is compressed by time-of-flight bunching.

to 26.5 MeV at the tail. Also seen in Fig. 5.7 is the rippling of the beam due to coherence effects in the ion's betatron trajectories. This local pinching of the ion beam can result in current driven instabilities and must be carefully controlled.

In a related topic, Fig. 5.9 shows the precession of ions as they propagate at an average axial velocity V_{z_o} or energy of E_{z_o}. This accounts for the axial spreading of the beam but also has the important feature of washing out convective instabilities that might otherwise disrupt the beam. These slight variations in the ions' axial velocity mean that electromagnetic waves cannot have phase velocities that match up with these travelling ions and hence cannot be pumped by the ion beam.

These calculations represent a good start toward understanding and modeling of ion beam propagation in plasma channels. The computer models developed to simulate these processes will also serve to describe near term experiments and they are being developed with this thought in mind. The codes will be carefully written according to structured programming/structured design principles and will be fully documented.

At the FPA-KfK LIBRA meeting in October 1982 in Madison, we heard a guest lecture by S. Goldstein of JAYCOR/NRL. He described the state-of-the-art in ion generation, focusing and propagation with a review of the most recent experimental work at NRL. A particularly intriguing idea that he presented was the use of large plasma channels, 5 cm in diameter, with a separate focusing cell near the target. This concept is depicted schematically in Fig. 5.10. These large plasma channels allow very high currents (i.e., power) to be propagated because the limiting current scales as r_{ch}^4. Hence ~ 100 TW can theoretically be propagated in a single channel! On an experimental basis

AXIAL SPREADING OF THE ION PULSE

PULSE FRAME AXIAL VELOCITY Vz_0

Ez_0 9.85 MEV X_0 .22 CM

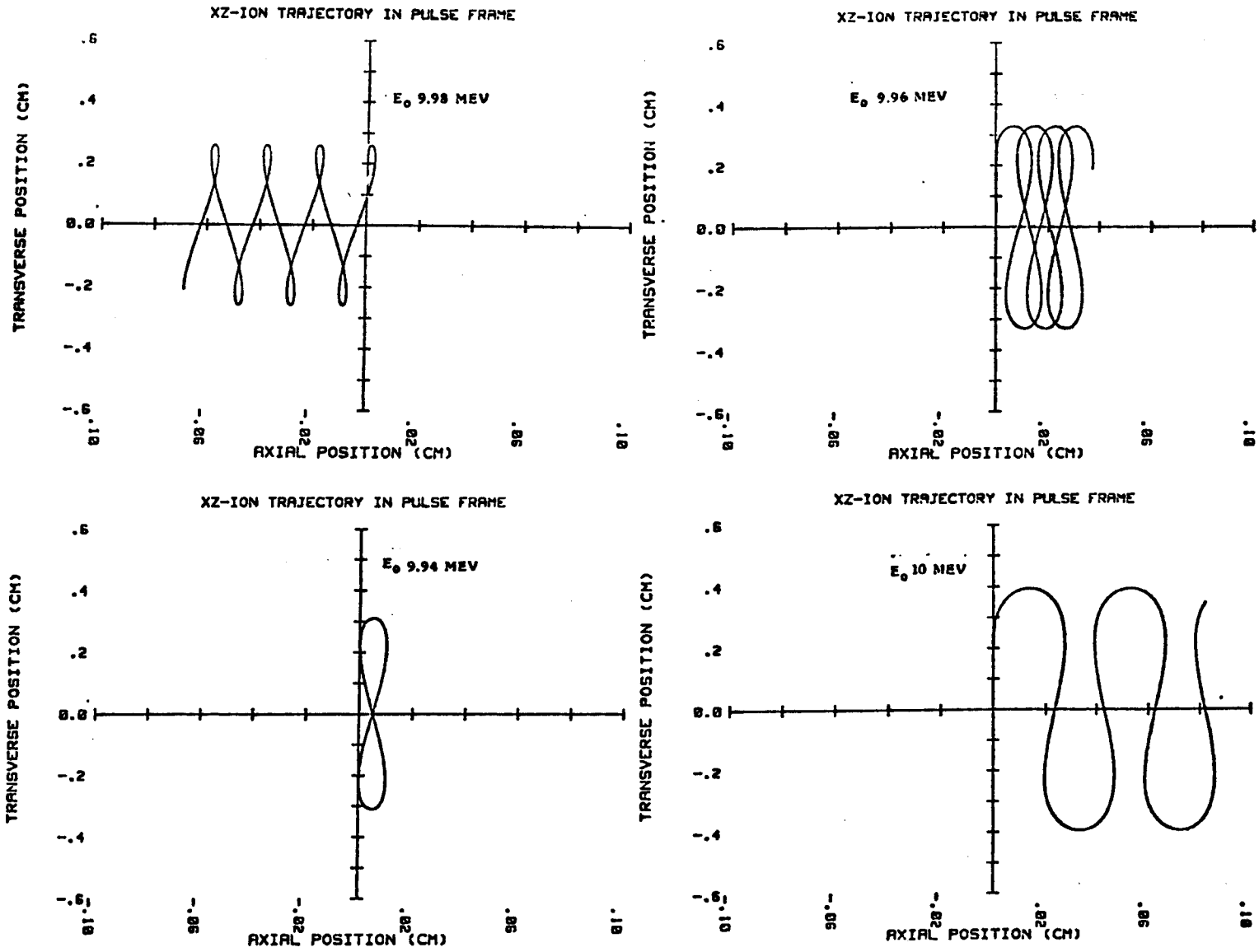

Fig. 5.9 Precession of ions as they propagate in the channel.

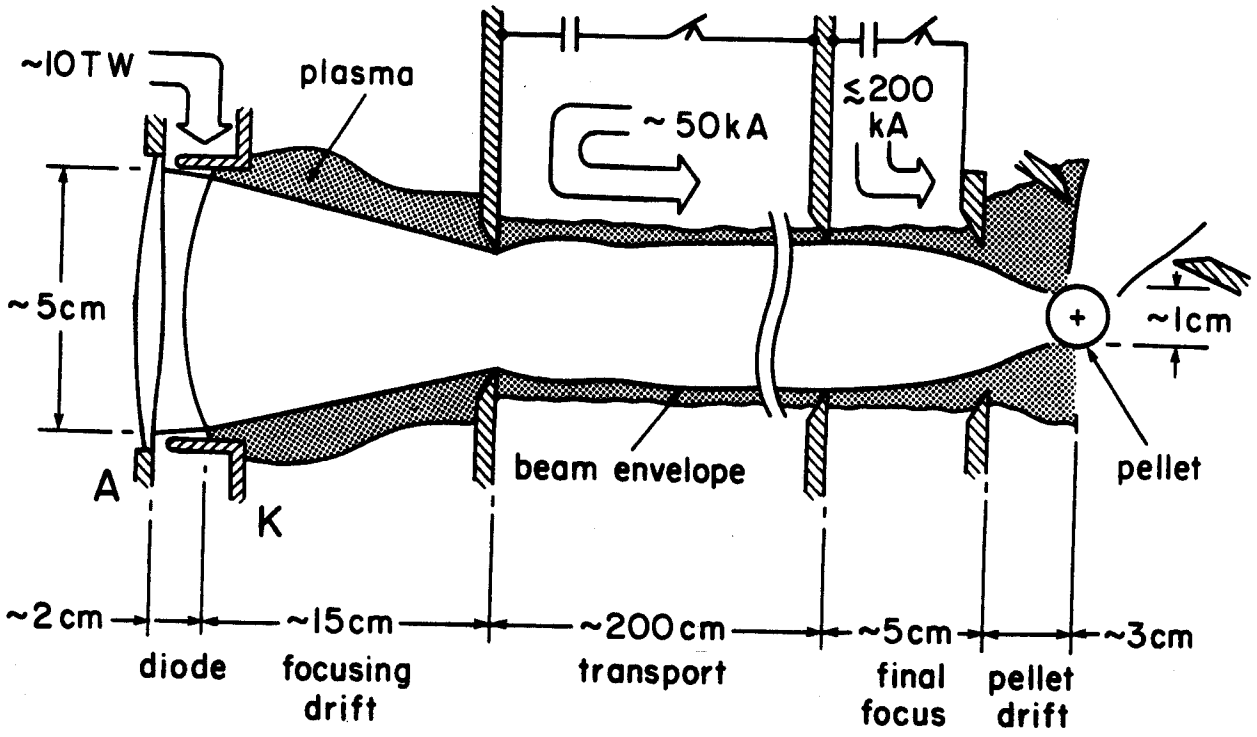

Fig. 5.10 Large diameter plasma channels with an active focusing cell at the target.

this can be accomplished using two sets of capacitor banks to generate the channel and focusing cell as shown in Fig. 5.10. However, the inclusion of this hardware in the proximity of the target would not be possible in a reactor where it would be destroyed after each target microexplosion. Hence, some other mechanism must be found to focus the ions from this 5 cm diameter channel down to the 0.5-1.0 cm target diameter. Goldstein had two suggestions. The first was to place a focusing structure around the target to provide current paths to create essentially a mirror B field to pinch the ion beam down to the size of the target. The second suggestion was to use a long wavelength laser to irradiate a structure around the target to create locally intense azimuthal magnetic fields that would serve to focus the ions.

All of these ideas have merit and demonstrate the wealth of possible schemes that could lead to the successful implementation of light ion beam driven fusion. This large channel formation and final focusing falls neatly within our original picture of the ion generation, focusing, propagation and focusing picture. We plan to pursue these ideas further.

6. Light Ion Driver System

A pulsed-power driver relevant to the LIBRA reactor must convert a fraction of the electrical energy produced by the plant into a high-intensity high-brightness light ion beam at a repetition rate of a few Hertz with an efficiency of about 20% for a lifetime of 10^9 shots.

Light ion beam generators fall into two classes, depending upon the mode of energy transfer to ions:

Single-stage generators: ion diodes

Multi-stage generators: Pulselac.

Each of these generator types is being considered as a driver system for the LIBRA study. Prior to developing a specific point design, a low level of preliminary work is being carried out to develop an understanding of the technologies involved in each driver concept so that we can determine their impact on the cavity and blanket design. Important issues are: identification of critical components, extrapolation from existing technology to reactor-relevant technology, and evaluation of present day confidence in development of crucial components. This should give us a crude picture of the design features of the driver.

We are attempting to gain an overall appreciation of state-of-the-art driver technologies, as well as a feeling for the development necessary to achieve reactor relevant components. S. Humphries, Jr. of the University of New Mexico, presented a seminar to our design group concerning recent developments in ion diode technology and multistage technology. S. Goldstein of Jaycor Inc. spoke to us concerning diode technology, and several novel concepts for light ion beam transport which could be important for both ion diode

and multistage-generator reactor systems. We have conducted a review of the theory that has been developed to describe ion diode behavior.

Treating the driver as a black box, important parameters can be identified which characterize either the single or the multistage generators as far as the rest of the plant is concerned. These parameters are:

stored energy fraction

number of driver modules

ion beam energy per beam

transfer efficiency

peak output voltage

peak output current

ion beam current per beam

peak electrical power

average electrical power

pulse width.

Specific values of these parameters will be determined in principle by coupling the driver to the transport channel and target. The combined driver-channel-target system is characterized simply by the target gain and the overall driver efficiency, including losses in ion propagation. This will of course determine the economic attractiveness of the LIBRA reactor.

6.1 Single-Stage Generators

Single-stage generators, as the name implies, accelerate ions by the application of a single megavolt pulse to an ion diode. Since the acceleration is not gradual or incremental this approach is highly dependent upon the ability to generate and handle megavolt, short pulse length voltage pulses.

Several components in present day ion diode drivers cannot meet the requirements necessary for ICF reactor applications. Ion diode drivers employ either capacitive, inductive, or inertial energy storage, or some combination of these. These systems will be briefly described in order to point out the components which are in need of substantial further development.

Capacitive systems, such as PBFA-I at Sandia Labs, Fig. 6.1, employ Marx generators which charge a water dielectric transmission line which compresses the voltage pulse to the required pulse-length (50 ns). The pulse-forming stages are coupled sequentially by closing switches. Currently water switches are used. After pulse shaping, the high voltage pulse travels through an output line to a vacuum interface which separates the dielectric from the magnetically insulated vacuum transmission line. Finally the pulse is compressed geometrically prior to application to the ion diode.

The key components are the vacuum interface insulator and the closing switches. Present day vacuum tube insulators are too large and at reactor power and voltage levels are prohibitively large. Further development is needed to inhibit flashover in smaller insulators.

Closing switches capable of satisfying reactor specifications do not at present exist. Such switches must be invented.

Inertial charging systems are similar to capacitive systems with Marx units replaced by rotating machinery. Component development considerations are similar to capacitive systems.

Inductive storage systems operate as follows: an inductor is charged to high energy density and switched into the pulse line with an opening switch. Inductive energy storage can be achieved in volumes several orders of magnitude smaller than capacitive storage. No vacuum insulators are needed.

Fig. 6.1

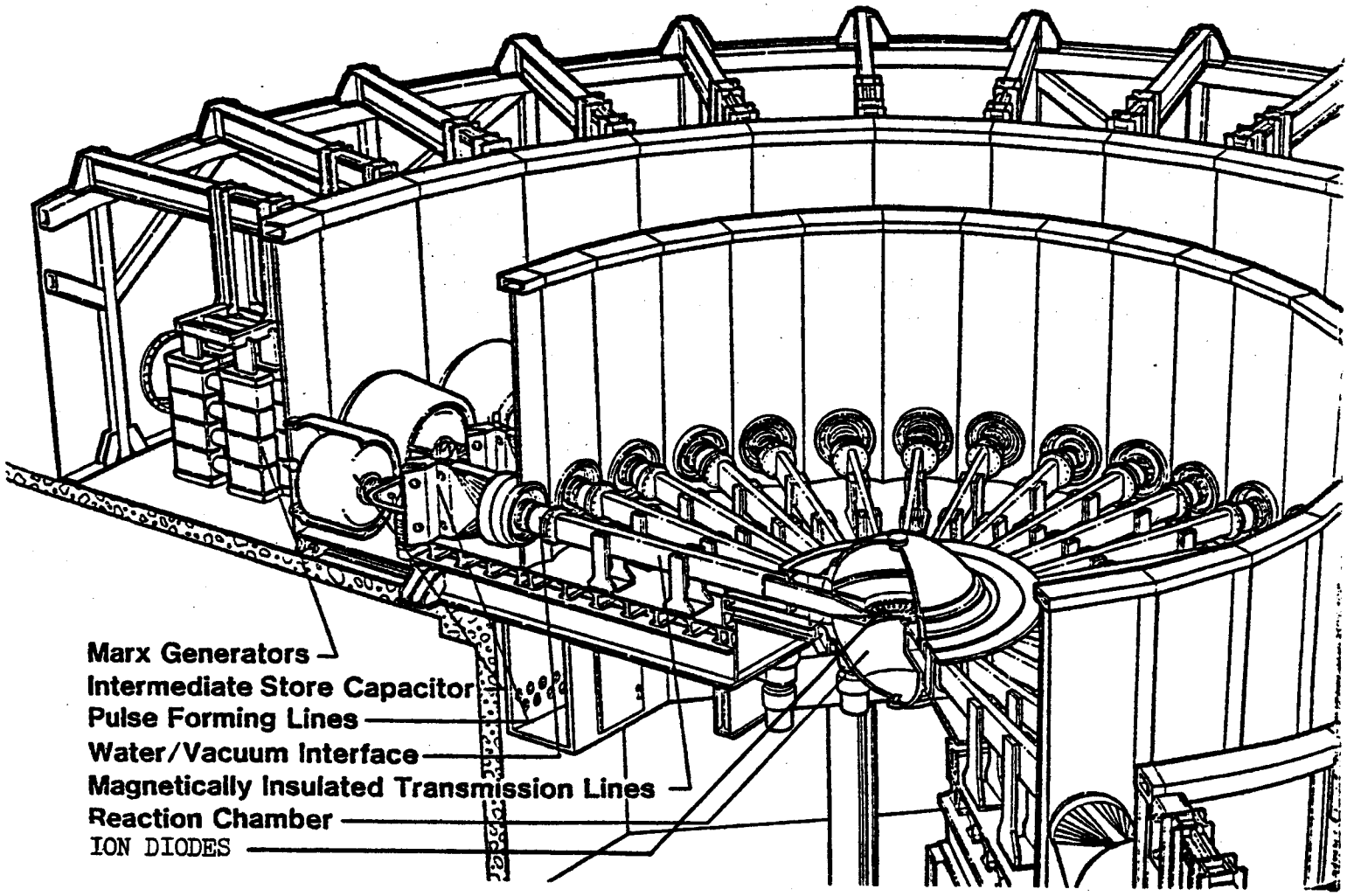
Marx Generators
Intermediate Store Capacitor
Pulse Forming Lines
Water/Vacuum Interface
Magnetically Insulated Transmission Lines
Reaction Chamber
ION DIODES

Auxiliary equipment requirements reduce the overall system size benefit to about one order of magnitude smaller than capacitive systems.

The crucial component is the opening switch. This switch must open to voltages of about 10 MV and must produce short (50 ns) pulses. Opening switches must be substantially developed before reactor specifications can be approached.

The ion source and accelerator in each of the systems described above is an ion diode. A survey of the scientific literature relating to the theory and experimental verification of ion diode designs, and in particular, reports on the progress in the quest to achieve the single-pulse intensity necessary for light ion fusion demonstration of feasibility leave the distinct impression that this technology is evolving very rapidly. It has only been in the past decade that the use of ion diodes to produce high intensity focusable ion beams has been considered. Furthermore, only in the last few years has the idea really been considered as a serious contender in the ICF concept.

As regards the application of ion diodes to the longer term goal of commercial ICF, great difficulties remain to be overcome, despite the substantial near-term progress. Although questions of cost, efficiency, and scalability to reactor application appear to have been answered in the affirmative, the technology of repetitively pulsed ion diodes is still fledgling. If ion diodes can be made to operate efficiently in a repetitive mode they will be prime candidates for ICF drivers.

A point design is difficult, as regards the ion diode, since a firm concept for a repetitively firing diode does not exist. The LIBRA study will proceed on the assumption that reactor-relevant diodes will eventually be developed.

6.2 Multistage Generators

Pulselac, the linear accelerator approach, will also be considered. We have not yet begun to explore the implications of a Pulselac driver. We intend to study the detailed physics of the propagation channel for ions in the self-pinching propagation mode which is appropriate for Pulselac driver systems. Channels of radius greater than the target radius will be considered. This necessitates the final focusing of such beams onto the target and this will also be analyzed.

7. Fireball Calculation

In a light ion fusion reactor where ions are propagated through preformed z-pinch plasma channels there is the requirement for a background gas in the pressure range of 1-20 torr depending on the molecular weight of the gas and the specific channel formation magnetohydrodynamics. The presence of this gas results in the generation of a micro-fireball when the target explodes. This phenomenon is shown schematically in Fig. 7.1. Depending on the density and opacity properties of the gas this fireball can either deposit a very intense surface heat flux on the first wall or a very strong shock overpressure. To make a first estimate of this phenomenon we have run a fireball simulation using the MF-FIRE hydrodynamics computer code using the output spectra from the 320 MJ target described in Section 4 of this progress report. The input parameters for this calculation are listed in Table 7.1. As the cavity gas we chose 10 torr of argon seeded with 1% lithium to facilitate laser initiated breakdown of the channels. This simply represents a guess of the required pressure for plasma channel formation. A more accurate determination of the gas pressure and molecular weight awaits the completion of the MHD channel formation model. Figure 7.2 is an "R-t" plot of the lagrangian zones in this calculation showing that the shock is not very strong and it reaches the first surface of the chamber, 5 meters from the target, at about 1 ms after the target explosion. The maximum overpressure is 1.8 MPa. The pressure-time profile at the first wall is shown in Fig. 7.3. For this gas mixture the dominant fireball phenomenon is radiative heat transfer to the first wall. This is shown in Fig. 7.4 where the original target x-ray spectrum is plotted. About 2.5 MJ of the target x-rays at energies above 10 keV are unattenuated by the gas and reach the first wall. The remainder of the x-rays in the lower

TABLE 7.1

Parameters for Fireball Calculation

Target		
Yield	320. MJ	
Neutrons	228. MJ	
Gammas	0.48 MJ	Derived by scaling 1 mg HIBALL target
X-rays	72. MJ	
Debris	17. MJ	
Endothermic	2.52 MJ	
Cavity Gas		
Type	Ar + 1% Li and Ne + 1% Li	
Pressure	10 torr and 20 torr at 0°C	
Temperature	800°C	
First Wall		
Radius	5 m	

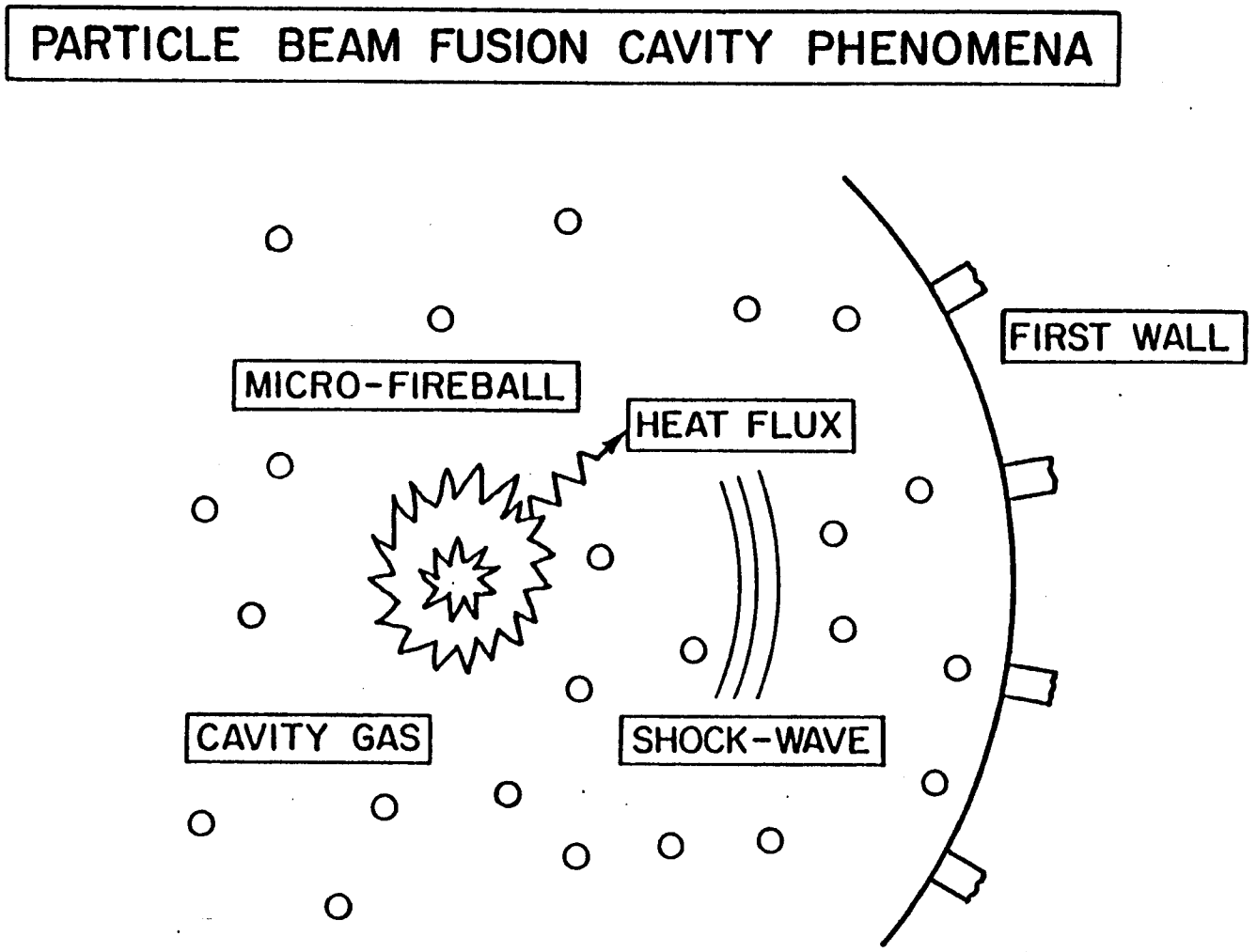

Fig. 7.1 Schematic picture of micro-fireball in light ion beam fusion reactor.

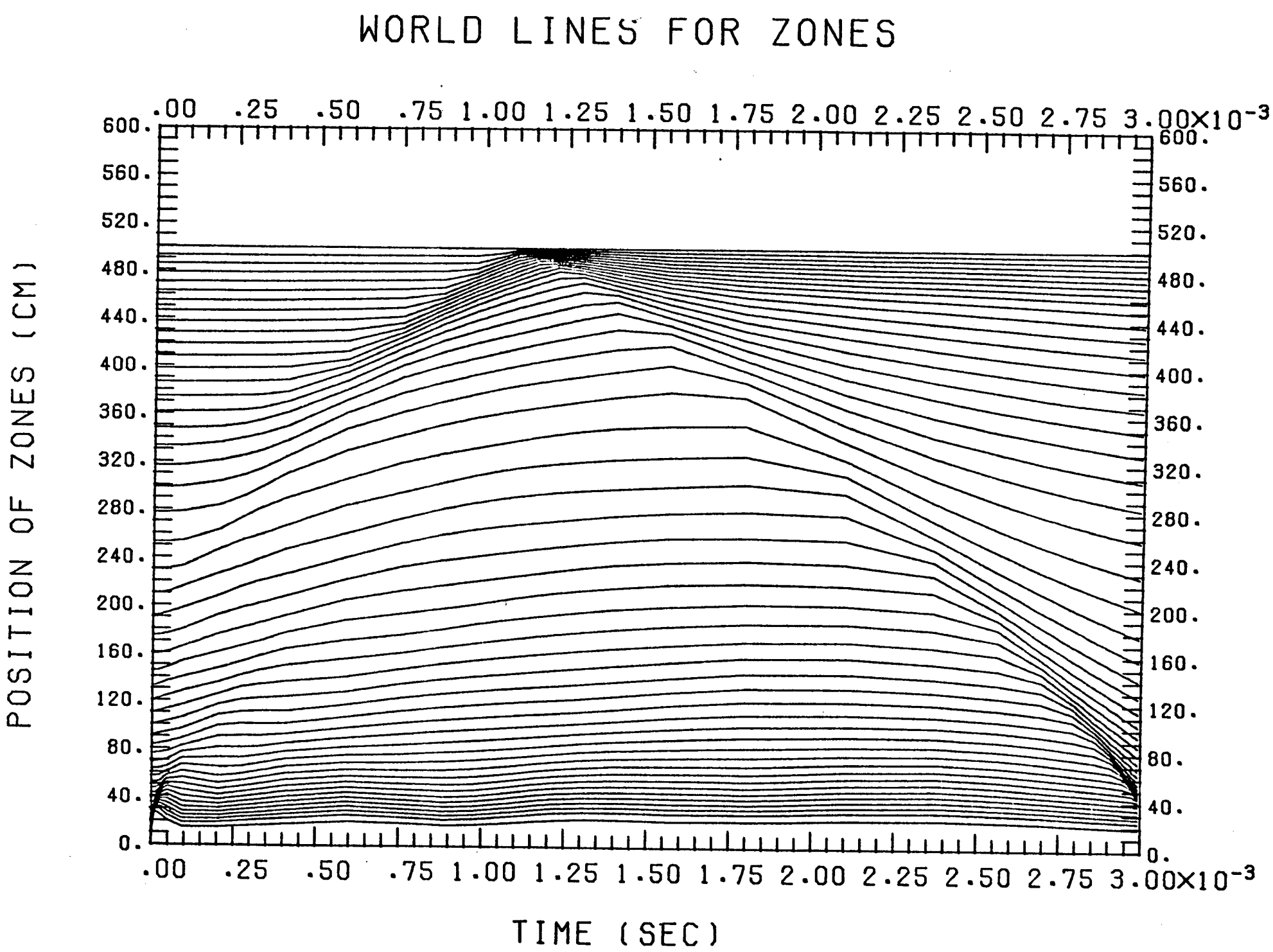

Fig. 7.2 R-t plot of fireball calculation.

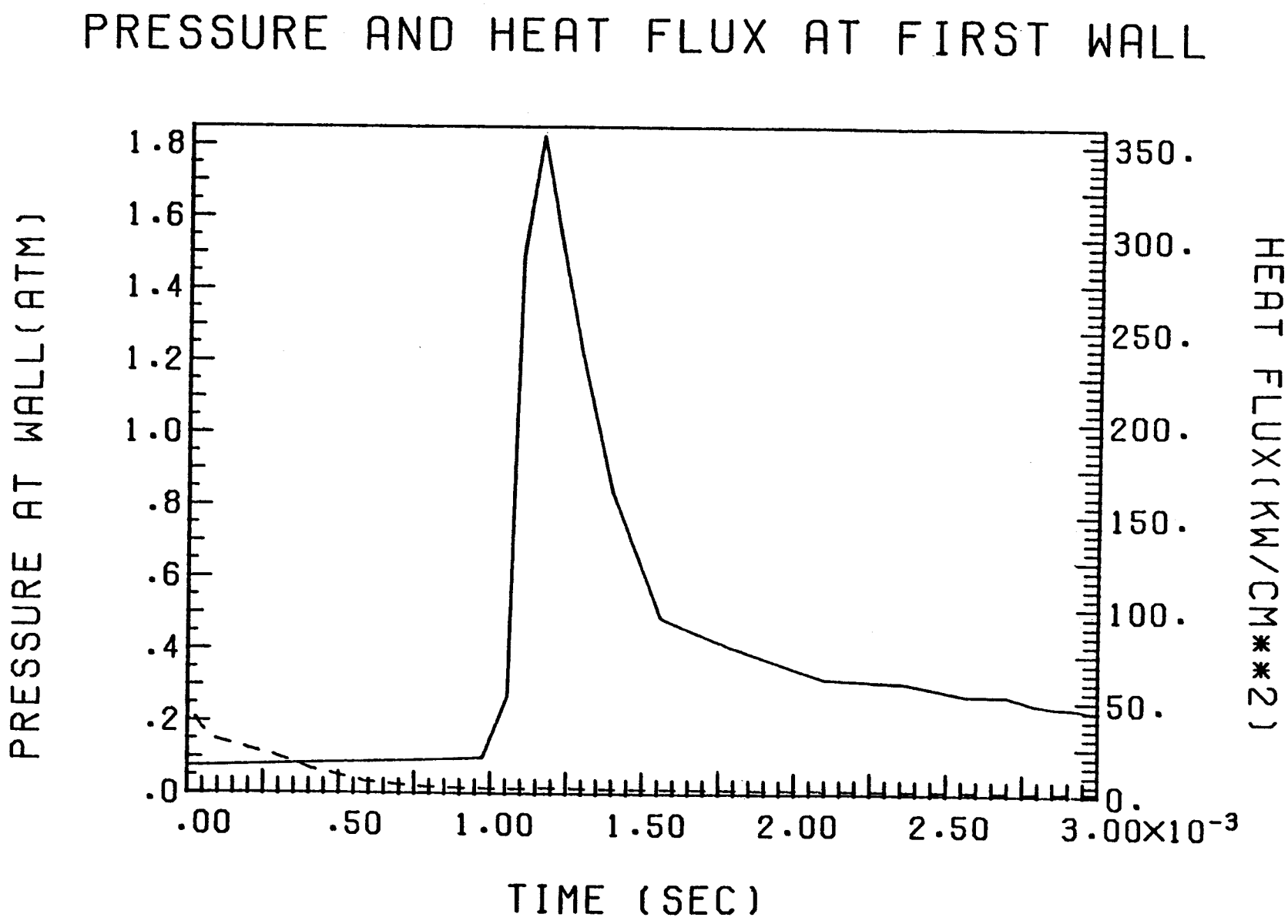

Fig. 7.3 Pressure vs. time at the first wall.

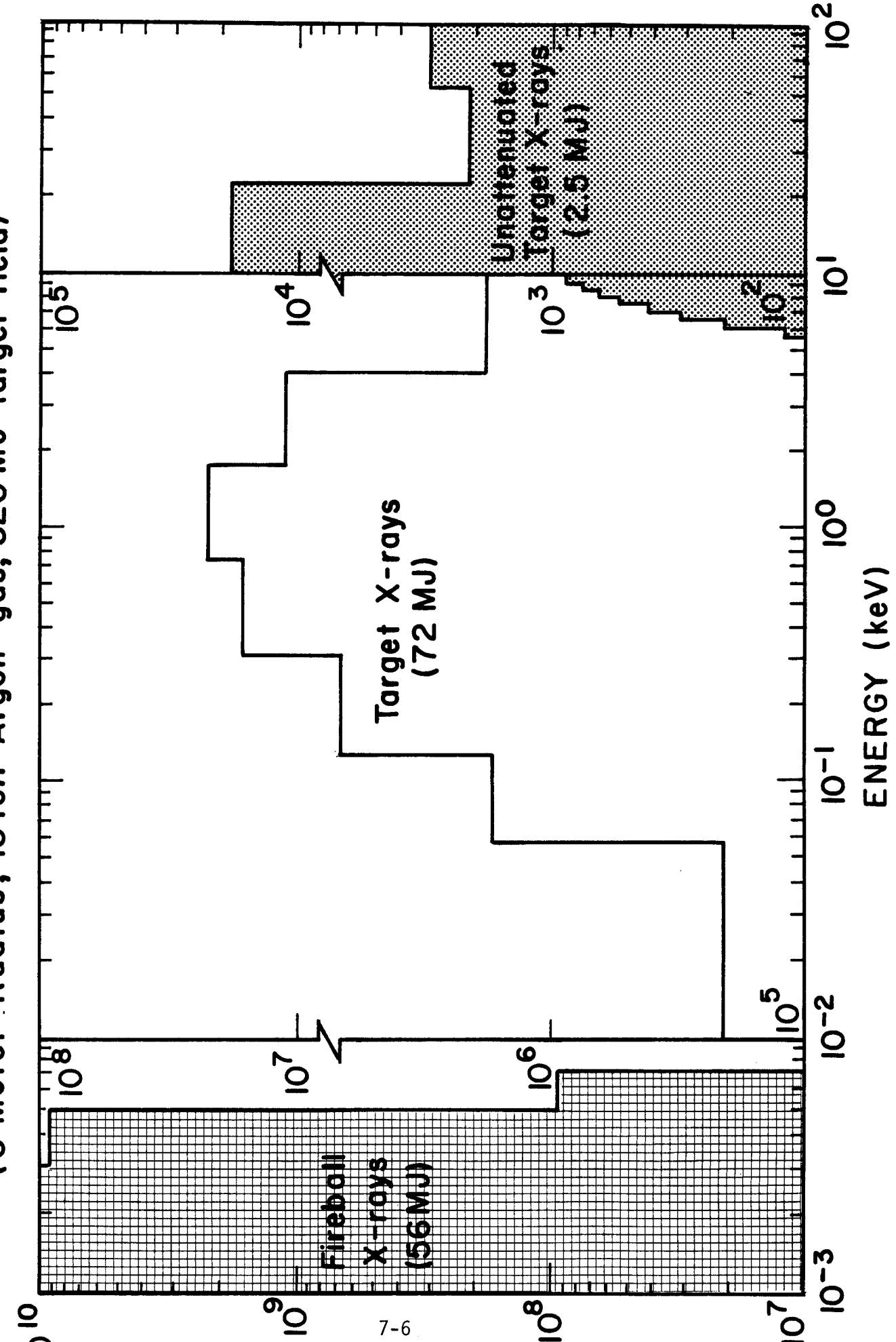

Fig. 7.4 Time integrated x-ray spectrum at the first wall.

energy part of the spectrum are totally absorbed by the gas and are transferred to the first surface at photon energies of 1-10 eV. In fact, 56 MJ of energy is deposited on the first surface in $\lesssim 10^{-3}$ sec, hence the average heat flux is $\sim 1.8 \times 10^5$ kW/m^2. The remainder of the energy, 30 MJ (13 MJ from x-rays and 17 MJ from debris), remains in the gas after 3 ms and is released over a much longer time scale. This residual energy must be recovered in other ways (see Section 8). These calculations illustrate that a severe heat flux must be handled in the light ion fusion reactor design even though a cavity gas is present. This was of course the situation in the HIBALL design where the chamber was evacuated to 10^{-4} torr. This leads to the conclusion that some type of wetted first surface is essential for this design to allow ablation of the liquid film. However, the recondensation of this vapor will be quite different in the presense of the non-condensible argon gas. Furthermore, a cavity radius of 5 meters with only 480 MW of fusion power corresponds to a wall loading of only 1 MW/m^2. This is quite low and indicates that a smaller cavity is desirable if possible.

Further fireball calculations must wait for a better determination of the optimum cavity size and the gas characteristics that are needed for channel formation.

8. Cavity Pumping

The repetition rate of LIBRA is 1.5 Hz. Therefore, the cavity has to be restored to its original condition within 0.67 seconds. The cavity conditions just before the shot are listed in Table 8.1. The gas pressure in the cavity is between 1 to 50 torr, and is picked at 10 torr at this stage. The Li impurity is added intentionally to enhance thermal radiation. The cavity temperature is picked to minimize gas ionization and for pellet delivery. This set of numbers is chosen for the initial calculation and can be varied as needed.

After the fireball explosion, there is ~ 90 MJ of energy associated with the cavity gas, of which 60 MJ is transferred to the first wall coolant by thermal radiation within 3×10^{-3} seconds. At this time, the cavity gas becomes cold so that thermal radiation is not effective. Therefore, other methods have to be used to reduce the cavity temperature and pump out the ashes to re-establish the initial cavity conditions. The mass balance and energy balance of the cavity are listed in Tables 8.2 and 8.3, respectively.

Three possible alternatives have been reviewed as possible cavity cleanup schemes. These are to be discussed separately:

1. Vacuum Pumping

This method was suggested by ADLIB[1] to clean up their cavity. Since the energy is associated with the cavity gas as thermal energy, the easiest method is to pump out the gas and recover the energy through a heat exchanger. The cavity gas density will have to be pumped down from $3.6 \times 10^{17}/cm^3$ to $1.8 \times 10^{15}/cm^3$. In order to keep the heat exchanger and piping to a reasonable size, this gas has to be compressed to a few atmos-

TABLE 8.1

Cavity Conditions

Ar density, cm^{-3}	3.6×10^{17}
Li density, cm^{-3}	3.6×10^{15}
Cavity temperature, °C	800°

TABLE 8.2

Mass Balance

	Before Shot	After Shot
Ar	1.9×10^{26}	1.9×10^{26}
Li	1.9×10^{24}	1.9×10^{24}
Pb		6.7×10^{20}
He		1.42×10^{20}
D		2.43×10^{20}
T		2.43×10^{20}

TABLE 8.3

Energy Balance

Initial cavity temperature	800°C
Energy associated with the gas	30 MJ
Specific heat (c_v)	12.6 J/mole-°C
Mass of gas	308 moles
Gas specific energy	9.7×10^4 J/mole
Gas temperature*	6600 K

*Gas temperature is lower than [specific energy/c_v] due to ionization of the gas.

pheres. The gas will be fed back to the cavity upon release of the thermal energy in a heat exchanger.

The main problem associated with this scheme is how to handle a gas at ~ 6600 K. If this gas is pumped out at sonic velocity, the thermal load at a stagnation point along the way will be ~ 10^4 W/cm^2 and, undoubtedly, the structure will melt. The time required to pump down the cavity gas density by a factor of 20 will require a pumping capacity of 6×10^5 liter/sec.

2. Gas Flooding

Since the cavity gas is too hot to handle, it is suggested that the cavity first be flooded by a high pressure gas to cool down. 6×10^3 moles of argon is fed into the cavity to bring the gas condition to 800°C and 800 torr. The cavity is pumped down to 40 torr. The gas pumped out from the cavity will be compressed to a few atmospheres and fed to a heat exchanger and cooled to 500°C. This gas will be fed back to the cavity after the next shot.

Since the gas is being pumped out of the cavity at 40 torr, it is necessary to compress the gas to a few atmospheres. This is necessary both to reduce the equipment size and at pressure high enough for feeding back to the cavity. Adiabatic compression of an ideal gas shows that to compress a gas from 40 torr to 1 atm, the resultant gas temperature is 4560 K. The compression energy required will be 261 MJ. This is clearly not possible.

3. Thermal Radiation

A passive cooling of the cavity, if possible, is the simplest method. The ash can be removed by pumping out a small volume of the cavity gas,

resulting in a relatively high cavity impurity level. The energy needed to be radiated away is 30 MJ, or 9.5 J/cm^2, which may be achievable if the cavity gas temperature is high.

Figure 8.1 shows the cavity gas temperature as a function of cooling time with different gas emissivities. If the gas emissivity is between 0.1 to 0.2, the cavity gas can be cooled to 1000 ~ 1300°C, which may be acceptable. If this is the case, the cooling and clearing of the cavity can be decoupled and this becomes a much easier process.

The clearing of the cavity depends on the allowable impurity level. If the maximum acceptable impurity level of Pb is 1% of the argon density, impurity control can be achieved by pumping out 0.1% of the cavity gas by the end of the cooling period, which corresponds to a vacuum pumping of only 280 liter/sec. The resulting cavity gas concentrations are listed in Table 8.4.

TABLE 8.4

Cavity Gas Impurities

Ar, cm^{-3}	1.9×10^{26}
Li, cm^{-3}	1.9×10^{24}
Pb, cm^{-3}	1.9×10^{24}
He, cm^{-3}	4.0×10^{23}
D, cm^{-3}	6.7×10^{23}
T, cm^{-3}	6.7×10^{23}

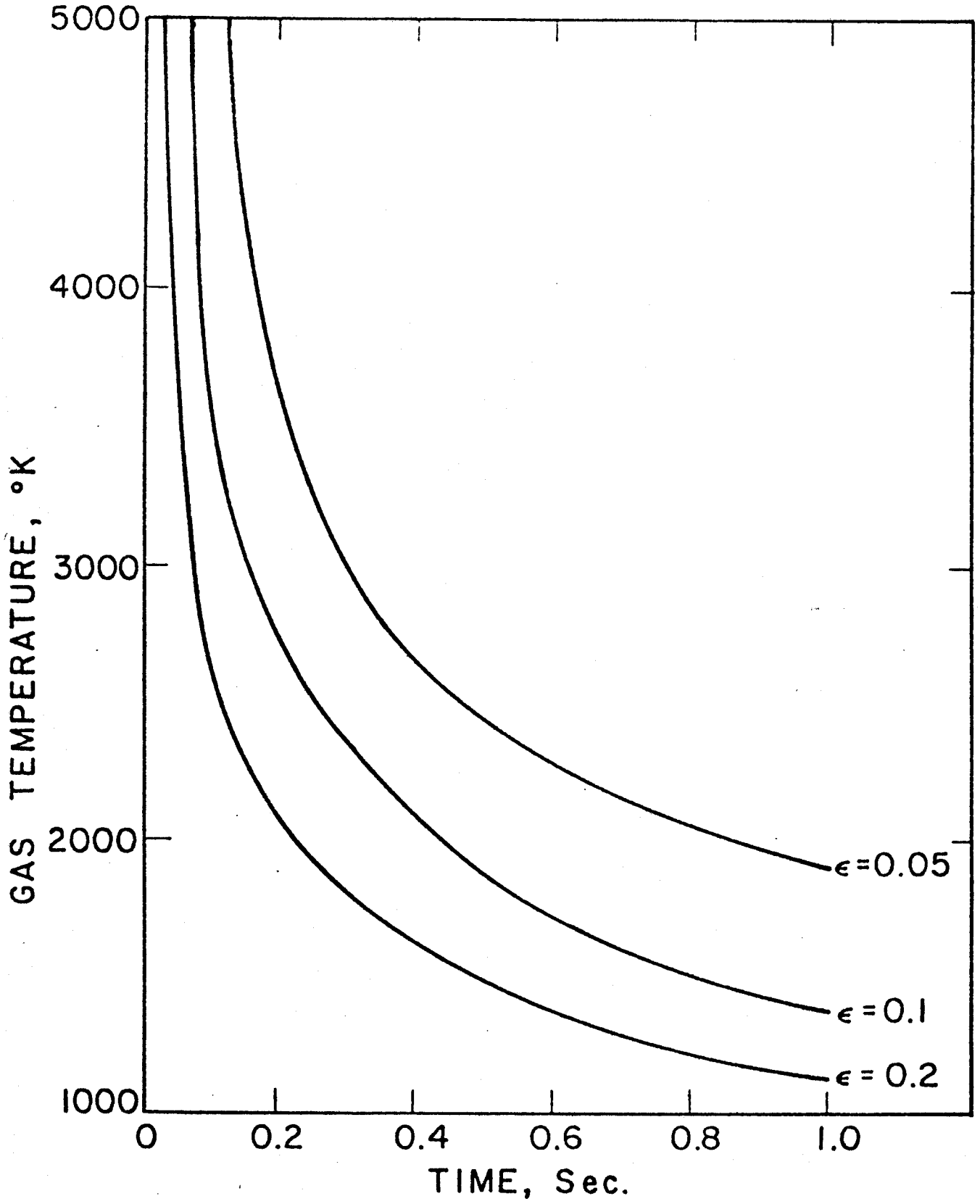

Fig. 8.1 Cavity gas cooled by radiation.

The following list of studies have to be performed to establish the cavity cleanup scheme:

1. Calculation of emissivity of the cavity gas as a function of temperature > 1000 K.
2. Calculation of apparent specific heat of gas (including ionization energy) as a function of temperature.
3. Establish acceptable cavity gas density and impurity levels.
4. Establish acceptable cavity gas temperature for pellet delivery and channel formation.
5. Study alternative cavity cleanup schemes.

Reference for Chapter 8

1. H. Madarame et al., "A Conceptual Design of Light Ion Beam Fusion Reactor - ADLIB-1," University of Tokyo Report UTNL-R 0144, 9/1982.

9. Cavity Design

Cavity design for LIBRA is in an infant stage. There are several general features of the cavity that have been identified as problematical and these features are receiving the most attention. The cavity is filled with approximately 5-10 torr of cavity gas to support the establishment of plasma channels for beam propagation. This gas also serves to protect the first surface from direct bombardment by debris ions and soft x-rays from the exploding target. However, the gas also supports the creation of a fireball which propagates to the first surface, imparting a significant overpressure. Our earlier calculations showed that a 1.8 MPa (18 atmosphere) overpressure was experienced at 5 meters from the target explosion. We believe that this overpressure can be managed with proper design of the first surface.

A more important problem is the cooling of the residual, hot cavity gas following the fireball dynamics. This gas will have a temperature of approximately 1000-3000 K. This is very hot, yet the temperature is likely to be too low for effective radiative heat transfer. This leaves only conductive and convective heat transfer. To solve this problem we propose to study the following design features:

1. Low repetition rate, 0.75-1.5 Hz.
2. Convective and evaporative cooling of the gas.

The low repetition rate gives us the best chance for meeting our goals. If the analysis shows that the rate can be increased, as we hope, then the design will be automatically scalable to higher power levels. To cool the gas we propose to use both convective and evaporative cooling. At the low pressures in the cavity, convective cooling is not sufficient to cool the gas. Therefore we propose to use the heat of vaporization of $Li_{17}Pb_{83}$ to cool the

gas. Several different reactor design groups have proposed similar schemes; see part 1 of this report. The Japanese proposed flowing the hot gas through a bank of dry V-20 Ti tubes that constitute the blanket within the reaction vessel. The Bechtel-PI group proposed the use of a Li mist within the target chamber to quench the fireball. Our estimates show that convective cooling on dry tubes will not be effective in reducing the gas temperature due to the low gas pressure. We do not want to quench the fireball with a Li mist because the fireball is very effective at transferring heat via radiation at its high temperatures. Quenching it prematurely only worsens the low temperature heat transfer problem by leaving more energy in the gas at low temperature.

The LIBRA preliminary cavity and blanket design is a combination of the best features of two of our earlier designs. The Light Ion Fusion Target Development Facility, a single shot experimental facility, is shown in Fig. 9.1. Here the reaction chamber has no blanket and is submerged in a water pool shield. The familiar HIBALL cavity design with the INPORT concept is shown in Fig. 9.2. The preliminary LIBRA design is shown in cross section in Fig. 9.3. We have utilized the INPORT concept within the cavity and have submerged the cavity in a swimming pool water shield. The INPORT units serve several purposes in this design:

1. They protect the first structural wall from radiation damage.
2. The front rows of tubes evaporatively cool the hot cavity gas as it is pumped through them.
3. The back rows of tubes condense the liquid metal vapor in the cavity gas.

Using this radiation-evaporation-convection-condensation sequence, we hope to cool the cavity gas to sufficiently low temperatures so that it can be

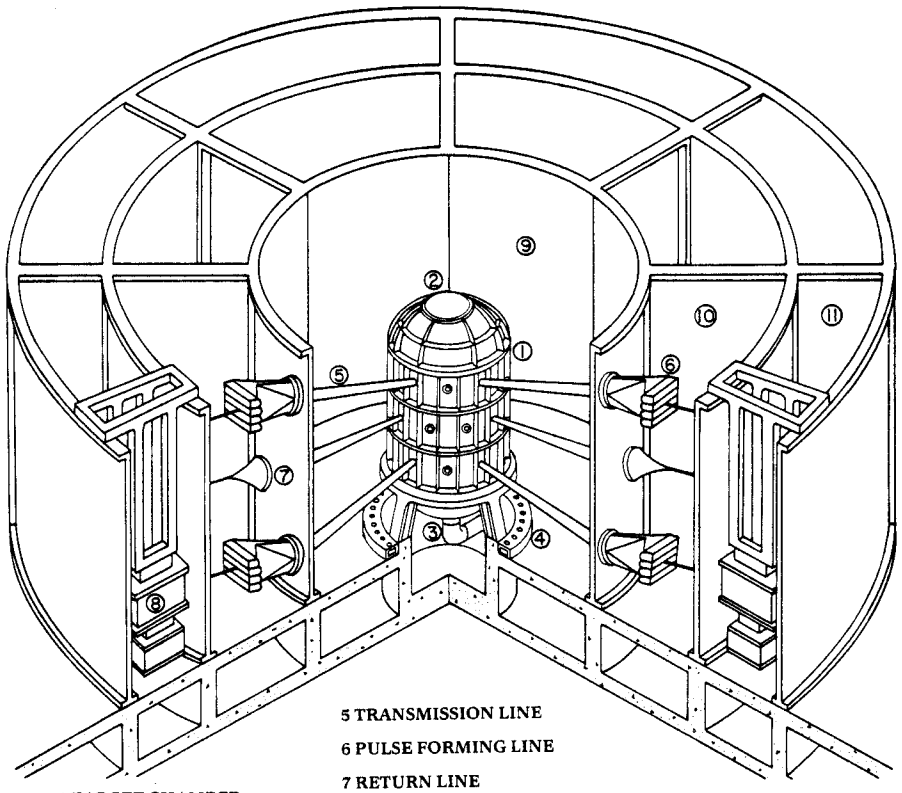

Fig. 9.1 Light Ion Beam Target Development Facility

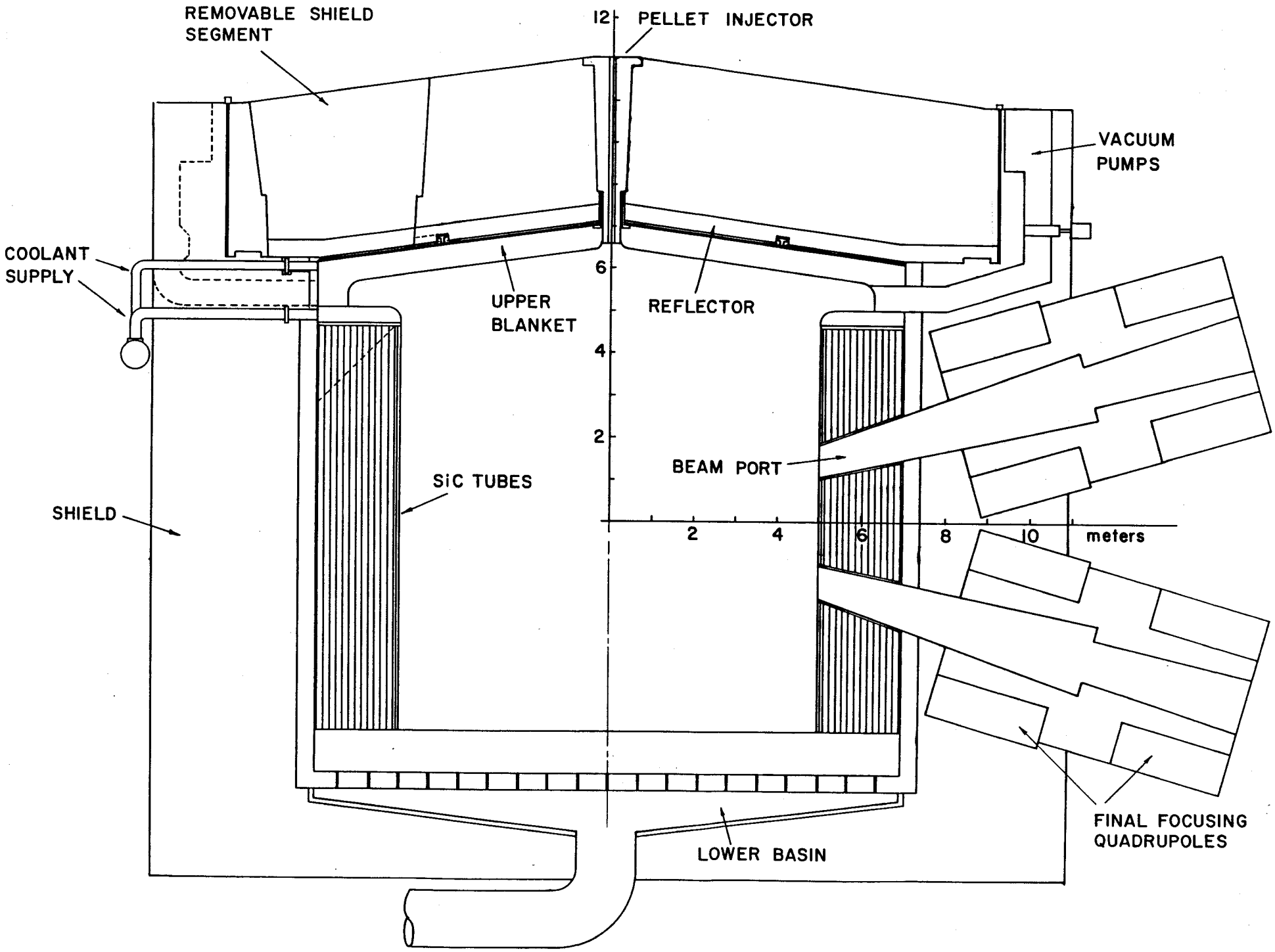

Fig. 9.2 HIBALL cavity design.

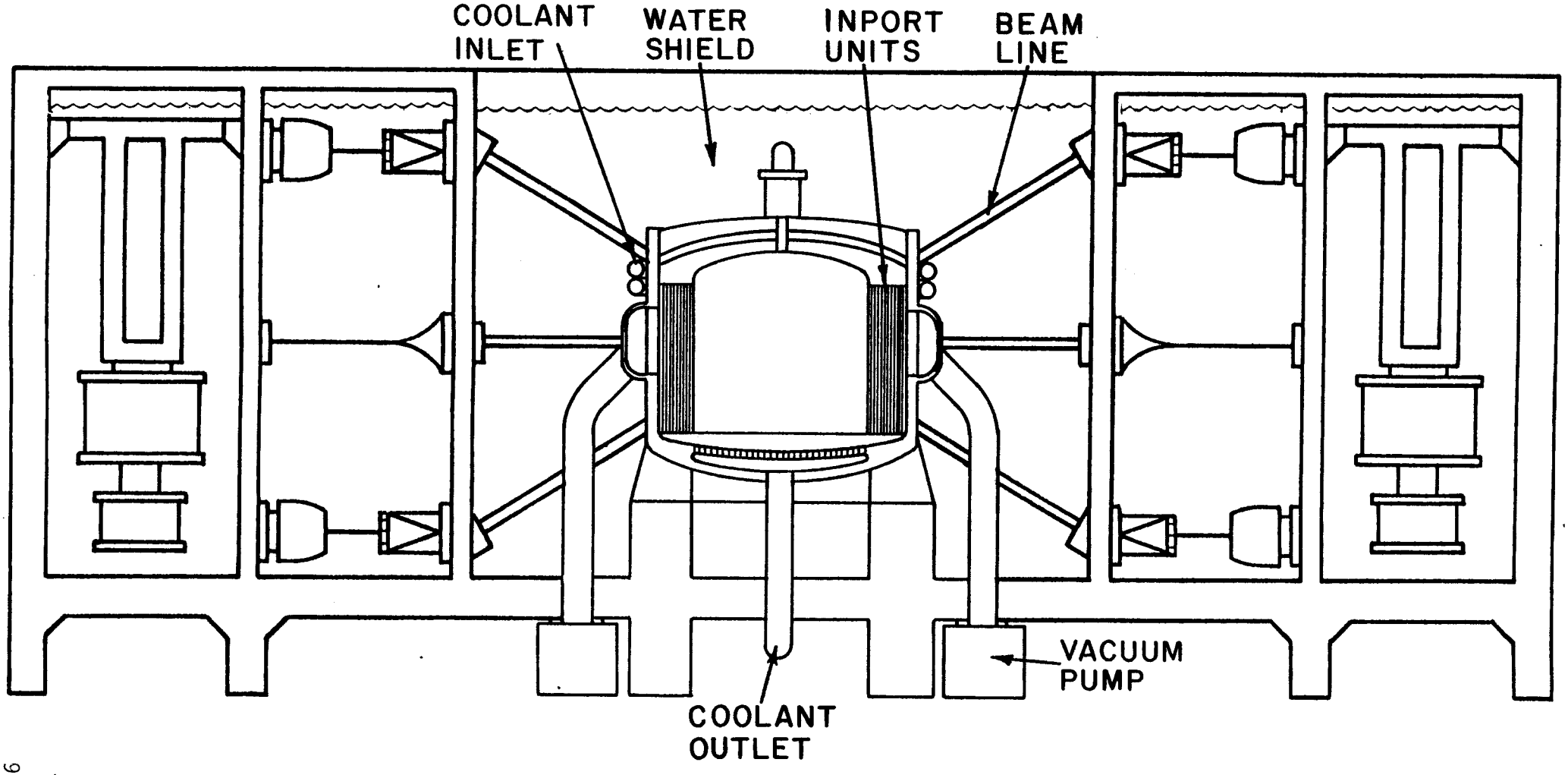

Fig. 9.3 LIBRA light ion beam reactor design.

handled by compressors and other gas handling equipment that is part of the gas cycle.

We must emphasize that this concept is preliminary and significant modifications could be made to it before it is established as the LIBRA design.

10. Reactor Shielding

We propose the use of a water shield in the LIBRA design. Such a shield design has been proposed by the Japanese for a tokamak reactor and was used in the light ion beam TDF design discussed in Part 1 of this report. The TDF design with a water shield is shown in cross section in Fig. 10.1. The water shield has several advantages over conventional concrete shields. These include:

1. Extremely good accessibility to the reaction chamber.
2. No neutron streaming problems except through penetrations.
3. Low activation by continuous processing of the water.
4. Good containment during breach of vessel accident.
5. Good flexibility in design option.
6. Cost?

Possible disadvantages include:

1. Loss of shielding by leaks.
2. No structural integrity.
3. Water-coolant interaction in case of leaks in the blanket.
4. Pressure wave propagation in the shield.
5. Ejection of submerged evacuated vessel.
6. Water is poor shielding material for high energy neutrons and gamma rays.
7. Radiolytic decomposition.

Further analysis must be done to assess the relative merits of a water shield within the context of a complete reactor design.

Fig. 10.1 Light ion beam target development facility with a swimming pool water shield.

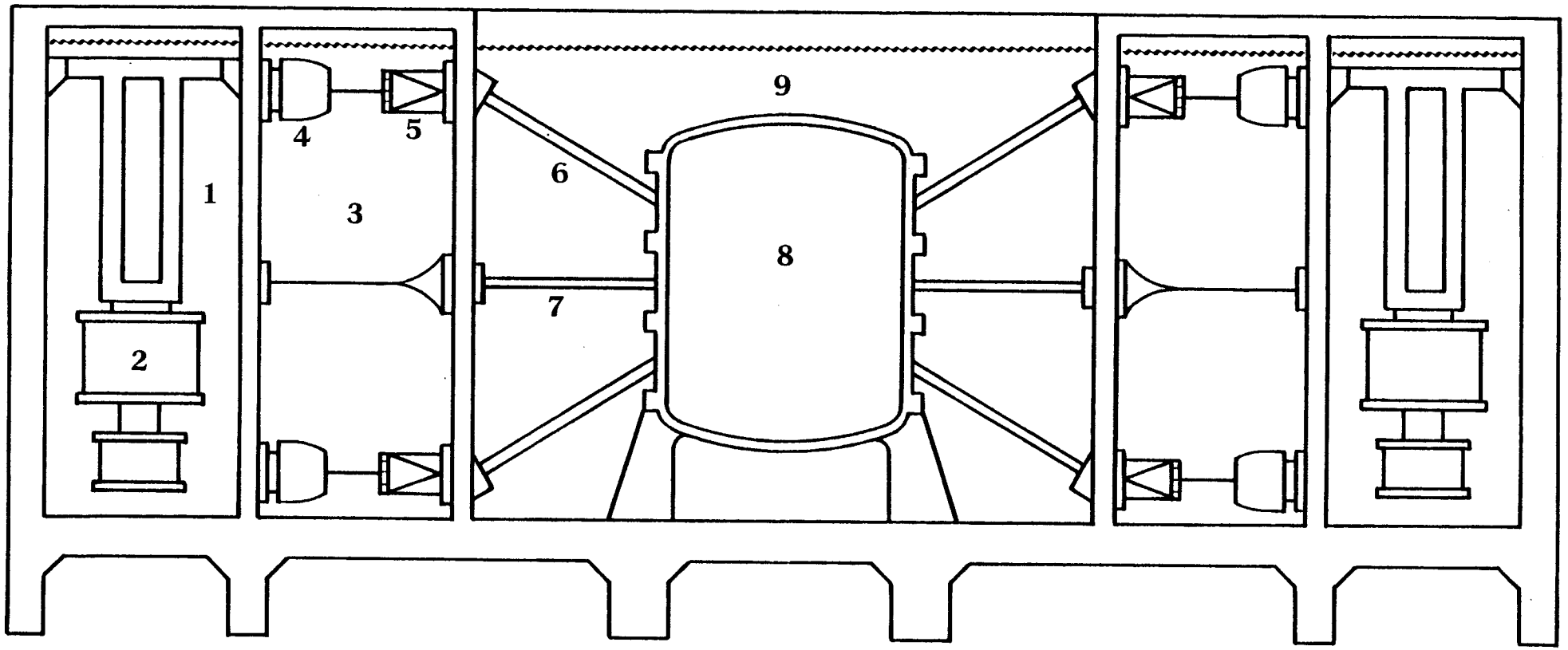

1 ENERGY STORAGE SECTION – OIL

2 BEAM MARX GENERATOR

3 PULSE FORMING SECTION – WATER

4 INTERMEDIATE STORAGE CAPACITOR

5 PULSE FORMING LINE

6 TRANSMISSION LINE

7 RETURN LINE

8 REACTION CHAMBER

9 SHIELDING POOL – WATER

11. Future Work

Calendar year 1982 was spent in background studies, scoping the LIBRA reactor parameters, and addressing some critical issues that arose during the scoping studies. For CY83 there are at least two directions that might be taken, depending on the resources available.

The first option would be to move into a full scale reactor design a la HIBALL. This is the preferred option, but it would require a significant increase in the effort on diode and target designs. These studies could be performed at KfK or in the U.S.

There are many issues which can be fruitfully addressed even though specific target or diode designs are not available. For example, an integrated cavity design which begins with a "generic" target output, that is coupled to a cavity gas and which allows reasonable beam propagation, could be analyzed. The interaction of the neutrons and cavity gas with a cavity wall can be determined and blanket modules could then be designed. The method used to exhaust the cavity gas is a critical area of investigation which can only be analyzed when a specific cavity is designed. Therefore a significant first wall, blanket, and shield design effort would be required.

The coupling of the LIBRA reactor chamber to a useful power cycle and the associated safety, environmental, and economic factors are areas of study which have a large impact on the overall system desirability. Therefore, such studies need to be performed early in the project so that appropriate feedback can be analyzed. Finally, the publication of a self-consistent LIBRA design document (e.g., on the scale of UWMAK, HIBALL, TASKA, etc.) could have a large impact on the ICF community in general and could be extremely important in maintaining public interest in the overall FRG-ICF program.

The second option is to limit the next year's work to critical issues that have arisen from the CY82 work. Specifically, the areas which could be studied somewhat independent of the entire reactor design are:

A. Channel formation and beam propagation.

B. Fireball analysis.

C. Cavity gas exhaust.

D. Cavity first wall design.

We have a start on developing beam propagation codes (see Chapter 5) and depending on the level of resources applied, such codes could be available for general use in 18 months to 2 years. These codes would give important insight into beam dimensions, space charge effects and cavity rep rate requirements (i.e., when will the cavity be "ready" for another beam injection sequence?).

The fireball analysis (Chapter 7) continues to show how we can mitigate the heat and shock wave effects of a thermonuclear explosion in a cavity gas. However, more detailed physics is required to completely analyze the propagation of the fireball back down the channels through which the beam was injected. Other atomic physics modifications need to be made as we add doping materials to alter the time sequence of radiation emission.

The exhaust of the hot cavity gas, even though it is at a low density, has been a problem with no satisfactory solution for over 5 years. The reduction in the cavity pulse rate in LIBRA has alleviated that problem somewhat, but it has transferred the problem to the blanket where the time between shots is now long enough that fatigue problems could arise. Therefore, even more work is required to come up with a credible scheme that will be consistent with the entire reactor operating sequence.

Finally, the design of a cavity wall for the LIBRA reactor is of major importance. The details of the design depend on how successful we are at modifying the radiation spectra from the target. Whether or not the INPORT scheme will work, or whether the "mist" configuration of EAGLE is necessary are important questions to be decided. Once those decisions are made a structural design of the first metallic wall facing the cavity gas can be made. Stress and fatigue analyses will be required to estimate wall lifetimes in the LIBRA environment.

In summary, we feel that significant progress on LIBRA has been made in CY82 to go to a full scale conceptual reactor design. However, this would require a significant increase in manpower and financial resources. If this is not possible, then there are several critical issues which can be studied during CY83 until such time as resources are available to initiate a larger conceptual reactor study.

APPENDIX

A bibliography of light ion beam fusion-related papers and articles was prepared during CY82. A listing follows.

LIGHT ION BEAM BIBLIOGRAPHY

Argonne National Laboratory

Magelssen, G.R. no date
X-Ray and Pressure Conditions on the First Wall of a Particle Beam Inertial Confinement Reactor

Australian National University

Marshall, R.A.
Railguns rec'd. 6/1982

Bechtel Inc.

no author 4/1982
Light Ion System Analysis and Design Phase I: Engineering Test Reactor Goal Specification Final Report (DRAFT)

no author no date
Light Ion Fusion Chamber Design Issues (Set of Viewgraphs)(no other information)

Thomson, S. 12/1978
Electron Beam Fusion-Fission Reactor Systems Study

no author no date
Viewgraphs relating to EAGLE Reactor

Allen, W.O. no date
Light Ion System Analysis and Design

Caird, J.A. Allen, W.O. 1980
Technical Research and Development Project 90307

no author 10/1978
1075 MWe Electron Beam Fusion-Fission Power Plant Captial Cost Estimate

Cornell University

Nation, J.N. Sudan, R.N. editors 10/1977
Proceedings of the 2nd International Topical Conference on High Power Electron and Ion Beam Research and Technology, 3-5 Oct. 1977 (2 Vols.)

Electric Power Research Institute

EPRI AP-1371 Brueckner, K.A. et al. 2/1980
Assessment of Drivers and Reactors for Inertial Confinement Fusion Final Report

Euratom – C.E.A.

Chevallier, J. et al. no date
Pulsed Electron Beam Generators Operating in C.E.A.

International Atomic Energy Agency

Kuswa, G.W. 7/1980
Progress Toward Fusion with Light Ions (SAN)

IAEA-CN-41/N-1 Yonas, G. 9/1982
Inertial Fusion Research Based on Pulsed Power (from IAEA 9th International Conference on Plasma Physics and Controlled Nuclear Fusion Research)(SAN)

IAEA-CN-41/N-2 Cooperstein, G. et al. 9/1982
Light-Ion Inertial-Confinement-Fusion Research at NRL (NAV) (From 9th IAEA Conference on Plasma Physics and Controlled Nuclear Fusion Research)

IAEA-CN-41/N-4 Imasaki, K. et al. 9/1982
Light Ion Beam Fusion Research in Japan (from IAEA 9th International Conference on Plasma Physics and Controlled Nuclear Fusion Research)

Cooperstein, G. et al. 7/1980
Progress at NRL and Cornell in Light Ion Beam Research for ICF (NAV)(COR)

JAYCOR, Inc.

Sandel, F.L. et al. 7/1981
Experimental Studies of Intense Light-Ion Beam Transport

AD-A-081958 Mako, F. 2/1980
Investigation of Collection Ion Acceleration Using Intense Relativistic Electron Beams Final Report, 11 Dec. 1978 – 13 December 1979

Johann Wolfgang Goethe University

UFTP Pre. 90/1982

Buchwald, G. et al. rec'd. 11/1982
Geometrical Stability of Inertial Confrinment (sic) (ICF) Targets

Kernforschungszentrum Karlsruhe GmbH

KfK 3232 Long, K.A. Tahir, N.A. 10/1981
Energy Deposition of Ions in Materials, and Numerical Simulations of Compression, Ign. and Burn of Ion Beam Driven ICF Pellets

Kurchatov Institute for Atomic Energy

Baranchikov, E.I et al. no date
Transfer and Focusing of High-Current Relativistic Electron Beams onto a Target

Bogolyubskij, S. et al. no date
Demonstration of the Possibility of Using Electron Beams for Heating Thermonuclear Targets

Lawrence Berkeley Laboratory

LBL-10301 Guiragossian, Z. Hermannsfeldt, W (editor) 9/1980
Light Ion Fusion Experiment (LIFE) Accelerator System for ICF

Los Alamos National Laboratory

Bangerter, R.O. et al. no date
Stability and Symmetry Requirements of Electron and Ion Beam Fusion Targets

LA-7014-MS Bohachevsky, I.O 11/1977
Scaling of Reactor Cavity Wall Loads and Stresses

LA-8327-MS Slaughter, M.D. 4/1980
A Numerical and Theoretical Analysis of Some Spherically Symmetric Containment Vessel Problems

LA-UR-81-1408 Guiragossian, Z.G et al. 1981
Method of Active Charge and Current Neutralization of Intense Ion Beams for ICF

LA-UR-81-1873 Lemons, D.S. 1981
Electron-Temperature Requirements for Neutralized Inertial-Confinement-Fusion Light-Ion Beams

LA-UR-81-2989 Bangerter, R.O. Mark, J.W-K. Meeker, D.J. 1981
Target Gain for Ion Driven Inertial Targets

Riepe, K.B. Stapleton, R.E. no date
Electron-Beam-Controlled Gas Lasers: Discussion from the Engineering Viewpoint Part II. Problems in the Electrical Design of Very High Energy Systems

MOD (PE) Atomic Weapons Research Laboratory

Martin, J.C. no date
Short Pulse High Voltage Systems

Maxwell Laboratories

Harrison, J. et al. no date
Compact Electron Beam Generators for Laser and Fusion Research

Harrison, J. et al. no date
Design of Very Fast Rise and Fall Time, Low Impedance Megavolt Pulse Generators for Laser Excitation

McDonnell–Douglas Astronautics Company

Fraley, T.G. 8/1982
An Investigation into the Use of Graphite and Silicon Carbide in Ion Beam Reactors

Nagoya University

IPPJ-601 Kawata, S. Niu, K. Murakami, H. 6/1982
Formation of Z-Discharged Plasma Channel in LIB-Fusion Device

Kubota, Y. Miyahara, A. Kawasaki, S. no date
2 MV Coaxial Marx Generator for Producing Intense Relativistic Electron Beams

Naval Research Laboratory

AD-1–076154 Ottinger, P.F. Mosher, D. Goldstein, S.A. 10/1979
Electromagnetic Instabilities in a Focused Ion Beam Propagating through a Z-Discharge Plasma Interim Report

NRL 4380 Raleigh, M. et al. 2/1981
Laser-Initiated, Reduced Density Channels for Transporting Charged Particle Beams

NRL MR-3784 Ottinger, P.F. Mosher, D. Goldstein, S.A. 6/1978
Microstability of a Focussed Ion Beam Propagating Through a Z-Pinch Plasma

NRL MR-4088 Ottinger, P.F. Mosher, D. Goldstein, S.A. 10/1979
Electromagnetic Instabilities in a Focused Ion Beam Propagating through a Z-Discharge Plasma

NRL MR-4387 Cooperstein, G. et al. 11/1980
NRL Light Ion Beam Research for Inertial Confinement Fusion

NRL MR-4397 Mosher, D. Colombant, D.G. Goldstein, S.A. 11/1980
Beam Requirements for Light-Ion-Driven Inertial-Confinement Fusion

NRL MR-4462 Bleach, R.D. et al. 1981
X-Ray Diagnostic for Light-Ion Current Measurements

NRL MR-4726 Young, F.C. et al. 1/1982
Production of Intense Light Ion Beams from a Superpower Generator

NRL MR-4747 Grun, J. et al. 3/1982
Ablative Acceleratiion of Planar Targets to High Velocities

NRL MR-4773 Barker, R.J. Goldstein, S.A. 4/1982
The Use of Finite J_θ for Increasing the Ion Efficiency of High Impedance Diodes

NRL MR-4926 Obenschain, S.P. et al. 9/1982
Uniform Laser Ablative Acceleration of Targets at 10E14 W/cm^2

NRL MR-4948 Ottinger, P.F. Goldstein, S.A. Mosher, D. 11/1982
Constraints on Transportable Ion Beam Power

Burton, J.K. no date
The TRITON Electron Beam Accelerator

Ottinger, P.F. Mosher, D. Goldstein, S.A. 3/1981
Stability Considerations for Light-Ion Beam Transport in Z-Discharge Channels

Blaugrund, A.E. Stephanakis, S.J. Goldstein, S.A. no date
A Time Resolved Beam Profile Monitor for Intense Ion Beams

Mosher, D. 4/1981
Light-Ion-Beam Transport for Inertial Confinement Fusion

Goldstein, S.A. et al. 7/1981
Ion Beam Handling in Magnetized Plasmas

Mosher, D. et al. 7/1981
System Requirements for Light-Ion ICF

Mosher, D. 7/1981
Recent Progress in the NRL Light-Ion Program

Mosher, D. 7/1981
ICF Research Outside the United States Some Background Information and Highlights of the International Topical Conference on High-Power Electron and Ion Beam Research

Cooperstein, G. et al. 7/1981
Light Ion Production and Focusing with Pinch-Reflex Diodes

Osaka University

ILE 8119P Ozaki, T. et al. 9/1981
Generation and Focussing of Intense Ion Beams in Pinch–Reflex Diode

ILE 8127P Yamanaka, C. et al. 10/1981
Concept and Design of ICF Reactor "SENRI-I"

ILE 8128P Nakai, S. et al. 10/1981
Neutronics in ICF Reactor "SENRI-I"

ILE 8214P Nakashima, H. et al. 11/1982
Time Dependent Analysis of Radiation Damage to the Stainless Steel Walls of the Laser Fusion Reactor Design, SENRI-I(II)

ILE 8215P Ido, S. et al. 11/1982
Conceptual Design of ICF Reactor SENRI, Part II – Advances in Design and Pellet Gain Scaling

ILE 8216P Tsuji, R. Ido, S. 11/1982
Inner Frozen Metal Blanket Concept for an ICF Reactor

Nakai, S. Imasaki, K. Yamanaka, C. no date
Relativistic-Electron-Beam-Induced Fusion

Physics International

Aslin, H. no date
Fast Marx Generator

Smith, I. no date
Liquid Dielectric Pulse Line Technology

Sandia National Laboratory

SAND76-0615 Mogford, J.A. Garner, W.L. editors 10/1976
Sandia Technology: Particle Beam Fusion (various articles)

SAND76-5122 Vol. I&II Yonas, G. editor 2/1976
Proceedings of the International Topical Conference on Electron Beam Research and Technology Albuquerque, NM, 3-5 November 1975

SAND78-0110C Cook, D.L. Sweeney, M.A. 6/1978
Deisgn of Compact Particle-Beam-Driven Inertial-Confinement Fusion Reactors

SAND78-0753 Prestwich, K.R. Cook, D.L. Yonas, G. 1978
Pulsed Power Technology for Inertial Confinement

SAND79-0222C Cook, D.L. Sweeney, M.A. 1/1979
Critical Environmental Considerations for Particle-Beam-Driven ICF Reactor Materials

SAND79-0600C Sweeney, M.A. 1979
Sandia Particle Beam Fusion Program

SAND79-0734C Freeman, J.R. et al. 1979
Electron and Ion Beam Transport to Fusion Targets

SAND79-0819C Kuswa, G.W. Bieg, K.W. Burns, E.J.T. 1979
Progress Toward Fusion with Particle Beams

SAND79-0949C Van Devender, J. 1979
Pulsed Power Systems for Inertial Confinement Systems

SAND79-1011 Sweeney, M.A. Cook, D.L. 12/1979
Particle Beam Fusion Progress Report 4/78 - 12/78

SAND79-1411C Clauser, M.J. Burns, E.J. Chang, J. 1979
Particle Beam Interactions with Plasmas and their Application to Inertial Fusion

SAND79-1611 Cook, D.L. Sweeney, M.A. 11/1979
The Pellet Injection Problem in a Gas-Filled Particle Beam Reactor

SAND79-1673 Humphries, S.Jr. et al. 8/1979
Production and Post-Acceleration of Intense Ion Beams in Magnetically Insulated Gaps

SAND79-1927C Mehlhorn, T.A. 1980
Ion Beam Energy Deposition Physics for ICF Targets

SAND79-1942C Bieg, K.W. Chang, J. 1980
Target Fabrication for Particle Beam Fusion

SAND79-1944 Cook, D.L. 1979
Pellet Injection, Protection and Targeting

SAND79-2133C Yonas, G. 1979
Pulsed Power Particle Beam Fusion Research

SAND79-7044 no author 5/1979
Technical Review of the Sandia Laboratories Particle Beam Fusion Program

SAND80-0038 Mehlhorn, T.A. 1980
Finite Material Temperature Model for Ion Energy Deposition in Ion-Driven ICF Targets

SAND80-0154 Olsen, J.N. Baker, L. 2/1980
Laser Heating of a Molecular Gas Channel

SAND80-0367C Kuswa, G.W. 1980
Pulse-Power Driven Light Ion Accelerators for Fusion: The Sandia Approach

SAND80-0387C Wright, T.P. et al. 1980
Light-Ion Transport in Plasma Channels for ICF

SAND80-0466C Cook, D.L. 3/1980
Technological Aspects of Particle Beam Fusion

SAND80-0974 Sweeney, M.A. Cook, D.L. 1/1981
Particle Beam Fusion Progress Report 6/79 - 12/79

SAND80-1355C no author 1980
Progress Toward Fusion with Light Ions

SAND80-2425C Cook, D.L. et al. 10/1980
Light Ion Driven Inertial Fusion Reactor Concepts

SAND80-2436C Yonas, G. 1980
Light Ion Beams as a Potential ICF Ignition Source and Requirements for Reactor Application

SAND80-2788C Cook, D.L. Sweeney, M.A. 1981
Heating of Cryogenic Targets in a Light-Ion Fusion Cavity

SAND80-7001 Moses, G.A. Abdel-Khalik, S. Drake, D. 8/1980
First Wall and Cavity Design Studies for a Light Ion Beam Driven Fusion Reactor

SAND81-0445C Quintenz, J.P. Kuswa, G.W. 1981
Light Ion Ignitors for Inertial Confinement Fusion: Progress Toward Proof-of-Principle

SAND81-0672C Kuswa, G.W. Quintenz, J.P. Seidel, D.B. 1981
Scalability of Light Ion Beams to Reach Fusion Conditions

SAND81-0842C Mix, L.P. et al. . 1981
Low-Energy X-Ray Emission from Light Ion Targets

SAND81-1459 no author 3/1982
Particle-Beam Fusion Progress Report January 1981 through June 1981

SAND81-2009 Humphries, S.Jr. Lockner, T.R. November 1981
High Power Pulsed Ion Beam Acceleration and Transport

SAND82-1740 Mendel, C.W.Jr. Slutz, S.A. Seidel, D.B. 8/1982
Analytic, Two-Dimensional, Time-Dependent Theory of Magnetically Insulated Electron Flow

SAND82-0304 Mendel, C.W.Jr. 10/1982
Analytical Theory of Series Field Coil Ion Diodes

Humphries, S.Jr. 4/1980
Magnetic Field Effects in Light Ion Fusion Transport (Internal Memo)

Cook, D.L. rec'd. 6/1982
Engineering Aspects of Particle Beam Fusion Systems

Cook, D.L. Sweeney, M.A. no date
Critical Environmental Considerations for Particle-Beam-Driven ICF Reactor Materials

Kuswa, G.W. et al. no date
Progress Toward Fusion with Particle Beams

Quintenz, J.P. Kuswa, G.W. no date
Light Ion Ignitors for Inertial Confinement Fusion: Progress Toward Proof-of-Principle

Olsen, J.N. Leeper, R.J. 1981
Ion Beam Transport in Laser Initiated Discharge Channels

Prestwich, K.R. Cook, D.L. Yonas, G. no date
Pulsed Power Technology for Inertial Confinement

Kuswa, G.W. et al. no date
High Power Magnetically Insulated Radial Diode

Prestwich, K.R. no date
Pulse Power Technology Application to Lasers

Kuswa, G.W. no date
Inertial Confinement Fusion Energy with Particle Beams

Martin, T.H. no date
High Power Laser Exciter Accelerators

Cook, D.L. 10/1979
Impulse and Overpressure on PBFA-I (Memo to J.P. VanDevender)

no author no date
Viewgraphs relating to LIB Reactors

VanDevender, J.P 10/1981
Drivers for Light Ion Fusion (In "Particle Beam Fusion Articles", SNL)

Cook, D.L. et al. 10/1981
Light Ion Driven Inertial Fusion Reactor Concepts (In "Particle Beam Fusion Articles", SNL)

Yonas, G. 10/1980
Light Ion Beams as a Potential ICF Ignition Source and Requirements for Reactor Application (In "Particle Beam Fusion Articles", SNL)

Yonas, G. 4/1980
Testimony on Particle Beam Fusion Research House Armed Services Committee

Cook, D.L. Sweeney, M.A. no date
Design of Compact Particle-Beam-Driven Inertial-Confinement Fusion Reactors

Sweeney, M.A. Cook, D.L. 11/1979
Blast-Wave Kinetics and Thermal Transport in a Particle-Beam Reactor Chamber

Clauser, M.J. Sweeney, M.A. no date
Charged-Particle Beam Implosion of Fusion Targets

Yonas, G. 9/1981
Inertial Fusion Research Using Pulsed Power Drivers

Olsen, J. no date
Ion Beam Transport Experiments In Laser- or Wire-Triggered Discharges

Johnson, D.L. no date
Parallel Plate Transmission Line (Lecture Notes)

Miller, P.A. et al. no date
REB Propagation and Combination in Plasma Channels

Ramirez, J.J. Prestwich, K.R. no date
REBLE, A Radially Converging Electron Beam Accelerator

Humphries, S.Jr. no date
Intense Pulsed Linear Ion Accelerators for Inertial Fusion

Mendel, C.W.Jr. Goldstein, S.A. no date
Electron Beam Pinching from Discrete Large Diameter Cathodes

Miller, P.A. et al. no date
REB Pinching, Transport, and Combination in Plasma Channels for ICF

no author 1/1980
Particle Beam Fusion

Kuswa, G.W. no date
Pulse-Power Driven Light Ion Accelerators for Fusion - The Sandia Approach

Kuswa, G.W. et al. 7/1981
Scalability of Light Ion Beams to Reach Fusion Conditions

Freeman, J.R. et al. no date
Particle Beam Fusion Research

various authors 10/1981
Presentations from: Light Ion Design Review and R&D Plan Workshop s

Science Applications, Inc.

Drobot, A.T. et al. 7/1981
Electromagnetic and Quasi-Static Simulations of Ion Diodes

University of Illinois

Johnson, G.B. 1980
Ion Bunching at High Energies

University of New Mexico

NE-74 Cooper, G.W. 10/1979
A Feasibility Study of Laser Guided Discharges

University of Tokyo

UTNL-R 0135 Oka, Y. et al. 6/1982
Preliminary Design of Light Ion Beam Fusion Reactors, UTLIF(1) & ADLIB-I

UTNL-R 0142 Madarame, H. 9/1982
A Conceptual Design of Light Ion Beam Fusion Reactor - UTLIF(I)

UTNL-R 0144 Madarame, H. et al. 9/1982
A Conceptual Design of Light Ion Beam Fusion Reactor - ADLIB-I

University of Toronto

Measures, R.M. Cardinal, P.G. no date
Laser Ionization Based on Resonance Saturation - A Simple Model Description

Measures, R.M. Cardinal, P.G. Schinn, G. no date
A Theoretical Model of Laser Ionization of Alkali Vapours Based on Resonance Saturation

University of Wisconsin

UWFDM-307 Peterson, R.R. Moses, G.A. 6/1979
MFP - A Calculation of Radiation Mean Free Paths, Ionization and Internal Energies in Noble Gases

UWFDM-315 Peterson, R.R. Moses, G.A. 10/1979
Blast Wave Calcualtions in Argon Cavity Gas for Light Ion Beam Fusion Reactors

UWFDM-320 Moses, G.A. et al. 10/1979
First Wall and Cavity Design Studies for a Light Ion Beam Driven Fusion Reactor

UWFDM-322 Engelstad, R.L. Lovell, E.G. 12/1979
First Wall Mechanical Design for Light Ion Beam Fusion Reactors

UWFDM-323 Moses, G.A. Peterson, R.R. 10/1979
First Wall Protection in ICF Reactors by Inert Cavity Gases

UWFDM-336 Moses, G.A. Peterson, R.R. 1/1980
FIRE - A Computer Code to Simulate Cavity Gas Response to Inertial Confinement Target Explosions

UWFDM-371 Peterson, R.R. Cooper, G.W. Moses, G.A. 8/1980
Cavity Gas Analysis for Light Ion Beam Fusion Reactors

UWFDM-372 Peterson, R.R. Moses, G.A. 9/1980
MIXER - A Multi-Species Optical Data and Equation of State Computer Code

UWFDM-382 Peterson, R.R. et al. 12/1980
TSTRESS - A Transient Stress Computer Code

UWFDM-405 McCarville, T.J. Kulcinski, G.L. Moses, G.A. 1/1981
An Analytical Model for the Motion and Radiative Response of a Low Density Inertial Confinement Fusion Buffer Gas

UWFDM-406 McCarville, T.J. Kulcinski, G.L. Moses, G.A. 1/1981
A Model for the Deposition of X-Rays and Pellet Debris from Inertial Confinement Fusion Targets into a Cavity Gas

UWFDM-407 McCarville, T.J. Peterson, R.R. Moses, G.A. 2/1982
Improvements in the FIRE Code for Simulating the Response of a Cavity Gas to ICF Target Explosions

UWFDM-414 Badger, B. et al. 1/1982
Progress Report to Sandia for Light Ion Beam Activities During 1980-1981

UWFDM-421 Lovell, E.G. et al. 8/1981
Transient Elastic Stresses in ICF Reactor First Wall Structural Systems

UWFDM-423 Hassanein, A.M. McCarville, T.J. Kulcinski, G.L. 8/1981
First Wall Evaporation in Inertial Confinement Fusion Reactor Utilizing Gas Protection

UWFDM-442 Peterson, R.R. Lee, K.J. Moses, G.A. 10/1981
Low Density Cavity Gas Fireball Dynamics in the Light Ion Beam Target Development Facility

UWFDM-455 Peterson, R.R. Lee, K.J. Moses, G.A. 1/1982
Fireball Propagation in Preformed Plasma Channels in the Light Ion Beam Driven Target Development Facility

UWFDM-456 Peterson, R.R. et al. 2/1982
Choice of First Wall Material in the Light Ion Beam Target Development Facility

UWFDM-457 Badger, B. et al. 2/1982
Report to Sandia Laboratory on University Wisconsin Fusion Engr. Program Design Activities for the LIB TDF from Aug. 1981 - Feb. 1982

UWFDM-458 Moses, G.A. McCarville, T.J. Peterson, R.R. 3/1982
Documentation for MF-FIRE, A Multifrequency Radiative Transfer Version of FIRE

UWFDM-476 O'Brien, K.J. Moses, G.A. 6/1982
Bubble Screen Shielding of Water Pressure Waves Emitted by a Harmonically Pulsating Vessel

UWFDM-486 Moses, G.A. 9/1982
Frequency Dependent X-Ray Fluences from a High Yield Light Ion Beam Fusion Target Explosion in a Gas Filled Chamber

UWFDM-487 Engelstad, R.L. Lovell, E.G. November 1982
Modal Analysis of Light Ion Beam Fusion Reactor Vessels

Other Reports and Articles

Bergeron, K.D.
Equivalent Circuit Approach to Long Magnetically Insulated Transmission Lines (SAN) [Reprint: J. Appl. Phys. 48, pp. 3065-3069 1977]

Bergeron, K.D.
Theory of the Secondary Electron Avalanche at Electrically Stressed Insulator-Vacuum Interface (SAN) [Reprint: J. Appl. Phys. 48, pp. 3073-3080 7/1977]

Bergeron, K.D. Poukey, J.W.
Relativistic Space-Charge Flow in a Magnetic Field (SAN) [Reprint: Appl. Phys. Lett. 27, pp. 58-60 7/1975]

Bergeron, K.D.
One- and Two-Species Equilibria for Magnetic Insulation in Coaxial Geometry (SAN) [Reprint: Phys. Fluids 20, pp. 688-697 4/1977]

Blaugrund, A.E. Cooperstein, G. Goldstein, S.
Relativisitic (sic) Electron Beam Pinch Formation Processes in Low Impedance Diodes (NAV)(UMD) [Reprint: Phys. Fluids 20, pp. 1185-1194 7/1977]

Blaugrund, A.E. Cooperstein, G.
Intense Focusing of Relativistic Electrons by Collapsing Hollow Beams (NAV) [Reprint: Phys. Rev. Lett. 34, pp. 461-464 2/1975]

Booth, L.A.
Considerations for Inertial Confinement Fusion Reactor Design [Atomkernerergie/Kerntechnik 36, pp. 211-212 1980]

Briggs, R.J. et al.
Transport and Self-Focused Relativistic Electron Beams [From: 2nd Int. Top. Conf. High Power E. & Ion Bea1977]

Buchanan, H.L. et al.
Transport of Intense Particle Beams with Application to Heavy Ion Fusion [From: Proc. 3rd Int. Top. Conf. on High Power E. 1979]

Colombant, D.G. Goldstein, S.A. Mosher, D.
Hydrodynamic Response of Plasma Channels to Propagating Ion Beams (NAV) [Reprint: Phys. Rev. Lett. 45, pp. 1253-1256 10/1980]

Cook, D.L. Sweeney, M.A.
Critical Environmental Considerations for Particle-Beam-Driven ICF Reactor Materials (SAN) [Reprint: J. Nucl. Matls. 85&86, pp. 127-131 1979]

Cook, D.L.
Technological Aspects of Particle Beam Fusion [20th Annual ASME Symp., pp. 37-46 1980]

Cooperstein, G. et al.
High-Intensity Light-Ion Beam Research at NRL(NAV) [From Japan-US Seminar, Thy. & Appl. of Multiply Ionized Plasmas Prod. by Laser & Part. Beams]

Destler, W.W. et al.
Collective Acceleration of Light and Heavy Ions (UMD) [Reprint: IEEE Trans. Nucl. Sci. NS-28 1981]

Didenko, A.N. et al.
Generation of High Power Ion Beams in Ballistic Focusing Diodes (TOM) [Reprint: IEEE Trans. Nucl. Sci. NS-28, p. 3436 1981]

Frazier, G. et al.
no title [From 3rd IEEE Int. Pulsed Power Conf. 6/1981]

Freeman, J.R. Baker, L. Cook, D.L.
no title [From: 4th Conf. on High Power E. & Ion Beam Res. 6/1981]

Freeman, J.R. Baker, L. Cook, D.L.
Plasma Channels for Intense-Light-Ion-Beam Reactors [Reprint: Nucl. Fus. 22 (1982) 383-393]

Freiwald, D.A. Axford, R.A.
Approximate Spherical Blast Theory Including Source Mass (LOS) [Reprint: J. Appl. Phys. 46, pp. 1171-1174 3/1975]

Goldstein, S.A. Lee, R.
Ion-Induced Pinch and the Enhancement of Ion Current by Pinched Electron Flow in Relativistic Diodes (UMD)(NAV) [Reprint: Phys. Rev. Lett. 35, pp. 1079-1082 10/1975]

Goldstein, S.A. et al.
Focusing of Intense Ion Beams from Pinched-Beam Diodes (NAV) [Reprint: Phys. Rev. Lett. 40, pp. 1504-1507 6/1978]

Gorbulin, Yu. M. et al.
REB Focusing Analysis with High Time Resolution (KUR) [From Japan-US Seminar, Thy. & Appl. of Multiply Ionized Plasmas Prod. by Laser & Part. Beams]

Grieg, J.R. et al.
Electrical Discharges Guided by Pulsed CO_2Laser Radiation (NAV) [Reprint: Phys. Rev. Lett. 41, pp. 174-177 7/1978]

Guragossian, Z.G et al.
Method of Active Charge and Current Neutralization of Intense Ion Beamsfor ICF (TRW) [Reprint: IEEE Trans. Nucl. Sci. NS-28, p. 3398 1981]

Halbleib, J.A. et al.
Overlap of Intense Charged Particle Beams for Inertial Confinement Fusion [Nature (London) 286, pp. 366-368 1980]

Hovingh, J. et al.
Fluid Mechanics Considerations for Liquid Wall Inertially Confined Fusion Reactors (LAL) [From: 8th Symp. on Engr. Prob. Fus. Res. 11/1979]

Humphries, S. Jr et al.
Production and Postacceleration of Intense Ions Beams in Magnetically Insulated Gaps (SAN) [Reprint: J. Appl. Phys. 51, pp. 1876-1895 4/1980]

Humphries, S. Jr
Options for Light-Ion Fusion [Comm. Plasma Phys. Contrl. Fusion 6, pp. 45-52 1980]

Humphries, S. Jr
Intense Pulsed Ion Beams for Fusion Applications (SAN) [Reprint: Nucl. Fus. 20, pp. 1549-1612 1980]

Humphries, S.Jr.
Intense Pulsed Ion Beams for Fusion Applications [Nucl. Fusion 20, pp. 1549-1612 1980]

Humphries, S.Jr. et al.
Pulselac Program: Space Charge Neutralized Ion Beams for Inertial Fusion Applications (SAN) [Reprint: Nucl. Inst. Meth. 187, pp. 289-294 1981]

Humphries, S.Jr. Poukey, J.W.
Proposed Method for the Transport of Ions in Linear Accelerators Utilizing Electron Neutralization (SAN) [Reprint: Particle Accelerators 10, pp. 71-87 1979]

Humphries, S.Jr.
Longitudinal Instabilities of Pulseline Driven Neutralized Linear Ion Accelerators(SAN) [Reprint: J. Appl. Phys. 51, pp. 2338-2347 5/1980]

Humphries, S.Jr.
Velocity Lens Model for Longitudinal Beam Dynamics in Inductive Linear Ion Accelrators (SAN) [Reprint: J. Appl. Phys. 53, pp. 1334-1341 3/1982]

Humphries, S.Jr. Lockner, T.R. Freeman, J.R.
High Intensity Ion Accelerators for Inertial Fusion (SAN) [Reprint: IEEE Trans. on Nucl. Sci., NS-28, pp. 246/1981]

Humphries, S.Jr. et al.
One-Dimensional Ion-Beam Neutralization by Cold Electrons (SAN) [Reprint: Phys. Rev. Lett. 46, pp. 995-998 4/1981]

Humphries, S.Jr.
Intense Ion-Beam Neutralization in Free Space (SAN) [Reprint: Appl. Phys. Lett. 32, pp. 792-794 6/1978]

Imasaki, K. et al.
Implosion Efficiency of Light Ion Beam Driven Target (OSA) [Reprint: J. Phys. Soc. Japan 50, pp. 1819-1820 6/1981]

Imasaki, K. et al.
no title [From: 4th Conf. on High Power E. & Ion Beam Res. 6/1981]

Iners, J.D. Nation, J.A. Roth, I.
Proton Induction in an Induction Linac (COR) [Reprint: IEEE Trans. Nucl. Sci. NS-28, 3380 1981]

Johnson, D.J. et al.
Time-Dependent Impedance Behavior of Low-Impedance REB Diodes During Self-Pinching (NAV) [Reprint: J. Appl. Phys. 49, pp. 4634-4643 9/1978]

Johnson, D.J. et al.
Production of 0.5-TW Proton Pulses with a Spherical Focusing, Magnetically Insulated Diode(SAN) [Reprint: Phys. Rev. Lett. 42, pp. 610-613 2/1979]

Johnson, D.J. et al.
Dual-Current Feed Magnetically Insulated Light-Ion Diode [J. Appl. Phys. 50, pp. 4524-4531 1979]

Jorna, S. Metzler, N. Hammerling, P.
Dependence of Target Yield on Input Energy Profile [Phys. Lett. A 80, pp. 380-382 1980]

Kramer, J.M. Meek, C.C. Predebon, W.W.
A Generalized Analysis of Thermal and Mechanical Loads in Inertial Confinement Reactors (ARG)(MIC) [Reprint: J. Thermal Stresses 3, pp. 537-549 1980]

Lee, E.P. Cooper, R.K.
General Envelope Equation for Cylindrically Symmetric Charged-Particle Beams [Reprint: Particle Accelerators 7, p. 83 1976]

Lerner, E.J.
Electromagnetic Pulses: Potential Crippler [Reprint: IEEE Spectrum, pp. 41-49 5/1981]

Lockner, T.R. Humphries, S.Jr. Ramirez, J.J.
Experiments on the Acceleration and Transport of Multi-Kiloampere Ion Beams (SAN) [Reprint: IEEE Trans. Nucl. Sci. 28, pp. 3407-3409, 1981]

Maenchen, J. et al.
Magnetic Focusing of Intense Ion Beams (COR) [Reprint: Phys. Fluids 22, p. 555-565 1979]

Magelssen, G.R. Gula, W.P.
Scaling Laws for Single-Shell DT Gas-Filled Spherical Targets for Heavy-Ion Fusion (ARG)(LOS) [Reprint: Phys. Fluids 25, pp. 898-904 6/1982]

Martin, T.H. et al.
Particle Beam Fusion Accelerator–I (PBFA-I) (SAN) [Reprint: IEEE Trans. Nucl. Sci. NS-28,

p. 3365 1981]

Measures, R.M. Drewell, N. Cardinal, P.
Electron- and Ion-Beam Transportation Channel Formation by Laser Ionization Based on Resonance Saturation-Libors [Reprint: J. Appl. Phys. 50 1979]

Measures, R.M. Drewell, N. Cardinal, P.
Superelastic Laser Energy Conversion [From: Radiation Energy Conv. in Space Conf. 1978]

Mendel, C.W.
no title (paper 4C3-4) [From: IEEE Int. Conf. Plasma Science 1980]

Mendel, C.W. Jr. Goldstein, S.A.
A Fast-Opening Switch for Use in REB Diode Experiments (SAN) [Reprint: J. Appl. Phys. 48, pp. 1004-1006 3/1977]

Miller, P.A. et al.
Propagation of Pinched Electron Beams for Pellet Fusion (SAN) [Reprint: Phys. Rev. Lett. 39, pp. 92-95 7/1977]

Miller, P.A. Gerardo, J.B.
Relativistic Electron Beam Propagation in High-Pressure Gases (SAN) [Reprint: J. Appl. Phys. 43, pp. 3008-3013 7/1972]

Miller, P.A. et al.
Light Ion and Electron Beams for Inertial Fusion (SAN) [Reprint: Comments Plasma Phys. 5, pp. 95-104 1979]

Moses, G.A. Spencer, R.
Compact-Electron-Beam or Light-Ion-Beam Fusion Reactor Cavity Design Using Non-Spherical Blast Waves [Nucl. Fusion 19, pp. 1386-1388 1979]

Moses, G.A. Peterson, R.R.
First-Wall Protection in Particle-Beam Fusion Reactors by Inert Cavity Gases [Nucl. Fusion 20, pp. 849-857 1980]

Mosher, D. Bernstein, I.B.
Magnetic-Field–Induced Enhancement of Relativistic-Electron-Beam Energy Deposition (NAV) [Reprint: Phys. Rev. Lett. 38, pp. 1483-1486 6/1977]

Mosher, D.
Interactions of Relativistic Electron Beams with High Atomic-Number Plasmas (NAV) [Reprint: Phys. Fluids 18, pp. 846-857 7/1975]

Mosher, D. et al.
no title [From: Conference on High-Power Electron and Ion-Beam Research, 6/1981]

Nakai, S. et al.
Light Ion Beam Fusion Research at ILE Osaka (OSA) [From Japan-US Seminar on Theory and Application of Multiply Ionized Plasmas Produced by Laser and Particle Beams]

Niu, K.
Modeling of LIB Fusion Targets (Tokyo Inst. Technology) [From Japan-US Seminar, Thy. & Appl. of Multiply Ionized Plasmas Prod. by Laser & Part. Beams]

Olsen, J.N.
Laser-Initiated Channels for Ion Transport: CO_2Laser Absorption and Heating of NH_3 and C_2H_4 Gases (SAN) [Reprint: J. Appl. Phys. 52, pp. 3279-3285 5/1981]

Olsen, J.N. Baker, L.
Laser-Initiated Channels for Ion Transport: Breakdown and Channel Evolution (SAN) [Reprint: J. Appl. Phys. 52, pp. 3286-3292 6/1981]

Olsen, J.N. Johnson, D.J. Leeper, R.J.
Propagation of Light Ions in a Plasma Channel [Appl. Phys. Lett. 36, pp. 808-810 1980]

Olson, C.L.
Pulsed Power Ion Accelerators for Inertially Confined Fusion [Fiz. Plazmy 3, pp. 465-486 1977]

Ottinger, P.F. Mosher, D. Goldstein, S.A.
Propagation of Intense Ion Beams in Straight and Tapered Z-Discharge Plasma Channels (NAV) [Reprint: Phys. Fluids 23, pp. 909-920 5/1980]

Ottinger, P.F. Mosher, D. Goldstein, S.A.
Electromagnetic Instabilities in a Focused Ion Beam Propagating Through a Z-Discharge Plasma (NAV)(JAY) [Reprint: Phys. Fluids 24, pp. 164-170 1/1981]

Ottinger, P.F. Mosher, D. Goldstein, S.A.
Microstability of a Focused Ion Beam Propagating Through a Z-Pinch Plasma (NAV)(SCI) [Reprint: Phys. Fluids 22, pp. 332-337 2/1979]

Ottinger, P.F. Mosher, D. Goldstein, S.A.
Stability Constraints on Transported Light-Ion Beams (Paper 4A8 at IEEE Mtg., Ottawa Canada, May 1982) [Naval Research Laboratory 5/1982]

Pasour, J.A. et al.
Reflex Tetrode with Unidirectional Ion Flow (NAV) [Reprint: Phys. Rev. Lett. 40, pp. 448-451 2/1978]

Phelps, D.A. Salisbury, W.W. Jorna, S.
Injector Based on Electric Insulation for the Controlled Ballistic Focusing of Light Ion Beams [J. Appl. Phys. 52, pp. 3761-3768 1981]

Phelps, D.A. Chang, D.B.
Stability of Bounded Electron Beams Neutralized by Co-Moving Electrons (OCC) [Reprint: IEEE Trans. Nucl. Sci. NS-28, p. 3427 1981]

Phelps, D.A. Somerstein, S.
Precision Intense Particle Beam Accelerators Using In-Situ Tuning Techniques (OCC) [Reprint: IEEE Trans. Nucl. Sci. NS-28, p. 3424 1981]

Poukey, J.W. Humphries, S.Jr. Lockner, T.R.
Flow Enhancement in Magnetically Insulated Ion Injectors [Reprint: Phys. Fluids 25(8) (August 1982) 1471-1479]

Poukey, J.W. et al.
Focused Intense Ion Beams Using Self-Pinched Relativistic Electron Beams (SAN) [Reprint: Phys. Rev. Lett. 35, pp.1806-1808 1975]

Poukey, J.W.
Ion Effects in Relativistic Diodes (SAN) [Reprint: Appl. Phys. Lett. 26, pp.145-146 1975]

Poukey, J.W.
Two-Dimensional Ion Effects in Relativistic Diodes (SAN) [Reprint: J. Vac. Sci. Technol. 12, pp. 1214-1217 12/1975]

Prestwich, K.R.
HARP, A Short Pulse, High Current Electron Beam Acclerator (SAN) [Reprint: IEEE Trans. on Nucl. Sci. NS-22, 975-978, 1975]

Quintenz, J.P. Poukey, J.W.
Ion Current Reduction in Pinched Electron Beam Diodes (SAN) [Reprint: J. Appl. Phys. 48, pp. 2287-2293 1977]

Ranger, A.A.
Shock Wave Propagation Through a Two-Phase Medium [Reprint: Astonautica Acta 17, pp. 675-83 1972]

Ryutov, D.D.
High-Current Electron and Ion Beam Research and Technology. Report on the 3rd Int. Top. Conf.,Novosibirsk, USSR, 3-6 July 1979 [Nucl. Fusion 19, pp. 1685-1688 1979]

Sandel, F.L. et al.
no title [From: 4th Conf. on High Power E. and Ion-Beam Res.6/1981]

Slutz, S.A. Mehlhorn, T.A.
no title [Reprint: Appl. Phys. Lett. 39 12/1981]

Stephanakis, S.J. et al.
no title [Reprint: Bull. Am. Phys. Soc. 26, p. 921 9/1981]

Stephanakis, S.J. et al.
Production of Intense Proton Beams in Pinched-Electron-Beam Diodes (NAV) [Reprint: Phys. Rev. Lett. 37, pp. 1543-1546 12/1976]

Stringfield, R. et al.
no title [J. of Vac. Tech. 18, p. 146 1980]

Swain, D.W. et al.
The Characteristics of a Medium Current Relativistic Electron-Beam Diode (SAN) [Reprint: J. Appl. Phys. 48, pp. 1085-1093 3/1977]

Swain, D.W. et al.
Measurements of Large Ion Currents in a Pinched Relativistic Electron Diode (SAN) [Reprint: J. Appl. Phys. 48, pp. 118-124 1977]

Sweeney, M.A. Widner, M.M.
Thick-Shell Shock-Focusing Electron Beam Targets (SAN) [Reprint: Nucl. Fus. 13, pp. 429-433 1978]

Sweeney, M.A. Farnsworth, A.V.
High-Gain, Low-Intensity ICF Targets for a Charged-Particle Beam Fusion Driver [Nucl. Fusion 21, pp. 41-54 1981]

Thayer, W.J. et al.
Pressure Wave Suppression for a Pulsed Chemical Laser [Reprint: AIAA Journal 18, pp. 657-64 6/1980]

Thomson, S.L.
Hydrodynamic Effects in Inertial Fusion Reactors (BEC) [Reprint: 5th SMIRT Conf., Berlin 8/1979]

VanDevender, J.P
Long Self-Magnetically Insulated Power Transport Experiment(SAN) [J. Appl. Phys. 50, p. 3928 1979]

Varnado, S.G. Carlson, G.A.
Considerations in the Design of Electron-Beam-Induced Fusion Reactor Systems (SAN) [Reprint: Nucl. Tech. 29, pp. 415-427 6/1976]

Winterberg, F. Swegle, J.
Comments on "Linear Waves and Instabilities on Magnetically Insulated Gap" and reply to those comments (UNV)(SAN) [Reprint: Phys. Fluids 25, p. 913 6/1982]

Wright, T.P.
Multi-Channel Ion Beam Overlap (SAN) [Reprint: Phys. Fluids 24, p. 370-372 2/1981]

Wright, T.P. Halbleib, J.A.Sr.
Theoretical Multiple Beam Overlap from Channel Transport of Intense particle Beams (SAN) [Reprint: Phys. Fluids 23, p. 1603-1619 8/1980]

Wright, T.P. Green, T.A. Mehlhorn, T.A.
Charge Exchange and Energy Loss of Carbon Ions in Air-Plasma Channels [J. Appl. Phys. 52, pp. 147-150 1981]

Yamanaka, C. editor
Proceedings of the Japan – U.S. Seminar on Theory and Application of Multiply Ionized Plasmas Produced by Laser and Particle Beams, Osaka University [1981]

Yonas, G.
Developments in Sandia Laboratories Particle Beam Fusion Programme [Plasma Phys. Control. Nucl. Fus. Res., IAEA 1979]

Yonas, G.
Intense Particle Beams [IEEE Trans. Nucl. Sci. NS-26, pp. 4160-4165 1979]

Yonas, G.
Inertial Fusion Research Based on Pulsed Power (SAN) [From Japan-US Seminar, Theory and Application of Multiply Ionized Plasmas Produced by Laser and Particle Beams]

Yonas, G.
Fusion Power with Particle Beams (SAN) [Reprint: Scientific American 239 pp. 50-61 1978]

Yonas, G. et al.
Electron Beam Focusing Using Current-Carrying Plasmas in High γ/ν Diodes (SAN) [Reprint: Phys. Rev. Lett. 30, pp.164-167 1973]

Yonas, G. et al.
Electron Beam Focusing and Application to Pulsed Fusion [Reprint: Nuclear Fusion 14, pp. 731-740 1974]

Yu, S. Lee, E.P. Buchanan, H.L.
Focal Spot Size Predictions for Beam Transport through a Gas-Filled Reactor [From: Proc. of the Heavy Ion Workshop, p. 504 1979]

Yu, S. et al.
Beam Propagation through a Gaseous Reactor - Classical Transport [From: Proc. of Heavy Ion Fusion Workshop 1978]

Yu, S. et al.
Propagation of a Heavy Ion Beam in a Gas-Filled Reactor [From: Proc. of Heavy Ion Fusion Workshop 1977]

various authors
Conference Record – Abstracts, 1982 IEEE Int'l. Conf. on Plasma Science, Carleton University, Ottawa, Ontario, 17-19 May 1982 [IEEE 6/1982]

various authors
Proceedings of the 4th Internation Topical Conference on High-Power Electron and Ion-Beam Research and Technology, Palaiseau, France [Conference Proceedings 6/1981]